A medicinal chemistry study in nitrogen containing heterocycles

A thesis submitted in fulfilment of the

requirements for the degree of

Master of Science (Pharmacy)

Of

Rhodes University

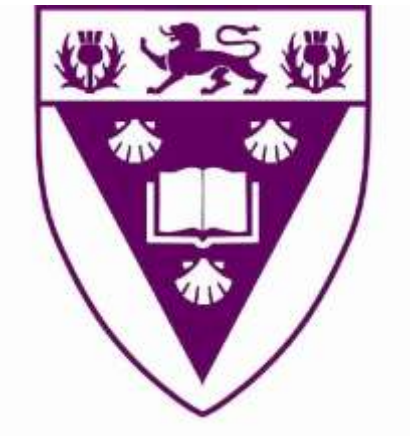

by

Mayibongwe J. Lunga

January 2017

Abstract

Heterocyclic structures have found extensive utility in the field of medicinal chemistry, as prominent regions of pharmacophores resulting in numerous drug treatments for many diseases. Accordingly, in this project we explored the respective antimalarial and anticancer activity exhibited by compounds featuring nitrogen containing indole and tetrazole heterocycles respectively. This thesis therefore comprises of two distinct parts.

Part 1.

Following the development of resistance towards traditional antimalarial therapy such as chloroquine and emerging resistance towards artemisinin combination therapies, the WHO reported the urgent need for new, effective drugs and identification of new drug targets to combat the *Plasmodium falciparum* parasite. In 2015 the parasite was the cause of 429 000 deaths, the majority occurring in the sub-Saharan region of Africa. This highlights the failing effectiveness of vector control strategies, reiterating the need to develop alternative control and treatment strategies. In response to this need we wanted to expand and further describe the SAR of the indole based series, indolyl-3-ethanone-α-thioethers, previously synthesized in our laboratory. These compounds were found to exhibit antimalarial activity with compounds **2.26** and **2.27** exhibiting activity against *P. falciparum* 3D7 in the nanomolar range. Based on these compounds we synthesized compounds **3.21** and **3.24** – **3.32** following a three step reaction pathway. Our results in this study, indicate that compound **3.28**, a *p*-nitrothiophenol analogue of **2.27** was the most active of the compounds we synthesized and furthermore was superior in activity against *Plasmodium* compared to **2.27**. This result indicated that the presence of *p*-NO_2 is important in enhancing anti-plasmodial activity. Comparing compounds **3.25** and **3.26** with an oxygen on the ether bridge to compounds **3.29** and **3.30** with a sulfur, we observed an increase in hydrophilicity coupled to a decrease in anti-plasmodial activity in the compounds, thus, highlighting the importance of sulfur for enhanced activity. Furthermore, we investigated bioisosteric replacement of the 5-chloro substituent present in hit compounds **2.27** and **3.28**, with an electron withdrawing nitrile (**3.27**) and electron donating methyl (**3.29**) and methoxy (**3.31**) substituents. These

substituents decreased anti-plasmodial activity, confirming that a chlorine substituent is optimal for biological activity. This study furthered our understanding of the SAR of indolyl-3-ethanone-α-thioethers for the development of potent anti-plasmodial lead compounds.

Part 2.

Triple negative breast cancer (TNBC), which disproportionately affects women of sub-Saharan Africa, is unresponsive to hormone-based therapies. This emergence presents a population of patients devoid of effective drug treatment, signaling the urgent need to develop new effective therapies with novel drug targets. Therefore, we identified our target in TNBC cells as the protein-protein interaction between the co-chaperones HOP and HSP90. We reasoned that a disruption of this interaction would ultimately result in cancer cell death via the degradation of essential oncogenic client proteins. Following a fragment screening campaign, which identified several acid and tetrazole containing hits (**4.56** – **4.58**) which bound to HOP, with low anticancer activity, we sought to develop synthetic methodology to elaborate our fragment hits synthesizing tetrazole containing fragments to target TNBC cell lines. We therefore proceeded to synthesize a range of multi substituted fragments (**4.59** – **4.63**), utilizing a nitrile (**4.66**) to access tetrazoles via 1,3-cycloaddition and an acid by nitrile hydrolysis. We successfully synthesized the tetrazole and acid fragments which are currently undergoing characterization for activity against TNBC.

Table of Contents

List of Tables

List of Schemes

List of Figures

List of Abbreviations

^{13}C-NMR	Carbon-13 Nuclear Magnetic Resonance
^{1}H-NMR	Hydrogen Nuclear Magnetic Resonance
brs	Broad singlet
calcd	Calculated
CD_3OD	Deuterated methanol
CQ	Chloroquine
δ	Chemical shift

d	Doublet
DCM	Dichloromethane
dd	Doublet of doublets
DMF	*N,N*-dimethyl formamide
DMSO	Dimethyl sulfoxide
EC_{50}	Half maximal effective concentration
eq	Equivalent
HMBC	Heteronuclear Multiple Bond Correlation
HOP	Heat shock protein organising protein
HRESMS	High Resolution Electrospray Mass Spectrometry
HSP90	Heat shock protein 90
HSQC	Heteronuclear Single Quantum Coherence
Hz	Hertz
IC_{50}	Half maximal inhibitory concentration
IR	Infrared
J	Spin-spin coupling constant
LD_{50}	Median lethal dose
LT	Leukotriene
M	Molar
m	Multiplet

mg	Milligram
MHz	Megahertz
mL	Millilitre
mmol	Millimolar
µM	Micromolar
mp	Melting point
NMR	Nuclear Magnetic Resonance
*P*LDH	*Plasmodium* lactate dehydrogenase
ppm	Parts per million
q_c	Quaternary carbon
rt	Room temperature
s	Singlet
SAR	Structure activity relationship
SP	Sulfadoxine-pyrimethamine
TLC	Thin layer chromatography
TMSCN	Trimethylsilyl cyanide
WHO	World Health Organisation

Acknowledgements

I am humbled and filled with great gratitude for a phenominal mom (Ivy) and dad (Godden), and remarkable big brother (Thamsanqa), for being the best family ever and believing in me. The unwavering support emotionally, financially and the encouragement through the highs and lows, you guys always carried me forward, the prayers, the phone calls, God bless and I love you guys.

My lab mates and friends Don, Faith, Carli, Tanyi, Tiaan, Hugan you guys are great. Ma Prudence for her tireless efforts to make available what we needed in the lab and for the lovely conversations. Lissa, Siya and Lola, we were in this degree and life hustle together, through thick and thin you guys remain G, my friends for life. B. Faro, includes you my guy.

To my supervisor Dr. Clinton G.L. Veale, thank you for being awesome and the coolest. The guidance and support was impeccable, under your wing I learnt a lot as a researcher and person. Thank you to yourself and Prof. Adrienne Edkins for the means of financial support towards my studies. God bless.

My family at River of Life Church has been a pillar to my life through and through. Special thank you to my God-given parents Ps Innocent and Mam' Milcah for everything; everything.

Dr. Roman Tandlich, thank you for the periodic conversations and all the words of encouragement, loved our chat sessions.

Above all, I would like to thank my Heavenly Father and Sustainer of my life for everyone who has contributed to my journey during this period and prior; be it in kind, encouragement, thoughts, prayers and just being there. Thank You Lord for Your grace that is sufficient for me. You started this and You have faithfully seen it to completion. I give You all the glory.

Chapter 1: Introduction

1.1 General overview of Malaria

Plasmodium falciparum induced malaria remains a highly endemic infection affecting mostly the sub-Saharan region of Africa, with less endemicity in South East Asia and the Americas.[1,2] In 2015, the WHO reported 212 million new cases of malaria, with a disease burden of 429 000 deaths, Africa accounting a colossal proportion of 90% of the reported global cases.

1.2 Plasmodium parasite life cycle

Development of the *Plasmodium* parasite occurs sexually in a mosquito following the asexual phase in a human host. As depicted in **Fig 1.1**, the sporozoite form of the *Plasmodium* is injected into the human blood stream during feeding by an infected female *Anopheles* mosquito. The sporozoites proceed from the injection site to invade the host liver cells where they divide asexually to form merozoites that rapidly multiply leading to cell rupture. This phenomenon accounts for clinical symptoms of fever, chills and night sweats experienced by an infected human host. The merozoites then infect red blood cells, further multiplying and causing cell rupture. More red blood cells are re-infected with merozoites propagating parasite multiplication while merozoites develop into gametocytes. When a mosquito feeds on the infected human host, gametocytes are assimilated with blood, maturing into gametes in the mosquito stomach resulting in formation of ookinetes on fusion of developed male and female sexual gametes. The ookinetes proceed to embed the mosquito stomach wall forming an oocyst on the outer stomach wall. Numerous sporozoites are formed within the oocysts causing a subsequent burst and release of sporozoites that migrate to the mosquito salivary glands for reinjection into a human host on feeding.[3–6]

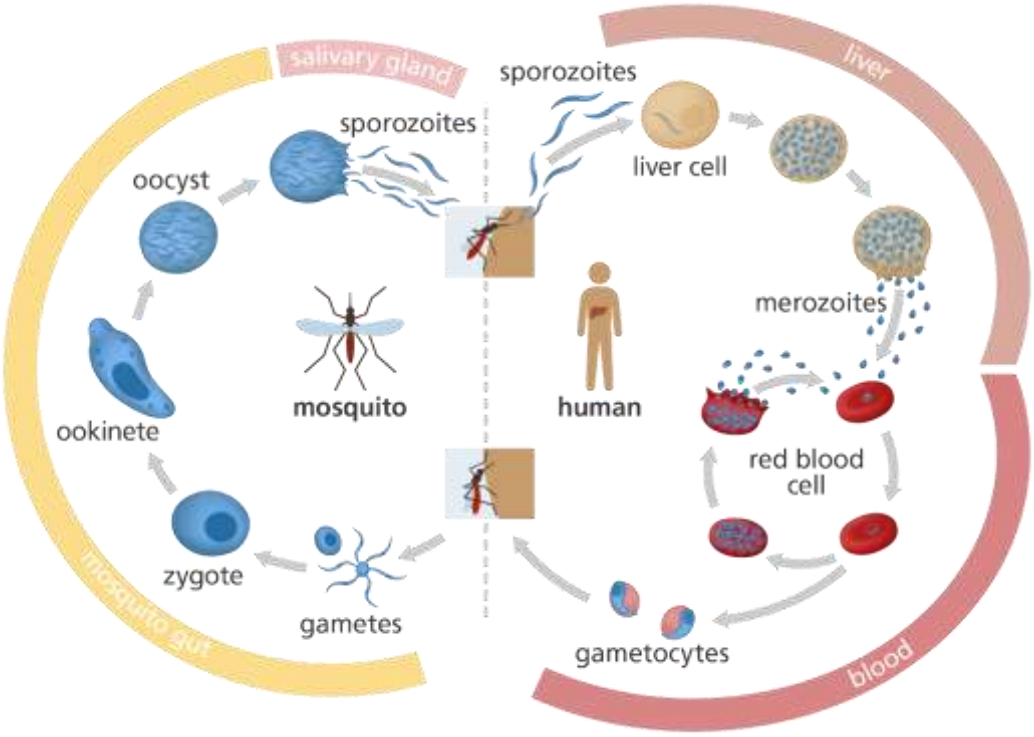

Fig 1.1 Life cycle of *Plasmodium* parasite. Image reproduced with permission from authors.[7] *Photo Credit: Genome Research Limited*.

1.3 Control, treatment and resistance

The insight into the *Plasmodium* parasite life cycle presents multiple opportunities to explore methods of prevention, control and treatment of malaria. Circumvention of mosquito feeding through the use of nets has been enhanced by vector control strategies such as use of insecticide-treated nets and mosquito repellents in the form of sprays, creams and coils.[8,9] Permethrin (**1.1**) is one such example of pyrethroid insecticides used to treat indoor nets, diethyl toluamide (**1.2**) on the other hand is used in mosquito repelling formulations.[10,11] Methoprene (**1.3**) is an example of environmentally less toxic insecticides, referred to as bio rational insecticides, used in mosquito breeding sites to block the reproductive and maturation stages of mosquitos, resulting in death.[12] However, mosquito resistance to insecticides such as dichloro-diphenyl-trichloroethane, (DDT, **1.4**) and pyrethroids has been

reported in African regions like Zambia, Cameroon, Mali, Ethiopia, calling for prompt resistance management strategies and development of new effective insecticides.[12–14]

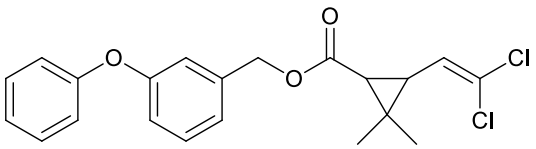

1.1 Permethrin

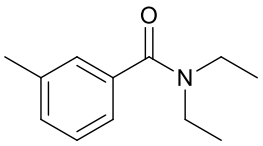

1.2 Diethyl toluamide

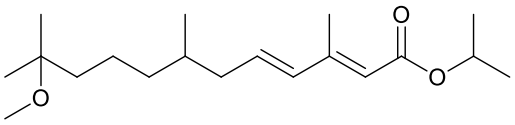

1.3 Methoprene

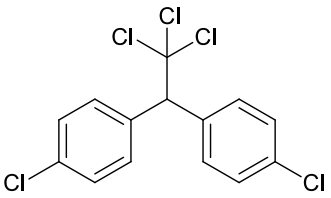

1.4 DDT

In the treatment of malaria infections, an array of antimalarial agents with different modes of action have been identified and developed for use as reported in the 2015 *WHO Guidelines for the treatment of malaria*. These agents included chloroquine (CQ, **1.5**), mefloquine (**1.6**), artemisinin and its derivatives (**1.7 – 1.9**) along with other combination treatments such as sulfadoxine/pyrimethamine (SP, **1.10** and **1.11**) and proguanil/atovaquone (**1.12** and **1.13)**. Most of the existing antimalarial agents have been plagued by decreasing efficacy against *P. falciparum* owing to parasitic gene mutations leading to the emergence and spread of resistance.[15,16] White suggests that these mutations are spontaneous changes in genes coding for drug target sites or protein transporters, affecting effective drug levels in the parasite.[16]

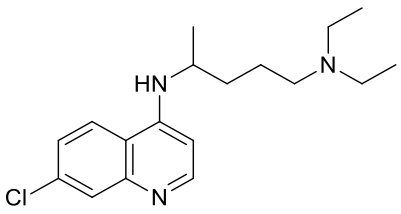

1.5 Chloroquine

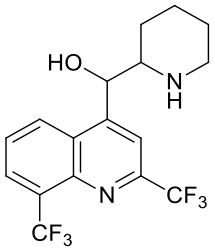

1.6 Mefloquine

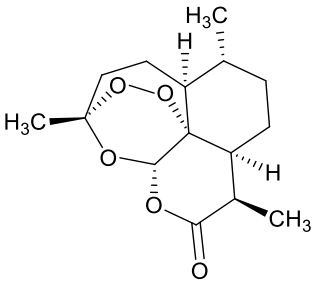

1.7 Artemesinin

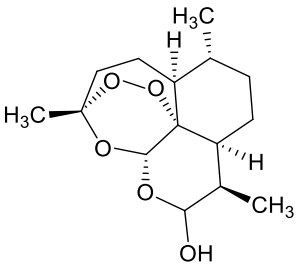

1.8 Artemether

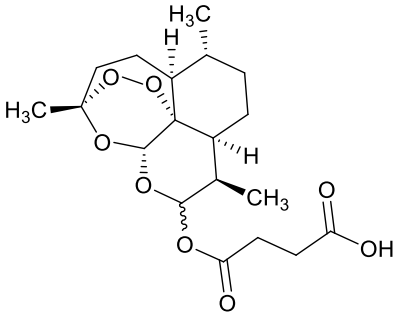

1.9 Artesunate

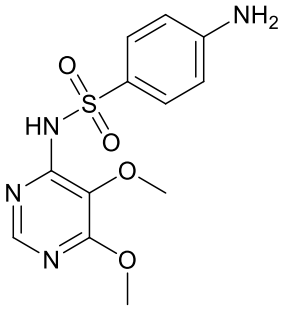

1.10 Sulfadoxine

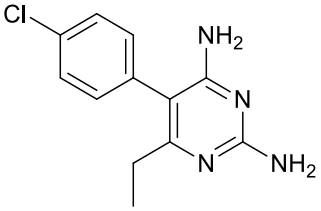

1.11 Pyrimethamine

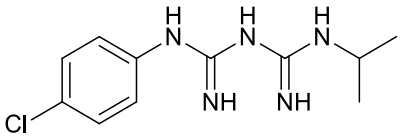

1.12 Proguanil

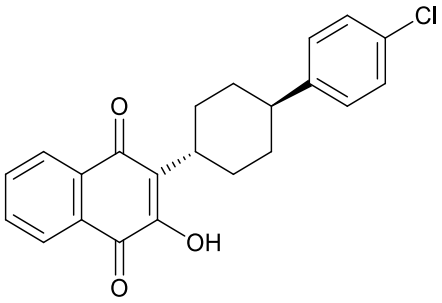

1.13 Atovaquone

In the 20th century, CQ was the first line drug of choice in the treatment of malaria, due to its oral bioavailability, safety profile and cost effectiveness.[17] Resistance to the drug emerged in Asia and the Americas in the 1960s with parts of Africa reporting emergence and its subsequent spread between 1978 – 1988.[17,18]

Many countries in Africa and South-East Asia then employed SP as a cost effective and safe alternative first line drug to CQ[17,19,20,21], but resistance to the drug emerged in the late 20th century spreading through Africa, Asia and the Americas.[20,22,23]

With increasing and widespread resistance to available antimalarial agents, the WHO advocated for the use of artemisinin combination therapy (ACT) to curb the rates of mortality and morbidity.[24] According to the 2001 *WHO* report on *Antimalarial Drug Combination Therapy,* the combination of antimalarial agents in therapy attempts to amplify therapeutic efficacy and retard the emergence of resistance in contrast with monotherapy outcomes. Agents with different mechanisms of action and target sites are combined to yield a concerted cumulative effect against the malaria parasite.[25]

Bosman and Mendis reported the widespread adoption of ACTs as a first line treatment in most malaria endemic countries between 2001 – 2006.[24] The safety profile and rapid efficacious nature of ACTs against multi–drug resistant parasites supported the implementation of treatment in spite of the highly inflated cost of procurement.[16,26] In recent years, the effective first line ACTs have been marked with emergence of resistance in parts of South-East Asia and as of late Africa. The resistance is characterised by delayed parasite clearance time after administration of the 3-day ACT course to malaria infected patients. Residual *P. falciparum* parasites were detected in patient's blood after the normal dosing regimen.[27–29]

1.4 Known malaria parasite drug targets

Notwithstanding the currently unknown biochemical processes and viable target sites of the parasite along with still undefined modes of action for drugs such as mefloquine, halofantrine and primaquine, some targets have been identified.[30–32] In a recent review, potential drug target sites and metabolic pathways essential for the survival of *P. falciparum* were identified and discussed.[33] We will therefore proceed to highlight some of the known and suspected drug targets of antimalarial agents in current use.

While the mechanism of action of CQ [34] has not been fully unravelled, the currently accepted theory (**Fig 1.2**) suggests that CQ binds to the toxic haem moiety released from the digestion of haemoglobin in red blood cells, thus forming a complex. The CQ-haem complex inhibits the parasite from converting

haem to the non-toxic haemozoin. Increasing amounts of the CQ-haem complex results in cell lysis and parasite death. Mefloquine though structurally similar to CQ, exhibits a relatively lower affinity to the haem group, suggesting an additional different mode of action still yet to be understood.[35–37]

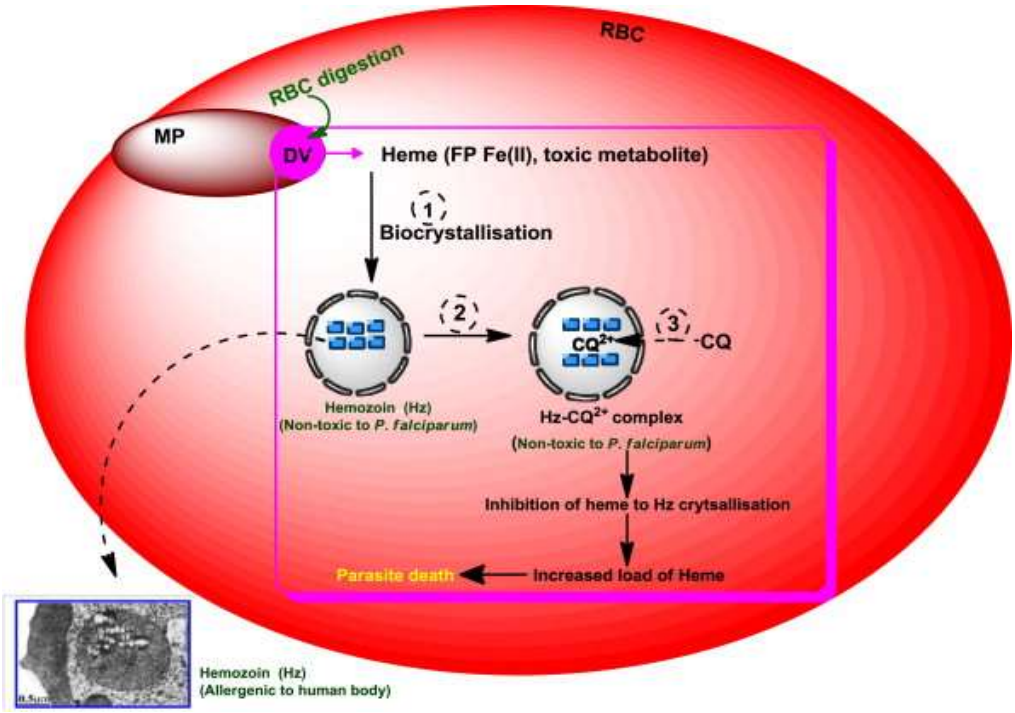

Fig 1.2 Chloroquine mechanism of action. Image reproduced with permission from authors.[37]

Studies are still inconclusive regarding the mechanism of resistance to CQ but amongst accepted theories, investigations have largely suggested that intra-parasitic concentrations of CQ are insufficient to inhibit haemozoin formation possibly due to the presence of an efflux pump in resistant strains. Genetic crosses have revealed that polymorphism of transporter protein genes have led to associated *P. falciparum* chloroquine resistance transporters (*pf*CRT), identified and found present in resistant strains with reduced intra parasitic CQ levels. Resistance is though, not thought to be entirely due to *pf*CRT polymorphism, *P. falciparum* multidrug resistance gene-1 (*pf*MDR1) has also been observed to modulate the extent of resistance to CQ by reducing drug target sensitivity.[40–43]

The more recent and widely used treatment is artemisinin and its derivatives (**1.7** – **1.9**), with a mechanism of action that has not been fully characterised. *In vivo*, artemisinin derivatives are thought to form radicals that bind to haem moieties to form adducts, in the process preventing formation of non-toxic haemozoin. Death of the parasite via this mechanism lacks conclusive evidence, as heamozoin levels were not affected in a study of artemisinin treated parasite cultures.[37,44,45] Nonetheless, the antimalarial activity of artemisinin compounds was found to be linked to the endoperoxide bridge, when one oxygen was substituted with a carbon, the compounds were inactive against *Plasmodium*.[44,46]

SP (**1.10** and **1.11**), which belong to the sulfonamides and anti-folate class of drugs respectively, target the malaria parasite's *de novo* folate biosynthesis pathway (**Fig 1.3**) which is essential for its survival. The folate derivatives from the pathway are cofactors in the synthesis of amino acids, purines and pyrimidines which in turn are substrates for DNA replication and protein synthesis. Sulfadoxine, a *p*-aminobenzoic acid analogue, and pyrimethamine, competitively inhibit two key enzymes in folate biosynthesis namely, dihydropteroate synthase (DHPS) and dihydrofolate reductase (DHFR) respectively. Proguanil is also a DHFR inhibitor.[47,48]

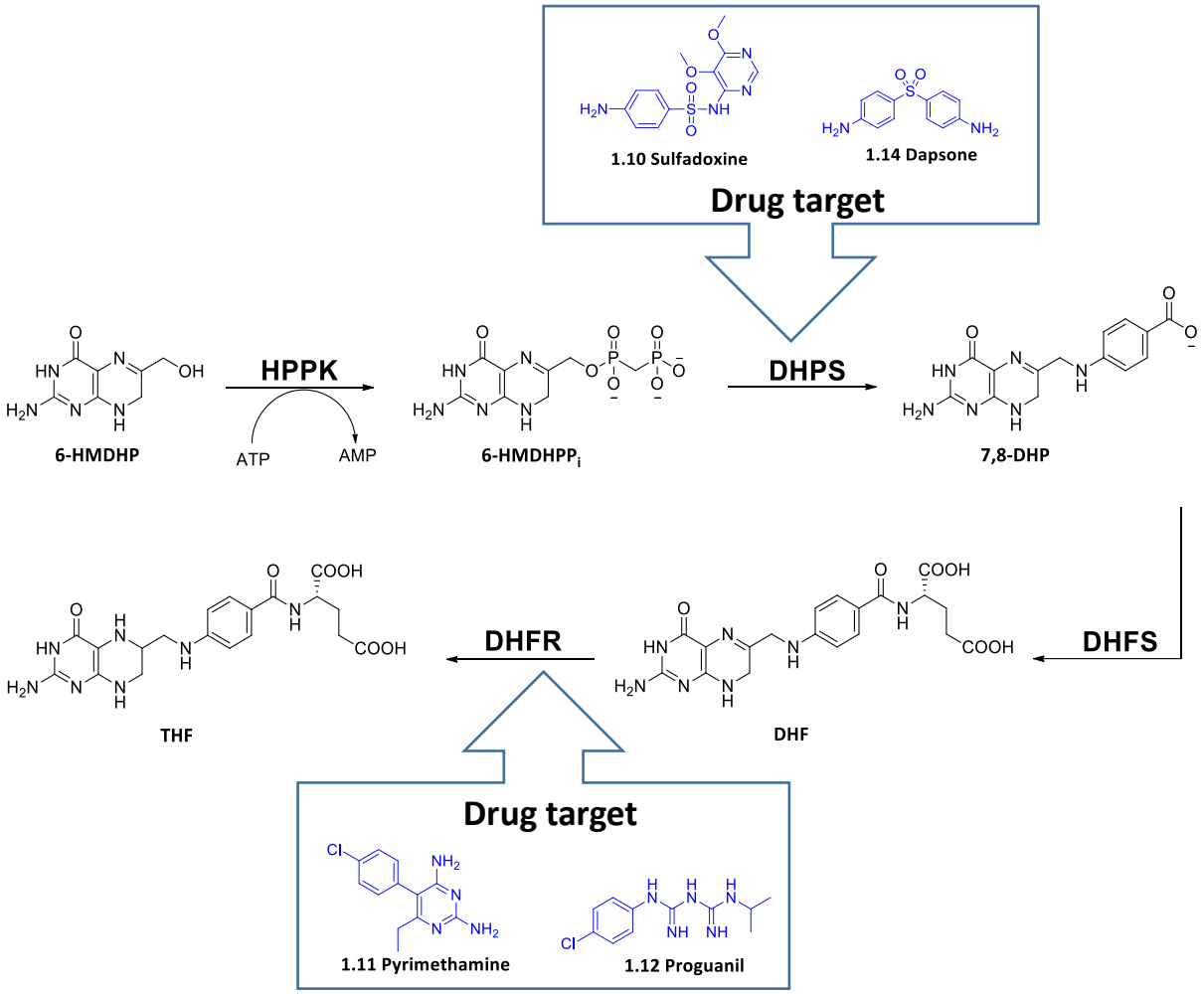

Fig 1.3 *De novo* folate biosynthetic pathway. ***Substrates****: 6-hydroxymethyl dihydropterin (6-HMDHP), 6-hydroxymethyl dihydropterin pyrophosphate (6-HMDHPP$_i$), 7,8-dihydropteroate (7,8-DHP), 7,8-dihydrofolate (DHF), tetrahydofolate(THF);* ***Enzymes****: 7,8-dihydro-6-hydroxymethylpterin pyrophosphokinase (HPPK), dihydropteroate synthetase (DHPS), dihydrodihydrofolate synthetase (DHFS), dihydrofolate reductase (DHFR).*

Efficiency of these drugs has been hindered by rapid resistance emerging due to point mutations in the respective genes of parasite DHPS and DHFR. High resistance was observed in folate enzymes where three gene sequence points had mutated whilst moderate resistance was conferred by one or

two gene sequences mutating. Use of trimethoprim and sulfa-containing drugs for the treatment of bacterial infections was also thought to contribute to the rapid emergence of resistance to SP treatment.[20,21,40,47] Studies were conducted to examine the effectiveness of SP treatment in malaria infected patients who had once used trimethoprim and sulfa-containing antibiotics for the treatment of bacterial infections. A high prevalence of SP resistant genes was found in malaria parasites of infected patients, naïve to SP treatment. These results confirmed the hypothesis of possible cross resistance being conferred on SP treatment.[49,50]

Atovaquone (**1.13**) is a drug, structurally related to ubiquinone (**1.15**), an electron transporter in the energy producing mitochondria. While often used in combination with the anti-folate, proguanil, the synergistic mechanism of atovaquone/proguanil has not yet been fully understood. It is known that ubiquinone binds to cytochrome bc_1 transferring electrons from dehydrogenase enzymes to the cytochrome complex which ultimately produces water using the electrons, free protons and O_2. Atovaquone exerts its function by competitively inhibiting the binding of ubiquinone to cytochrome bc_1 in electron transfer. This inhibition disrupts mitochondrial electron flow for ATP synthesis and further inhibits the activity of parasite mitochondrion-linked enzymes such as dihydroorotate dehydrogenase (DHOD). DHOD provides the orotate required for pyrimidine biosynthesis, substrates essential for DNA synthesis. Paucity thereof inhibits cellular proliferation causing parasite death.[51,52] In addition, DHOD has therefore been identified as a potential target in malaria parasites, with a new DHOD inhibitor, DSM265 (**1.16**), a triazolopyrimidine based compound currently undergoing clinical trials as a potential antimalarial agent.[53]

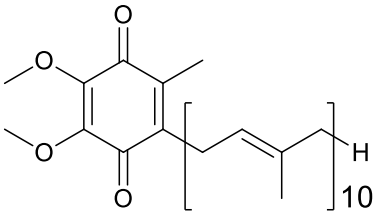

1.15 Ubiquinone

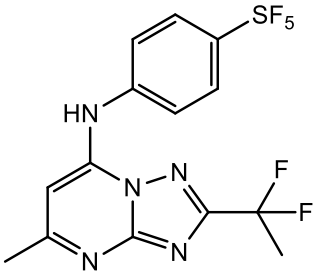

1.16 DSM265

Rapid emergence of resistance against atovaquone implied a prior natural resistance and is thought to be due to point mutations in genes coding for cyctochrome bc_1 which results in the exchange of an amino acid, at position 268, important in ubiquinone binding.[37,51,54,55] Akhoon *et al*. and Kessl *et al.* observed reduction in atovaquone interaction with cytochrome bc_1 binding site along with altered volume and surface area of binding site. The mechanism of resistance that has reduced atovaquone efficacy still requires further descriptive study for our understanding.[56,57]

1.5 The need for new antimalarial agents

The emergence and widespread resistance of *P. falciparum* against available treatment drugs and the decreased effectiveness of insecticides in vector control highlights the urgent need for new and effective strategies to combat malaria infection. A number of new antimalarial compounds have been synthesised in response to this urgency.

Compound NITD609 (rebranded to cipargamin after being renamed KAE609, **1.17**)[58] belongs to a new class of spiroindolone compounds and has been found active at nanomolar concentrations against drug resistant strains of *P. falciparum* and *P. vivax*. The compound was found to be active against all asexual blood stages of the parasite signifying presence of target site in all tested parasite stages, and though the mechanism of action had not been determined[59], successive studies strongly suggested that the compound's target site is the P-type cation-transporter ATPase4 found on the parasite's cell

membrane.[60] With an acceptable safety profile thus far, this drug candidate is undergoing development in clinical studies.[59,61]

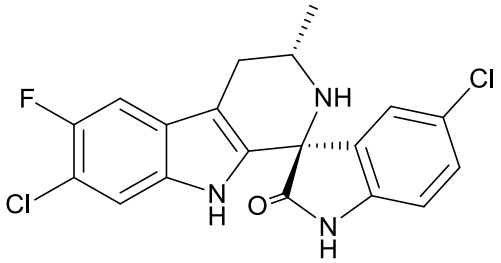

1.17 NITD609 (Cipargamin)

SKM13 (**1.18**) is a new CQ derivative with a phenyl methyl substituent and α,β-unsaturated amide representing a class of potential antimalarial drug candidates. Though still requiring further *in vivo* studies against CQ-resistant strains, the compound exhibited higher activity against CQ-resistant strains than CQ drug. These findings suggest that SKM13 may have an unknown mechanism of action separate to that of CQ, making it a potential new antimalarial agent.[62]

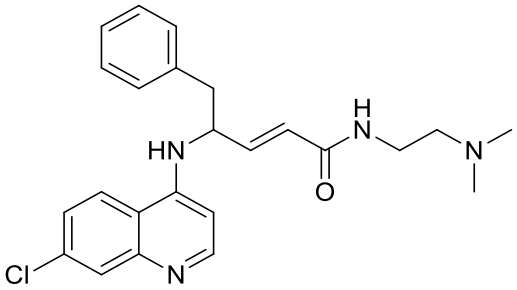

1.18 SKM13

The ongoing investigations into metabolic and biological processes of the malaria parasite are also encouraging new hypotheses and uncovering the nature of the parasite with proofs of various drug class mode of action.[63] Furthermore new potential drug targets for essential parasite bioprocesses are being discovered, exemplified by the aforementioned P-type cation-transporter ATPase4, whose disruption causes influx of Na^{2+}. The effect of increased intra parasitic Na^{2+} is not fully understood but is thought to affect important metabolic functions.[58]

In response to the need for new antimalarial agents, we want to investigate the reported antimalarial activity of indole based compounds[64], functionalising the scaffold to produce effective agents with a conceivably new target. This novelty would minimise the rapid development of resistance as opposed to a drug target similar to that of existing therapies already plagued by resistance.

Chapter 2: Indole nucleus and its derivatives in medicinal chemistry

2.1 General overview: Indoles

Indole is a heterocyclic compound comprising a fused benzene and pyrrole ring which was discovered in mid-1800 in the study of the natural dye, indigo.[64] The indole structure (**Fig 2.1**) shown below can undergo structural modifications yielding functional compounds that define new classes or expand existing classes of indole based derivatives.

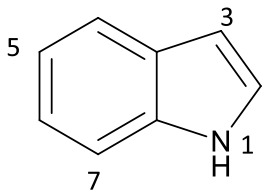

Fig 2.1 Structure of the indole nucleus.

The indole structure is prone to electrophilic substitution reactions with C-3 on the pyrrole ring having a high electron density.[65,66] When an electron withdrawing group is present on either the C-2 or C-3 positions, nucleophilic addition, cycloaddition and Diels-Alder reactions can occur, depending on the presence and nature of an *N*-protecting group, resulting in numerous indole derivatives.[67] Furthermore, the weakly acidic NH on the pyrrole can also undergo *N*-substitutions under basic reaction conditions,[68,69] and following substitutions on the more reactive pyrrole positions, the benzene ring can also undergo substitution.[68,70]

Indole, termed a privileged structure, can be fashioned into functionalised derivatives that elicit widely varying pharmacological effects of medicinal significance.[64,69] With a vast number of biologically active, naturally occurring alkaloids such as reserpine (**2.1**) an anti-hypertensive, yohimbine (**2.2**) for sexual dysfunction, melatonin (**2.3**) and serotonin (**2.4**) hormones, vindesine (**2.5**) an anti-tumour agent, development of synthetic indoles has become an area of important interest. Oxypertine (**2.6**) used as an anti-psychotic, fluvastatin (**2.7**) for hypercholesterolemia and zafirlukast (**2.8**) for asthma

are a few examples of synthetic indoles that have found clinical value.[69] We will therefore proceed to discuss more examples of natural and synthetic indoles used clinically, by classes of activity.

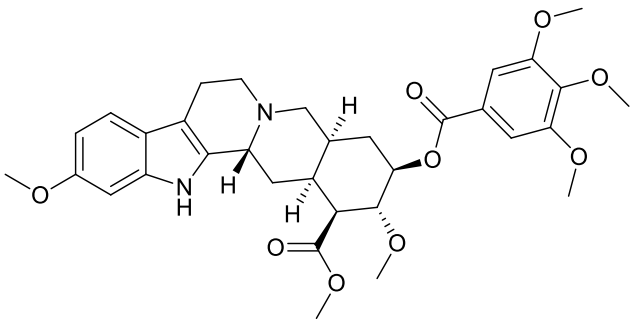

2.1 Reserpine

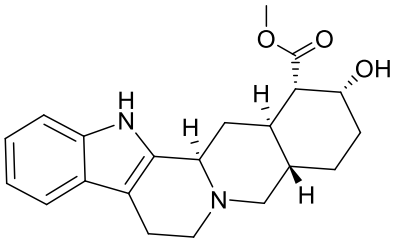

2.2 Yohimbine

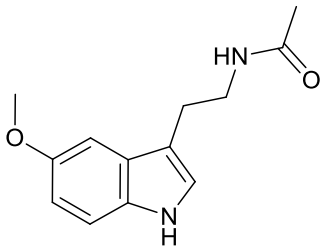

2.3 Melatonin

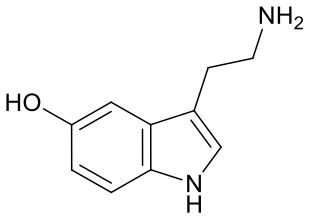

2.4 Serotonin

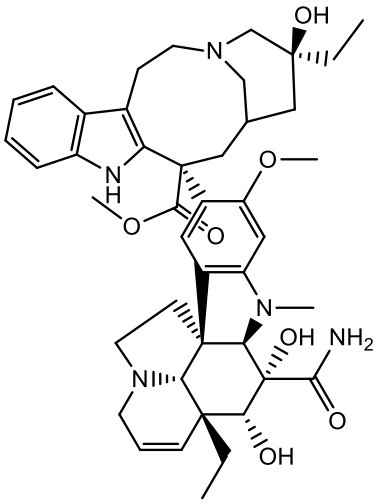

2.5 Vindesine

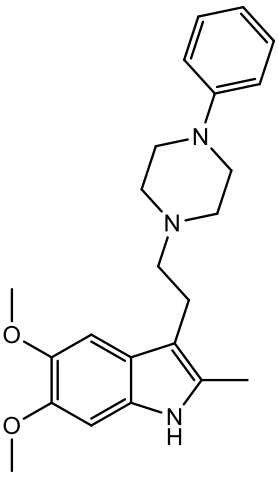

2.6 Oxypertine

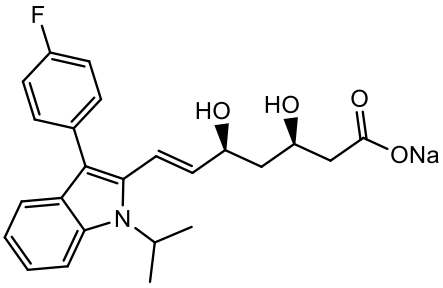

2.7 Fluvastatin

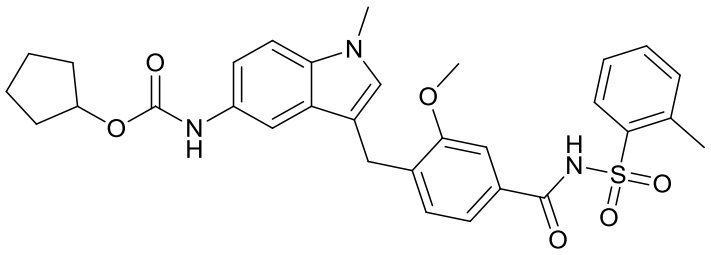

2.8 Zafirlukast

2.2 Indoles as anti-bacterial agents

Based on the therapeutic use of pyrazino[1,2-*a*]indoles as antidepressants, anticonvulsants, antihistaminic, thrombolytic, serotonin antagonistic, anxiolytic and anticancer agents Tiwari *et al.* sought to study the antibacterial activity of these indolic compounds.[71] 1,2,3,4-tetrahydropyrazino[1,2-*a*]indoles (**2.9a – i)** variably substituted on position 1 were synthesised and screened for antibacterial activity against pathogenic strains of *Staphylococcus aureus*, *Salmonella typhi, Streptomyces thermonitrificans, Escherichia coli and Pseudomonas aeruginosa* using the disc diffusion method. Gentamycin and doxycyline HCl were used as reference standards. Compounds **2.9d**, **2.9e** and **2.9f** were potent against all pathogenic strains compared to other screened compounds, with lower cytotoxicity than gentamycin.[71]

Interestingly, compounds **2.9a**, **2.9c** and **2.9h** exhibited a narrow spectrum of activity, each compound with MIC value of 3.75 µg/disc against *P. aeruginosa*, *S. thermonitrificans* and *S. aureus* respectively. In addition to substitutions on position 1, an unsubstituted NH at position 2 of 1,2,3,4-tetrahydropyrazino[1,2-*a*]indoles was also found to be important for antibacterial activity.[71] These observations present an opportunity to develop substituted compounds with increased antibacterial activity.

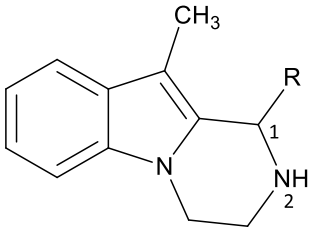

2.9a: R = C_6H_5
2.9b: R = *p*-*Br*C_6H_4
2.9c: R = *m*-*Cl*C_6H_4
2.9d: R = *p*-*F*C_6H_4
2.9e: R = *p*-$CH_3C_6H_4$
2.9f: R = *p*-$NO_2C_6H_4$
2.9g: R = *m*-$CH_3OC_6H_4$
2.9h: R = 2-pyridyl
2.9i: R = 2-thienyl

El-Sayed *et al.* investigated the reaction between indole and aliphatic di-aldehydes. A novel class of bisindolyl-cycloalkane indoles (**2.10a – f**, **2.11a – d**) was synthesised and compounds screened for antibacterial activity against *S. aureus* strains, MRSA standard ATC 43300 and clinically isolated MRSA. Ampicillin and sultamicillin antibiotics were employed as reference standards. Compounds **2.10a – f** and **2.11a – d** exhibited strong antibacterial activity against bacterial test strains. MIC values against MRSA standard and isolate ranged between 6.25 µg/ml – 12.5 µg/ml compared to the 25 µg/ml and 50 µg/ml of sultamicillin and ampicillin respectively. Save for **2.10a** and **2.10f** with MIC values of 50 µg/ml and 12. 5 µg/ml respectively against *S. aureus*, 3.125 µg/ml was observed for **2.10b – e** and **2.11a – d.**[72]

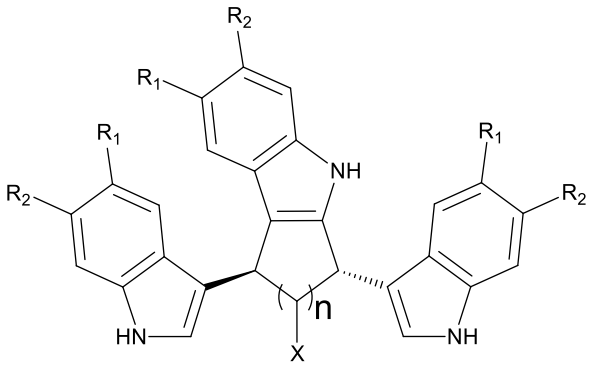

2.10a: n = 1, X = H, $R_1 = R_2 = H$
2.10b: n = 1, X = Cl, $R_1 = R_2 = H$
2.10c: n = 1, X = Br, $R_1 = R_2 = H$
2.10d: n = 2, X = H, $R_1 = R_2 = H$
2.10e: n = 2, X = H, R_1 = Cl, R_2 = H
2.10f: n = 2, X = H, R_1 = H, R_2 = Cl

2.11a: n = 3, $R_1 = R_2 = H$
2.11b: n = 3, R_1 = Cl, R_2 = H
2.11c: n = 3, R_1 = H, R_2 = Cl
2.11d: n = 4, $R_1 = R_2 = H$

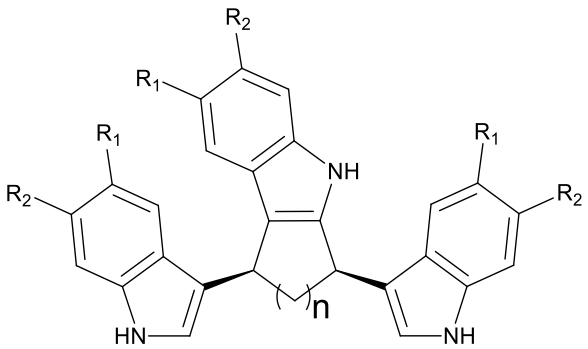

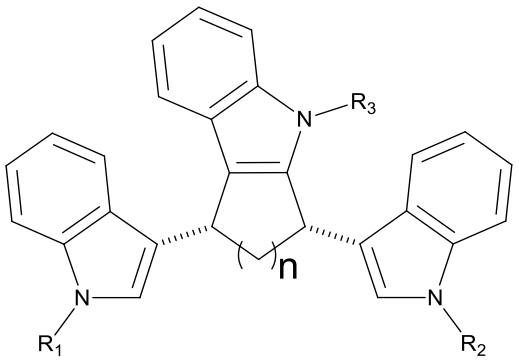

2.12a: n = 2, $R_1 = R_2$ = Ac, R_3 = H
2.12b: n = 2, $R_1 = R_2 = R_3$ = Ac
2.12c: n = 3, R_1 = Ac, $R_2 = R_3$ = H
2.12d: n = 3, $R_1 = R_2$ = Ac, R_3 = H

Furthermore, El-Sayed *et al.* discovered that a free indole NH is important for antibacterial activity, with N-substituted compounds, **2.12a** – **d**, exhibiting the lowest antibacterial activity in this class of compounds and against the antibiotic standards.[72] This class of bisindolyl cycloalkane indoles therefore presents an important library of lead compounds in antibacterial development. El Sayed *et al.* further optimised the reaction conditions to advance the development of bisindolyl cycloalkane indoles at room temperature using glacial acetic acid as a mild synthetic method.[73]

Choppara *et al.* developed another class of bis-indole analogues, with potent antibacterial activity.[74] These analogues were screened against *B. subtilis, K. pneumonia, P. auregenosa and E. coli.* Antibacterial activity of synthesised compounds was determined by measuring the zone where bacterial growth was inhibited, with reference to ciprofloxacin as a standard. Compounds **2.13a – f** and **2.14a – f** were active against the bacteria strains though inferior in activity compared to ciprofloxacin. Compound **2.13a** was more potent against *P. aeruginosa* whilst compound **2.13c** was found to be more potent against *E, coli*. [74]

As discovered by Tiwari *et al.*[71] and El Sayed *et al.*[72], Choppara *et al.* also observed a decrease in antibacterial activity with an *N*-substituent on compounds **2.14a – d** and **2.14f**.[74]

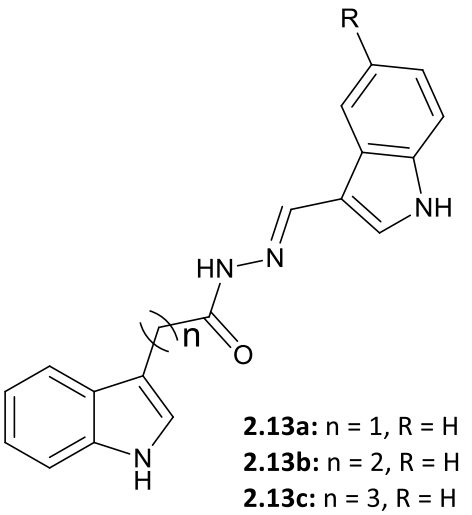

2.13a: n = 1, R = H
2.13b: n = 2, R = H
2.13c: n = 3, R = H
2.13d: n = 1, R = Br
2.13e: n = 2, R = Br
2.13f: n = 3, R = Br

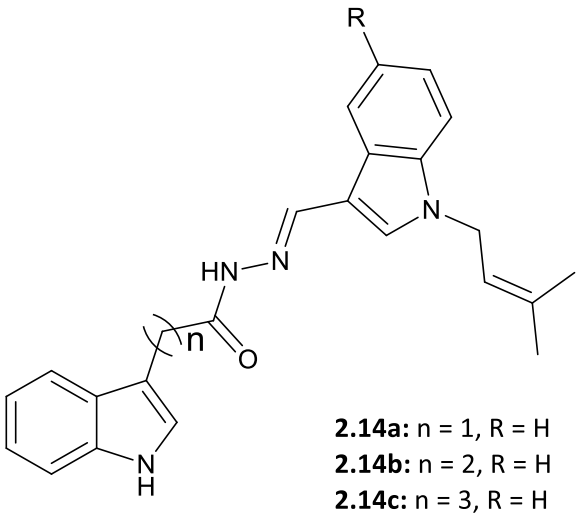

2.14a: n = 1, R = H
2.14b: n = 2, R = H
2.14c: n = 3, R = H
2.14d: n = 1, R = Br
2.14e: n = 2, R = Br
2.14f: n = 3, R = Br

Two new prenylated indole alkaloids (**2.15a** and **2.15b**) were isolated from the fungi *Aspergillus* sp., extracted from the gorgonian coral, *Dichotella gemmacea.*[75,76] Compounds were screened against gram-positive *Bacillus cereus*, *Micrococcus tetragenus*, *Staphylococcus epidermidis, S. aureus* and gram-negative *E. coli*, *Vibrio anguillarum*, *V. parahemolyticus, and Pseudomonas putida*.[76] There was little to no antibacterial activity exhibited by the prenylated compounds. However, another compound (**2.16c**) exhibited moderate antibacterial activity against *S. epidermis* with an MIC of 14.5 µM compared to 3.13 µM of the standard, ciprofloxacin.[75]

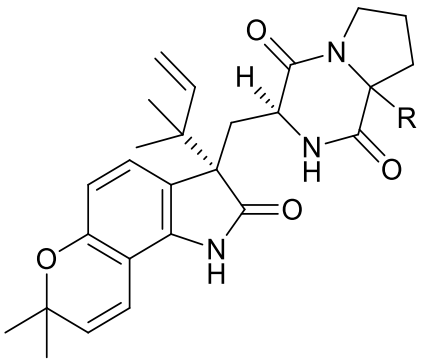

2.15a: R = β-OCH_3
2.15b: R = β-OH

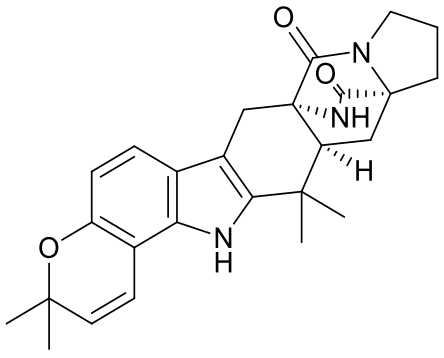

2.16c

2.3 Indoles as anti-inflammatory agents

The indole based indomethacin[77] (**2.17**) and tenidap[78] (**2.18**) are non-steroidal drugs that exhibit anti-inflammatory activity. Rani *et al.* synthesised a variety of chalcones, pyrazolines and azo compounds which were tested for anti-inflammatory activity on an oedemous rat's paw using indomethacin and phenylbutazone standards.[79] From the relatively more active class of compounds, compound **2.19b**, a pyrizoline was the most potent, inhibiting 47% of the oedema at 50 mg/kg with less ulcerative effects than phenylbutazone.[79]

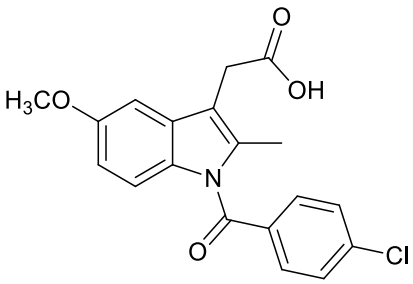

2.17 Indomethacin

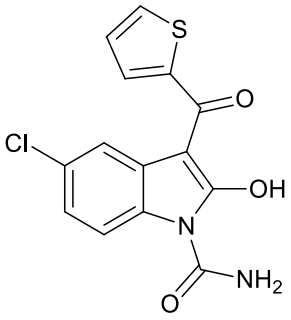

2.18 Tenidap

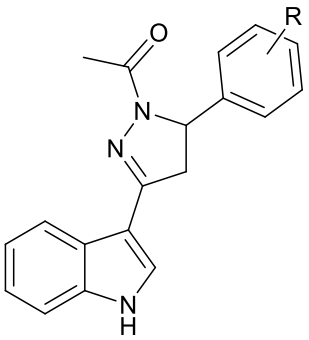

2.19a: R = *m*-OCH_3, *p*-OH
2.19b: R = *p*-OH
2.19c: R = H
2.19d: R = *p*-$N(CH_3)_2$
2.19e: R = *p*-OCH_3

2.4 Indoles as anti-cancer agents

Vinca alkaloids such as vincristine (**2.20**) and vinblastine (**2.21**) are indole based natural products, widely administered in adult and childhood cancer therapy.[80,81]

The alkaloids disrupt microtubules of the mitotic spindle apparatus from functioning, arresting the metaphase stage of cell division in both malignant and non-malignant cells.[80–82] Resistance to vinca alkaloids is due to the overexpression of membrane efflux proteins or multi-drug resistance associated proteins with additional cross-resistance from other bulky natural products of different function and structure.[83,84] Genetic mutations in the drug targeted tubulin structure also characterise this

resistance.[81–84] The emergence of resistance to widely used cancer treatment incites the need to formulate alternative strategies to retard resistance and develop novel cancer therapy.

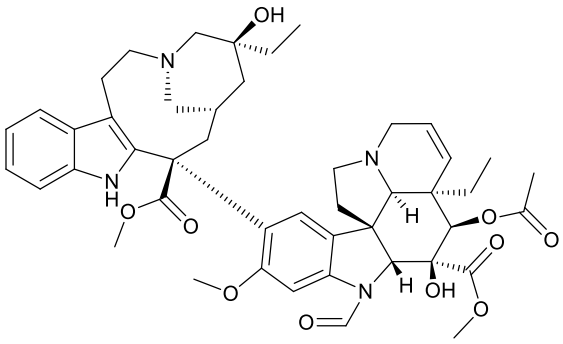

2.20 Vincristine

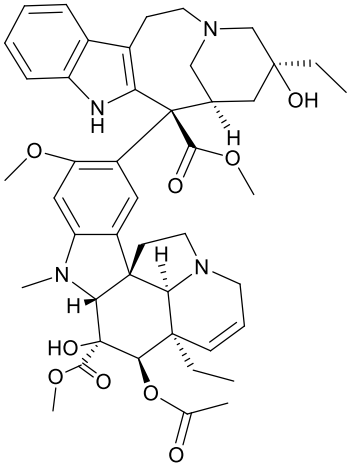

2.21 Vinblastine

Madadi *et al.* investigated (Z)-2-((1-benzyl-1*H*-indol-3-yl)methylene)-quinuclidin-3-one analogues as potential cannabinoid receptor ligands that would exert the desired therapeutic effects with reduced CNS side effects and addiction properties as seen with Δ^9-tetrahydrocannabinol (Δ^9-THC, **2.22**).[85] CB_1 and CB_2 are the two major G-coupled protein cannabinoid receptors found in mammals and have been found to be highly expressed in cancer cells.[85,86] CB_1 and CB_2 when stimulated, predominantly couple to G-inhibitory protein which inhibits the release of adenylyl cyclase.[86] Adenylyl cyclase is a 'secondary messenger' that stimulates the formation of cyclic monophosphate (cAMP) from ATP, cAMP subsequently binds to the protein kinases of that cell, stimulating or inhibiting essential metabolic pathways.[87] In this case, inhibition of adenylyl cyclase would initiate mitogen-activated protein kinase, inhibit some voltage gated calcium channels which decreases neurotransmitter release, and activate G-protein linked inwardly rectifying potassium channels which forces the cell membrane to remain at resting potential.[86] The induction of the cannabinoid receptors in animal cancer models has been found to induce apoptosis when ceramide, a 'secondary messenger' that activates ERK cascade (the

cascade mediates cell death, growth arrest or cell proliferation) is continuously released causing cell death, simultaneously inhibiting tumour growth and conferring neuron protection.[88]

In the study carried out, the non-classic cannabinoid analogues of Δ^9 THC, WIN 55212-2 (**2.23**), an aminoalkylindole, exhibited K_i (inhibitor constant) values of 1.9 nM and 0.3 nM for CB_1 and CB_2 receptors respectively. IPDN (**2.24**), an indolopyridone, had a greater affinity for CB_2 receptor than CB_1 with K_i values of 1.0 nM and 16 nM respectively.[85] Both compounds are potent cannabinoid ligands that inspired the synthesis of (Z)-2-((1-benzyl-1*H*-indol-3-yl)methylene)-quinuclidin-3-one analogues (**2.25a – g**). These analogues form a new class of compounds with **2.25b** and **2.25g** displaying a higher affinity for CB_2 receptor than CB_1, shown by K_i values of 1.33 nM and 2.50 nM respectively. **2.25g** also demonstrated strong receptor selectivity.[85]

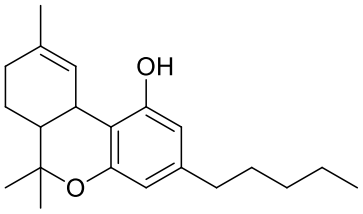

2.22 Δ^9 THC

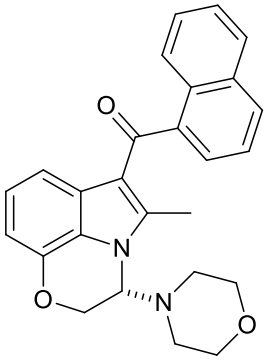

2.23 WIN 55212-2

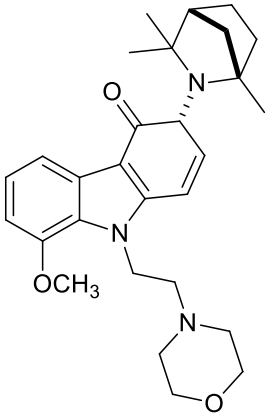

2.24 IPDN

Another study propelled by a bush willow isolate, combretastatin A4[89] (**2.26**), saw the synthesis of novel carbazole sulfonamide analogues containing an *N*-alkyl substituted indole motif linked to a 3,4,5-trimethoxyphenyl moiety via an unsubstituted sulphonamide bridge, components identified to be important for antiproliferative activity.[90] Compound **2.27** was found to be active against CEM leukaemia cells with an IC_{50} of 56 nM compared to 1.9 nM of **2.26**.[90] **2.27** was further tested against MCF-7 breast cancer cells, melanoma, Bel-7402 hepatoma, and PC-3 prostate cancer cells. The breast cancer cells were reported to have reduced in tumour volume by 75% after 35 days of initial administering of **2.27** while a 67% reduction in human hepatocarcinoma tumours was reported.[90]

From these *in vivo* tests, the improved activity of compound **2.27** to **2.26** was thought to be due to increased hydrophilicity, increasing *in vivo* absorption and therefore bioavailability.

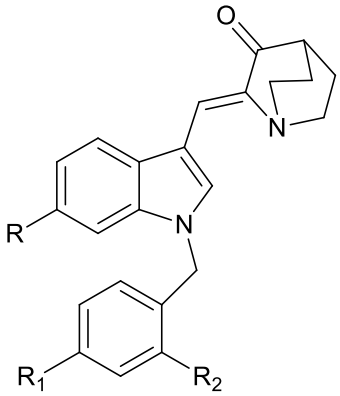

2.25a: R = R_1 = R_2 = H
2.25b: R = R_2 = H, R_1 = F
2.25c: R = R_2 = H, R_1 = Cl
2.25d: R = R_1 = H, R_2 = Br
2.25e: R = R_2 = H, R_1 = CN
2.25f: R = R_2 = H, R_1 = $COOCH_3$
2.25g: R_1 = R_2 = H, R = $COOCH_3$

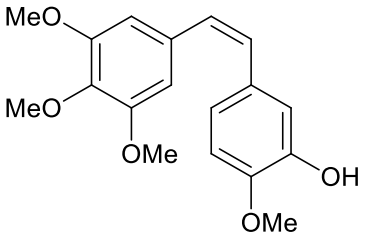

2.26 Combrestatin A4

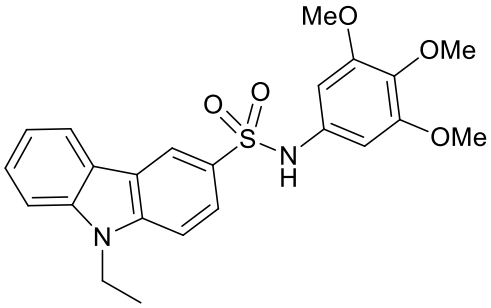

2.27

In further characterisation studies, lead compound **2.27** was observed to cause fragmentation of DNA, increased expression of tumour suppressing p53 protein while suppressing the Bcl-2 apoptosis inhibiting protein consequently causing apoptotic cell death.[90] The compound also blocked the metaphase stage of tumour cell division. With an LD_{50}>500 mg/kg and observed potency against tested cancer cell lines, **2.27** represents a novel class of anti-cancer agents.

On the other hand, 3,3'-diindolemethane (**2.28a**) presents a research opportunity into new, potent anticancer agents. In breast cancer cells, 3,3'-diindolemethane was seen to increase the expression of cyclin dependent kinase (CDK) inhibitor by stimulating mitochondrial reactive oxygen species.[91] CDK modifies various substrates in the stages of the cell cycle, propagating cell division.[92] Thus, inhibition of CDK arrests progression of cell division. Despite the potency of the drug in breast cancer cell lines,

low drug absorption impeded its use, inciting more bioavailable drug formulations to be developed successfully, resulting in their current clinical trials.[91,93,94] Of the synthesised 3,3'-diindolemethane derivatives, compounds **2.28b – d** were found more active against the melanoma cell lines ME18 and ME18/R with IC_{50} values for ME18/R ranging 17.0-17.4 µmol/ml compared to 40.7 µmol/ml of compound **2.28a**.[91]

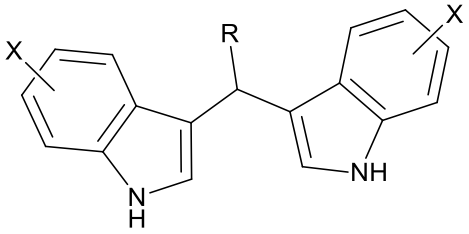

2.28a: X = H, R = H
2.28b: X = I, R = H
2.28c: X = Br, R = 4-methylphenyl
2.28d: X = H, R = 3,5-difluorophenyl

2.5 Indoles as anti-emetic agents

Currently on the market are indole based 5-HT_3 receptor antagonist drugs, ondansetron (**2.29**), alosetron (**2.30**) and tropisetron (**2.31**) used in the management of post chemotherapy and radiotherapy induced nausea and emesis.[69,95]

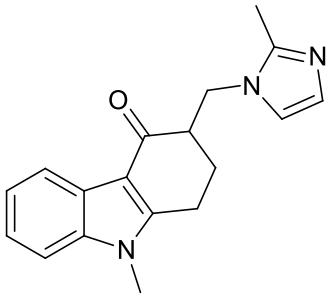

2.29 Ondansetron

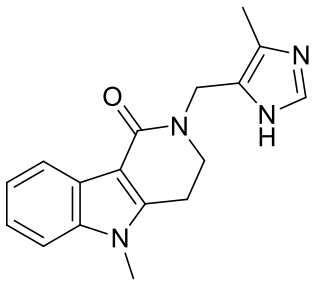

2.30 Alosetron

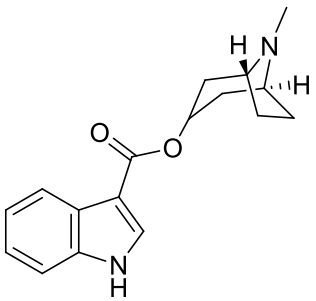

2.31 Tropisetron

Emesis is believed to be the result of the stimulation of 5-HT_3 receptors by the agonist serotonin released from enterochromaffin cells of intestinal membrane.[95] In the management of emesis, the 5-HT_3 receptor antagonists have been developed to possess a carbonyl group (involved in strong target binding) coplanar to an aromatic ring system and a basic motif (for target recognition), all occupying relative spatial positions.[96] The electronegative nitrogen of the indole nucleus has displayed important

electrostatic effects in the receptor region occupied, encouraging the anti-emetic activity of the indole based drugs.[96]

2.6 Indoles as anti-hypertensive agents

A number of indole based compounds have been found to exhibit anti-hypertensive activity and are presently used in the treatment of various heart related conditions.

Indapamide (**2.32**) is an indoline derivative of chlorosulfonamide used to treat heart failure and hypertension.[97] In hypertension, blood pressure is lowered by vasodilation of blood vessels, with marginal diuretic effects. Indapamide is therefore thought to lower blood pressure by inhibiting transmembrane calcium ion influx which depresses smooth muscle contractions and also by stimulating vasodilation via the modulator, prostaglandin PGE2.[97,98] Carvedilol (**2.33**) is a carbazole containing beta-blocker used to treat hypertension and congestive heart failure.[69] Mechanism of action is unknown but it is speculated that carvedilol exerts its function by reducing heart rate or regulating activity of systemic neuro-hormones.[99] Pindolol (**2.34**) is a selective beta blocker also used for hypertension, angina pectoris, arrhythmia, acute stress and depression.[69,100,101]

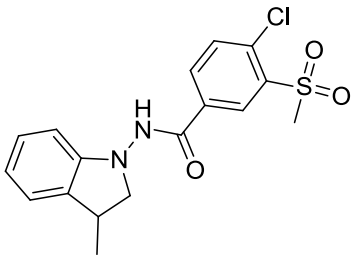

2.32 Indapamide

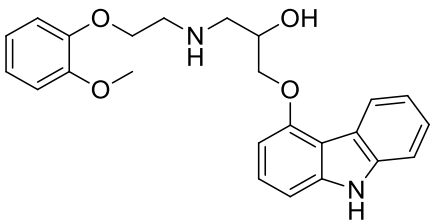

2.33 Carvedilol

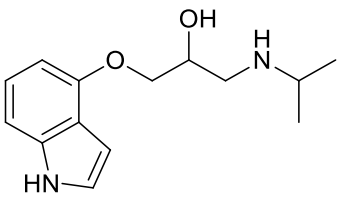

2.34 Pindolol

2.7 Indoles as anti-malarial agents

Natural extracts from plant species are still affording important biologically active isolates, including antimalarial agents. Some *Aspidosperma* species used in traditional treatment of malaria and fever were found to contain various indole alkaloids, extracts of which were tested against *Plasmodium*

falciparum 3D7 (chloroquine sensitive), W2 (chloroquine resistant) and K1 (multidrug resistant).[102] Of the known *Aspidosperma* species, de Paula *et al.* reported that 20 extracts and isolates were assayed and observed to exhibit antimalarial activity. Uleine (**2.35**) and ellipticine (**2.36**) were found to be the most active isolates *in vitro* and *in vivo* respectively, with ellipticine completely suppressing *Plasmodium* parasite growth. Uleine was reported to be non-toxic against tumour cells while, ellipticine was found to be cytotoxic.[102]

Dolabela *et al,* using *Aspidosperma pervifolium* species, tested uleine and its alkaloid ethanol extract against *P. falciparum* W2 and 3D7 strains. A highly selective *in vitro* antimalarial activity of uleine against W2 comparable to that of the ethanol extract was shown, establishing that uleine was the major alkaloid exhibiting antimalarial activity in the extract.[103] Chong and Sullivan Jr. conducted mechanism of action studies on ellipticine thought to be an inhibitor of haeme crystallisation to form the non-toxic haemozoin. In their study, ellipticine exhibited good results with an IC_{50} of 7.9 µM compared to 4.3 µM of chloroquine in inhibiting haeme crystal growth.[104] Ellipticine was therefore thought to act by substrate sequestration or surface binding.[104,105]

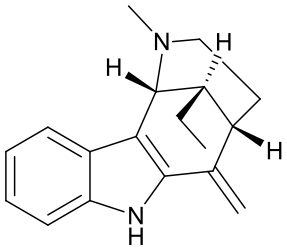

2.35 Uleine

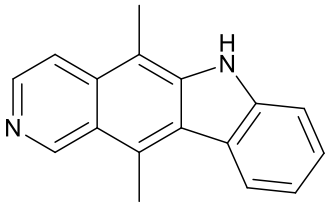

2.36 Ellipticine

A comparative study of ellipticine, its isomer olivacine (**2.37**), along with cryptolepine triflate (**2.38**) and its analogue (**2.39**) was conducted by Rocha e Silva *et al.* The study confirmed previously reported ellipticine *in vitro* activity against *P. falciparum* 3D7 and K1 with IC_{50} values of 0.35 µM and 0.81 µM respectively compared to the 0.058 µM and 0.13 µM values of chloroquine diphosphate. The isomer, olivacine was the least active while the cryptopeline triflate analogue (11-(4-piperidinamino) cryptolepine hydrogen dichloride) had the highest reported activity of 0.087 µM and 0.10 µM against

3D7 and K1 strains respectively. Acute toxicity was observed with cryptopeline triflate analogue and additionally, administration of a 2nd subcutaneous dose of 50 mg/kg/day to infected mice caused lethal toxicity. This toxicity impedes the use of cryptolepine derivatives as treatment drugs.[105] Further research in curbing this toxicity is required.

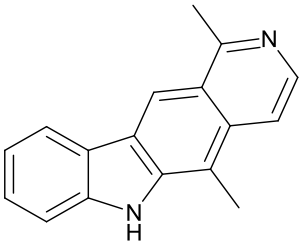

2.37 Olivacine

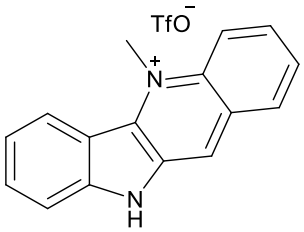

2.38 Cryptolepine triflate

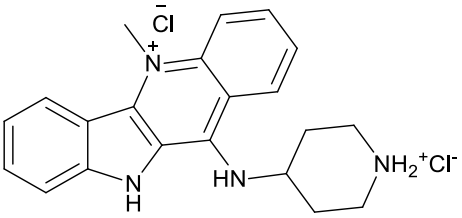

2.39 Cryptolepine hydrogen dichloride

Ashok *et al.* reviewed manzamine alkaloids, a novel class of indole containing compounds with antimalarial activity.[106] The manzamines are naturally occurring *ß*-carbolines compounds isolated from sponges, manzamine A (**2.40**) from *Haliclona sp.*[107]*,* manzamine B, E and ircinal A from *Acanthostrongylophora sp.*[108] Initially found to be active against cancer, manzamine A was seen to also exhibit *in vitro* antimalarial activity against *P. falciparum* chloroquine sensitive (D6) and chloroquine resistant (W2) strains with IC_{50} values of 4.5 ng/ml and 8.0 ng/ml respectively. The chloroquine standard exhibited IC_{50} values of 15.5 ng/ml and 170 ng/ml against the same strains.[108] In the 1990's, 8-hydroxymanzamine-A (**2.41**) was isolated from the sponge of *Pachypellina sp.*[109] whilst the N-oxides of manzamine A (**2.42**), manzamine J and 3,4-dihydromanzamine A were isolated from *Xestospongia ashmorica.* When screened against the D6 and W2 strains, the respective IC_{50} values of 6.0 ng/ml and 8.0 ng/ml were attained for 8-hydroxymanzamine-A[108] and 11.0 ng/ml and 13.0 ng/ml for manzamine A N-oxide.[106] Despite the potency of the outlined compounds, Ashok *et al.* further highlighted the cytotoxic nature of manzamines being the major drawback limiting their use. The comprehensive SAR study of manzamines offers a working reference for structural functionalisation to develop potent non-toxic derivatives.[106]

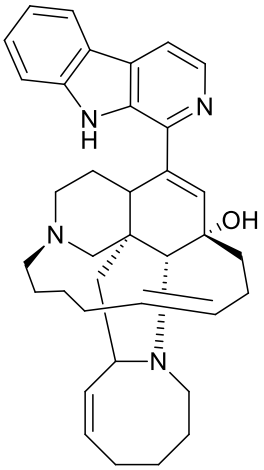

2.40 Manzamine A

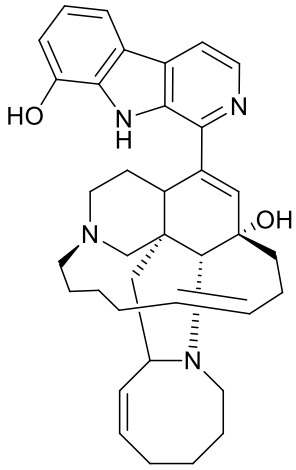

2.41 8-Hydroxymanzamine A

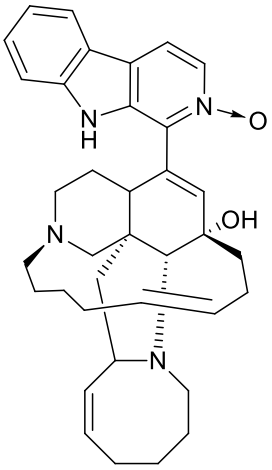

2.42 Manzamine A N-oxide

Urgaonkar *et al.* went on to investigate 2-amino-5-chloro-3-hydroxy-3-phenylindole (**2.43a**) which showed good *in vivo* activity against *Plasmodium berghei* infected mice without notable adverse effects. This motioned the synthesis of 2-amino-3-hydroxyindoles from isatin (**2.44**). The compounds were screened against *P. falciparum* 3D7 and Dd2 (multi-resistant) strains. The racemic mixture of 2-amino-5-chloro-3-hydroxy-3-phenylindole displayed superior activity to individual enantiomers with EC_{50} values of 207 nM against 3D7 and 507 nM against Dd2. Chloroquine was used as a standard with EC_{50} values of 16 nM and 216 nM against 3D7 and Dd2 respectively. Compounds **2.43b** and **2.43c** from the series were the most potent antimalarial agents, exhibiting activity superior to that of chloroquine with respective EC_{50} values of 24 nM and 30 nM against 3D7 strain, 57 nM and 37 nM against Dd2 strain. Compounds **2.43d** and **2.43e** were more active against the Dd2 strain compared to chloroquine with EC_{50} values of 139 nM and 152 nM respectively. Having established a reproducible synthesis of 2-amino-3-hydroxyindoles, this novel class of compounds could be modified, further describing the compound profile.[110]

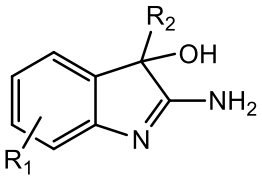

2.43a: R_1 = 5-Cl, R_2 = Ph
2.43b: R_1 = 5-Cl, R_2 = *o*-OMePh
2.43c: R_1 = 5-Cl, R_2 = 1-naphthyl
2.43d: R_1 = 5-Cl, R_2 = CH_2-(*o*-tolyl)
2.43e: R_1 = H, R_2 = *o*-tolyl

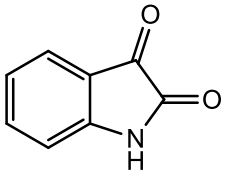

2.44: Isatin

Melatonin (**2.3**) has been observed to affect the development process of *P. falciparum* parasite. Alves *et al.* identified melatonin as an activator of inositol triphosphate (IP_3) dependent Ca^{2+} pumps by triggering IP_3 release.[111] Farias *et al.* further found that cysteine-proteases activated by Ca^{2+} in the parasite were important in haemoglobin degradation and merozoite release, processes that propagate parasite infection.[112] On this basis Schuck *et al.* synthesised a series of melatonin derivatives to inhibit this melatonin dependent pathway, disrupting parasite replication and development processes. Compounds **2.45a** and **2.45b** blocked melatonin effect while compounds **2.45c** – **e**, in addition, modulated the *P. falciparum* cycle exhibiting IC_{50} values ranging from 2.93 µM – 19.17 µM. These observations present a potential class of compounds that can be elaborated to increase antimalarial activity.[113]

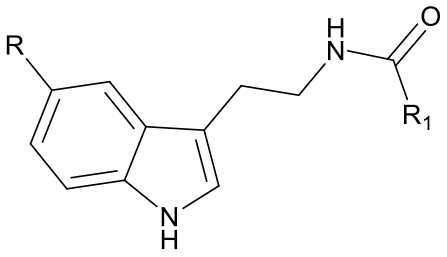

2.3: R = OMe, R_1 = Me
2.45a: R = H, R_1 = Me
2.45b: R = H, R_1 = $(CH_2)_4CH_3$
2.45c: R = OMe, R_1 = $(CH_2)_2CH_3$
2.45d: R = OMe, R_1 = $(CH_2)_4CH_3$
2.45e: R = OMe, R_1 = Ph

2.8 Rationale of project

The indole scaffold as discussed, presents a naturally occurring privileged structure allowing multi functionalisation of the nucleus to yield biologically active derivatives and synthetic compounds that bind to multiple targets of clinical importance in diseased conditions.

Accordingly, a study conducted in our lab has seen the synthesis of a novel class of indolyl-3-ethanone-α-thioethers exhibiting antimalarial activity with no significant toxicity to HeLa cells. Compounds **2.46** and **2.47** of the series were found active against the CQ-sensitive *P. falciparum* 3D7 strain in nanomolar concentrations of 0.24 µM and 0.09 µM respectively. It was hypothesised that the activity of this class was linked to the presence of a para-substituted α-thiophenyl ring. The nature of the para-substituent was also shown to affect activity, with the nitro substituted α-thiophenyl ring in **2.46** exhibiting the highest activity. Substitution on C-5 also lead to a further increase in antimalarial activity of **2.47**.[114,115]

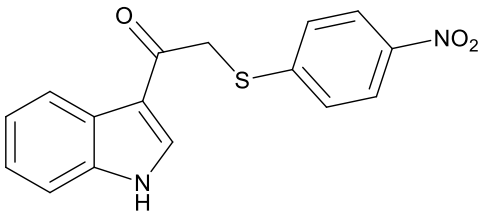

2.46

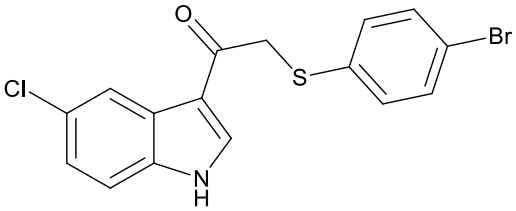

2.47

Our interest was to further expand this novel class of compounds, synthesising variably functionalised compounds in order to characterise the pharmacophore of these potent antimalarial agents simultaneously increasing our understanding of the properties of the compound's unknown target site. We proposed to structurally modify the scaffold are as outlined in **Fig 2.2.**

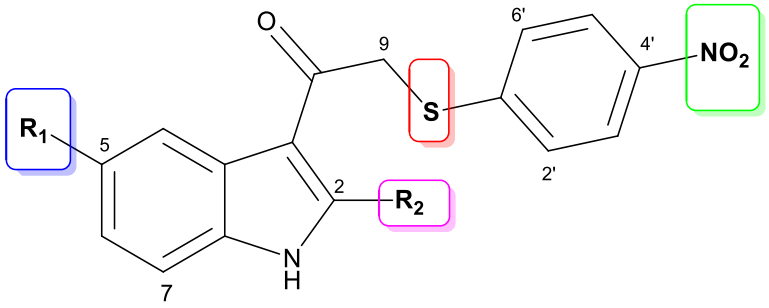

Fig 2.2 Proposed modifications to the indolyl-3-ethanone-α-thioether.

With the information gleaned from prior studies conducted in our lab, we sought to investigate the nature of activity enhancing C-5 substituents and further identify the possible interactions formed between the substituent and the target site and effect on antimalarial activity. We wanted to specifically compare the properties of the electronegative 5-chloro substituent with a nitrile substituent as its bioisostere along with the hydrophobic electron donating methyl and methoxy groups. We also wanted to investigate the effect on antimalarial activity of a C-2 substituent, predicting possible restriction of the rotation of C-3 substituent. Furthermore, we wanted to determine which α-thiophenol ring confers superior antimalarial activity between *p*-NO_2 and *p*-Br substituted rings.

Chapter 3: Synthesis of indolyl-3-ethanone-α-thioethers

Based on the research previously conducted in our lab,[114] we will proceed in this chapter, to discuss the synthetic procedures employed to generate desired analogues of indolyl-3-ethanone-α-thioethers, their characterisation and biological assay.

3.1 Outline of reaction pathway

To develop these compounds, we used the synthetic pathway derived in the investigations conducted by Svogie.[115] **Scheme 3.1** outlines the general three step synthetic route proposed for this project. We sought to utilise substituted analogues of **3.1** in the Friedel-Crafts acetylation method adapted in our lab[114,116], to yield the 3-acetylindole, **3.2** which in turn would undergo selective bromination affording the α-brominated ketone, **3.3**. The final step to yield the desired indolyl-3-ethanone-α-thioether, **3.4**, would be a coupling reaction involving the nucleophilic displacement of a α-brominated intermediate **3.3** with a thiophenol or phenol.

We wanted to explore the properties of the indole C-5 position by introducing varying substituents including the electron withdrawing nitrile group, the electron donating methyl and methoxy groups as comparisons to chlorine. Also of interest was the effect of a C-2 methyl substituent and the contrast between *p*-bromo and *p*-nitrothiophenol moieties.

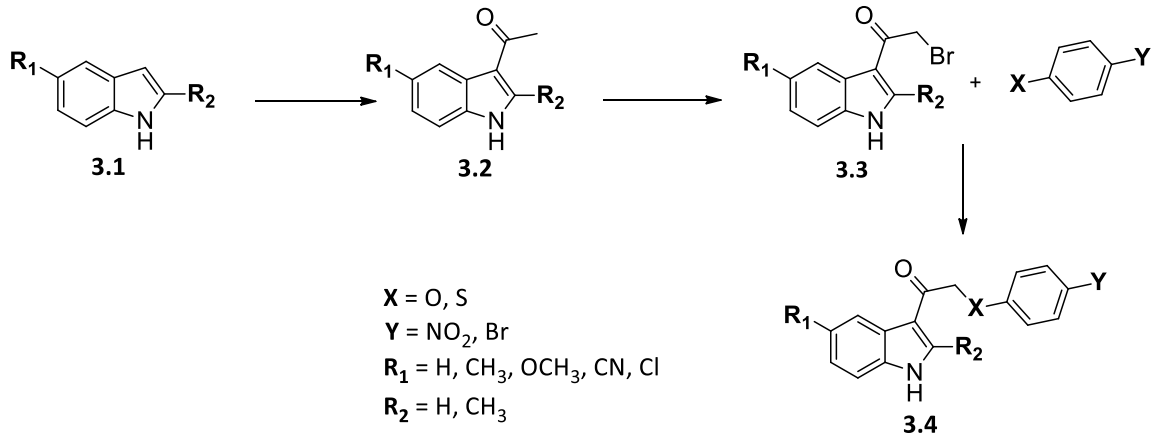

Scheme 3.1 General reaction pathway to synthesise indolyl-3-ethanone-α-thioethers.

3.2 Results and discussion

3.2.1 Synthesis of 1*H*-indole-5-carbonitrile (3.5)

The SAR trends noted in the study of Svogie *et al.*[114] found that a 5-chloro substituent was important for biological activity. As part of this study, we wanted to unravel whether the important contribution toward activity came from the chlorine's electronegativity or its lipophilicity. The nitrile moiety is also a very electronegative moiety[117], which we felt would be an appropriate bioisosteric replacement for chlorine. Furthermore, the nitrile is less lipophilic than the chlorine, which is an important element of consideration in our SAR. We initially employed the patented method **a**[118] in **Scheme 3.2** for its simplicity and use of reagents that were readily available in our lab. This method utilises CuCN as a source of nucleophilic nitrile anions that displace the bromine at the C-5 position. The reaction attempt was repeatedly unsuccessful with TLC and NMR data confirming presence of unreacted starting material in crude product mixture.

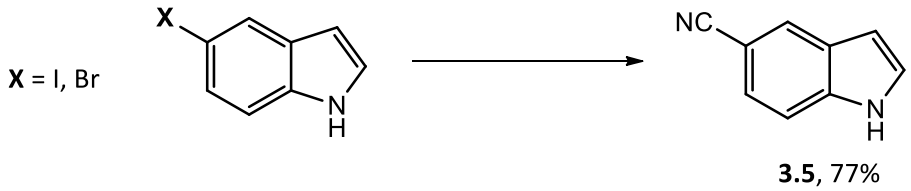

Scheme 3.2 Synthesis of 1*H*-indole-5-carbonitrile.

a) CuCN, *N,N*-dimethylformamide, Ammonia, 85 ^{o}C, 24 h
b) $Pd(OAc)_2$, PPh_3, Formamide, $POCl_3$, 140 ^{o}C, 48 h, N_2
c) CuI, PPh_3, Formamide, $POCl_3$, 140 ^{o}C, 24 h, N_2
d) CuI, CuCN, *N,N*-dimethylformamide, PPh_3, 140 ^{o}C, 24 h, N_2

We then attempted method **b** (**Scheme 3.2**) developed by Sawant *et al.* that utilises a $Pd(OAc)_2$ Triphenylphosphine (PPh_3) catalytic system and generates CN^- ions *in situ* via $POCl_3$ mediated dehydration of formamide.[119] Both 5-bromoindole and 5-iodondole were utilised as starting materials, however, both reaction attempts were unsuccessful, possibly due to the PPh_3 ligand we employed. Xantphos was used as the ligand in the original method and studies have revealed that ligand nature greatly influences catalyst effectiveness.[120–122] We went on to use the copper catalysed method by

Khemnar and Bhanage (**c** in **Scheme 3.2**).[123] Still generating the CN^- ions *in situ*, the method was again unsuccessful with 5-bromo and 5-iodoindole. We then adapted the method by Khemnar and Bhanage; our reasoning was to provide a ready source of nitrile anions (**d** in **Scheme 3.2**). Carried out under a nitrogenous atmosphere using anhydrous reagents, the reaction was reproducibly successful, at a 77% yield.

*3.2.1.1 Characterisation of compound **3.5***

The successful cyanation of 5-iodoindole was confirmed using NMR analysis. The ^{1}H-NMR spectrum showed a shift in chemical environment of compound **3.5** compared to that of 5-iodoindole (**Fig 3.1a**). ^{13}C-NMR spectrum was more definitive, with a new carbon signal characteristic of a nitrile carbon observed at 120.8 ppm (**Fig 3.1b**). 2D analysis confirmed the nitrile positioning at C-5 comparable to published analyses.[124]

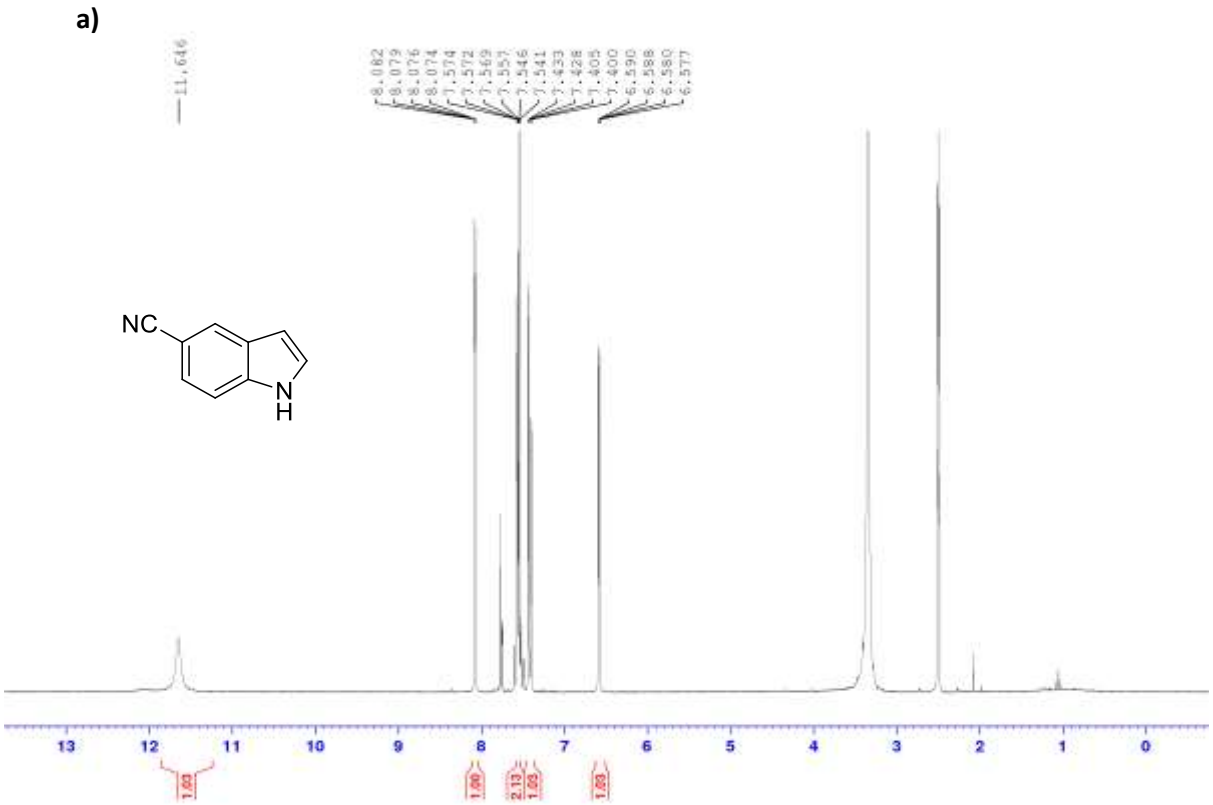

Fig 3.1a ^{1}H-NMR spectrum of **3.5**.

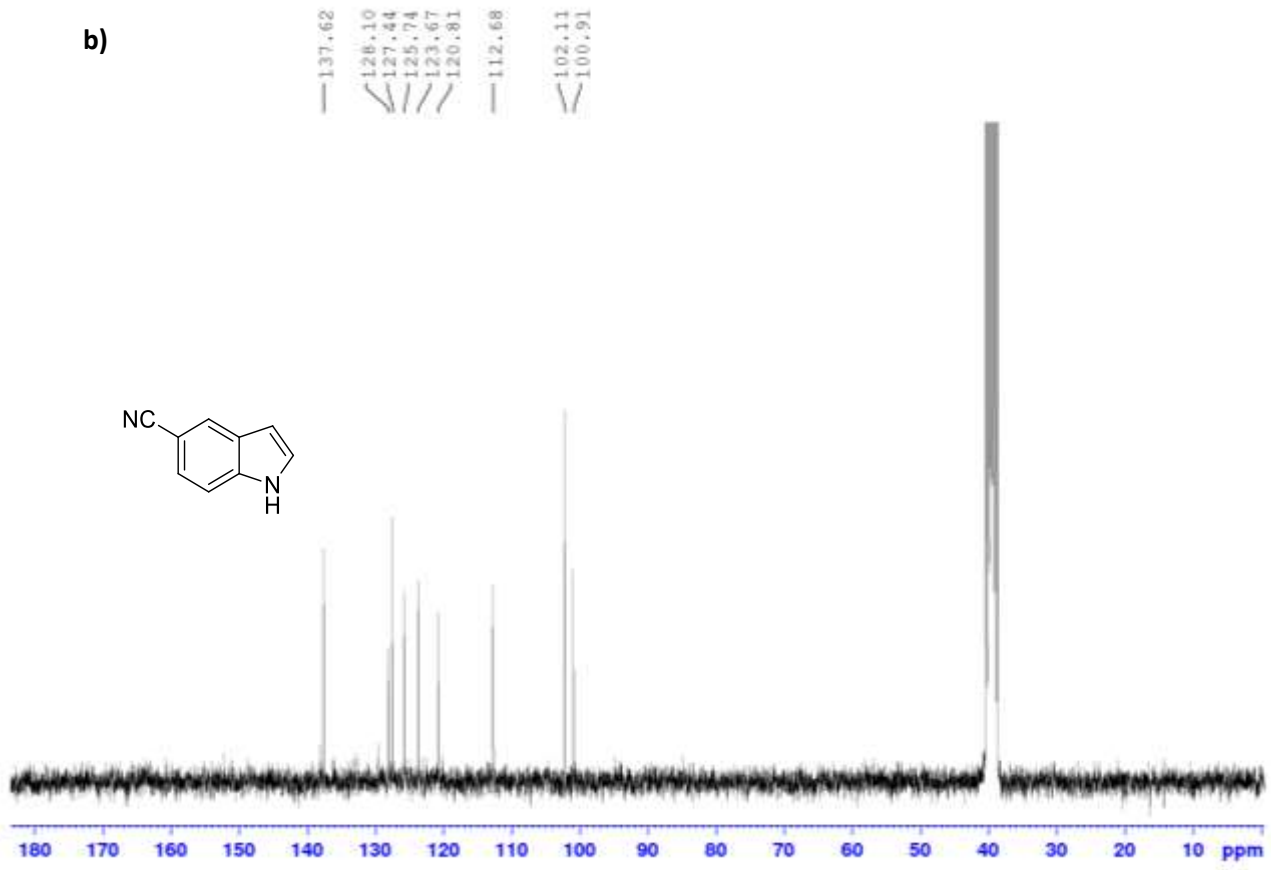

Fig 3.1b ^{13}C-NMR spectrum of **3.5**.

3.2.2 Suzuki-Miyaura cross-coupling reaction (3.6 – 3.7)

In our desire to further explore the nature of an optimal C-5 substituent, we attempted the synthesis of 5-methyl (**3.6**) and 5-phenyl (**3.7**) indole analogues. We anticipated that a Suzuki-Miyaura cross-coupling[125] between commercially available 5-indolylboronic acid with an appropriate organohalide would be appropriate to introduce the methyl and phenyl substituents (**Scheme 3.3**).

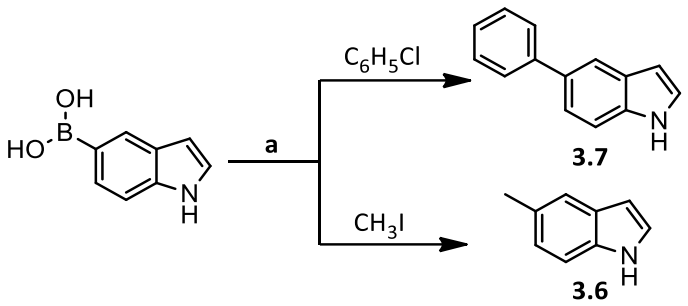

Scheme 3.3 Suzuki cross coupling of 5-indolylboronic acid and organohalides.

a) 10 wt% Pd/C, Na_2CO_3, Acetone:Water (3:1), 60 ^oC, 36 h

The reactions were allowed to proceed for 36 h owing to the reported slow conversion rate in aqueous conditions. However, the reactions were unsuccessful, yielding a mixture of compounds that could not be separated and purified. Fortunately, 5-methylindole was commercially available from Sigma-Aldrich allowing us to continue with the synthesis of the desired compound. Unfortunately, we could not obtain compound **3.7**.

3.2.3 Synthesis of 3-acetyindoles (3.8 – 3.12)

As depicted in **Scheme 3.4** we employed the adapted Friedel-Crafts acetylation method (**a**) by Veale *et al.*[116] stemming from the regioselective method described by Ottoni *et al.*[126] The method utilises $SnCl_4$ to catalyse the electrophilic attack of the indole on acetyl chloride. All reactions were allowed to proceed for 4 h under an inert nitrogenous atmosphere. Overall yields were low. Indoles featuring electron withdrawing groups e.g. 5-bromine (**3.9**) 5-chlorine (**3.10**) and 5-nitrile (**3.8**) exhibited the highest yields, while the electron donating 5-methyl substituted analogues (**3.11** and **3.12**) had the lowest yields, possibly due to their influence on the electron distribution of the indole.

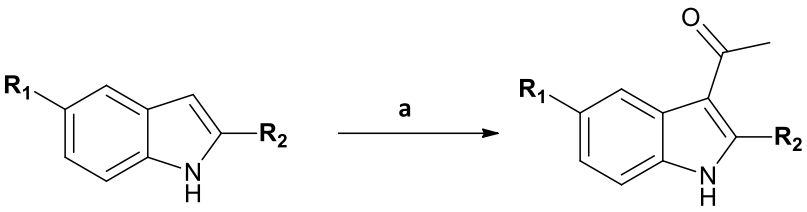

R_1 = H, Br, CN, Cl, CH_3
R_2 = H, CH_3

3.8: R_1 = CN, R_2 = H, 46%
3.9: R_1 = Br, R_2 = H, 69%
3.10: R_1 = Cl, R_2 = H, 45%
3.11: R_1 = CH_3, R_2 = H, 19%
3.12: R_1 = H, R_2 = CH_3, 30%

Scheme 3.4 Synthesis of substituted 3-acetyindoles.

a) $SnCl_4$, Acetyl chloride, Nitromethane, CH_2Cl_2, 4 h, 0 ^oC - rt, N_2

*3.2.3.1 Characterisation of compounds **3.8** – **3.12***

The successful synthesis of acetylated indoles was confirmed using NMR analysis. In the ^{1}H-NMR spectrum of **3.8** we observed a signal at 2.48 ppm integrating for three protons, characteristic of a methyl group (**Fig 3.2a**). In the ^{13}C-NMR spectrum we observed the carbonyl signal at 192.9 ppm and further, with 2D analysis we correlated via HSQC, the ^{13}C signal at 27.3 ppm to the ^{1}H signal at 2.48 ppm and using HMBC ascertained the acetylation to have occurred at C-3 (**Fig 3.2b**). Similar characteristics were observed with signals on the NMR spectra of compounds **3.9** – **3.12**. The results obtained were comparable to published analyses of **3.9**.[116]

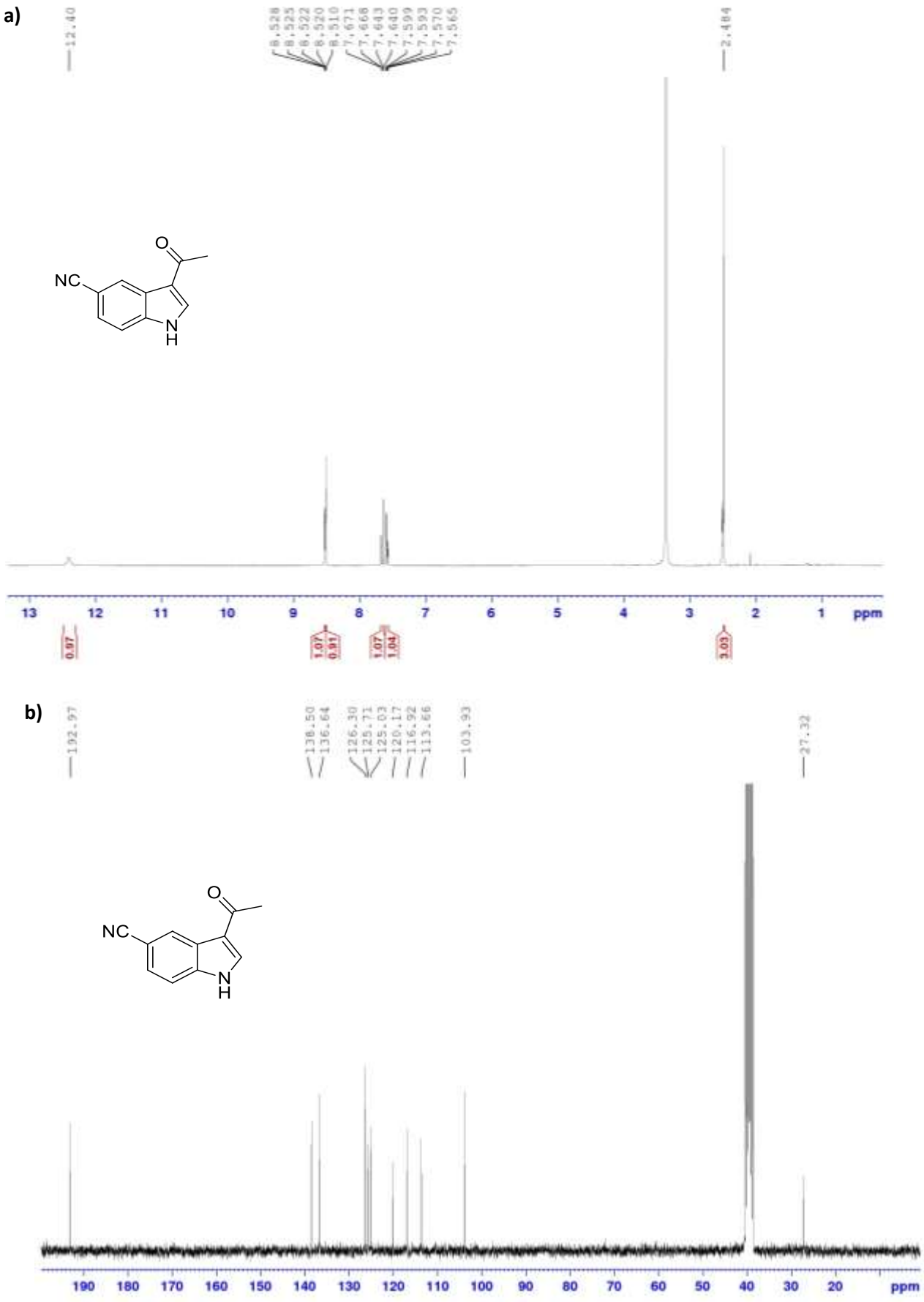

Fig 3.2 a) ^{1}H-NMR and b) ^{13}C-NMR spectra of **3.8**.

3.2.4 Synthesis of 1-(5-methoxy-1*H*-indol-3-yl)ethanone (**3.13**)

To further explore the parameters of the C-5 substituent, we wanted to introduce a hydrophobic methoxy residue, which in contrast to chlorine, is an electron donating substituent. Xu and Fan outlined a copper catalysed synthesis of 5-methoxyindole from 5-bromoindole using sodium methoxide as the source of $^{-}OCH_3$ ions for the nucleophilic displacement of the bromide.[127]

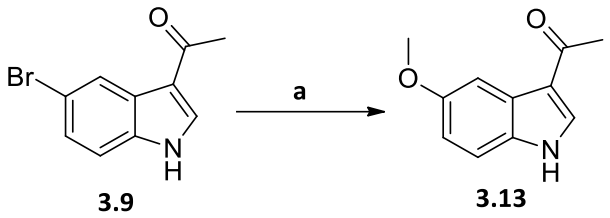

3.9 **3.13**

Scheme 3.5 Synthesis of 1-(5-methoxy-1*H*-indol-3-yl)ethanone from 1-(5-bromo-1*H*-indol-3-yl)ethanone.

a) CuI, NaOMe, *N,N*-dimethylformamide, 6 h, reflux, N_2

Due to the low yields observed in the Friedel-Crafts acetylation to form **3.11**, we decided to use the acetylated **3.9** as the substrate for this reaction (**Scheme 3.5**). While successful, we obtained the desired product at a low yield of 20%.

*3.2.4.1 Characterisation of compound **3.13***

The successful synthesis of **3.13** was confirmed by NMR. A new signal at 3.83 ppm integrating for three protons was observed on the ^{1}H-NMR spectrum, characteristic of a methoxy group (**Fig 3.3a**). Analysing the ^{13}C-NMR spectrum, we observed a signal at 54.6 ppm characteristic of the methoxy carbon (**Fig 3.3b**). These observations were confirmed by 2D analysis.

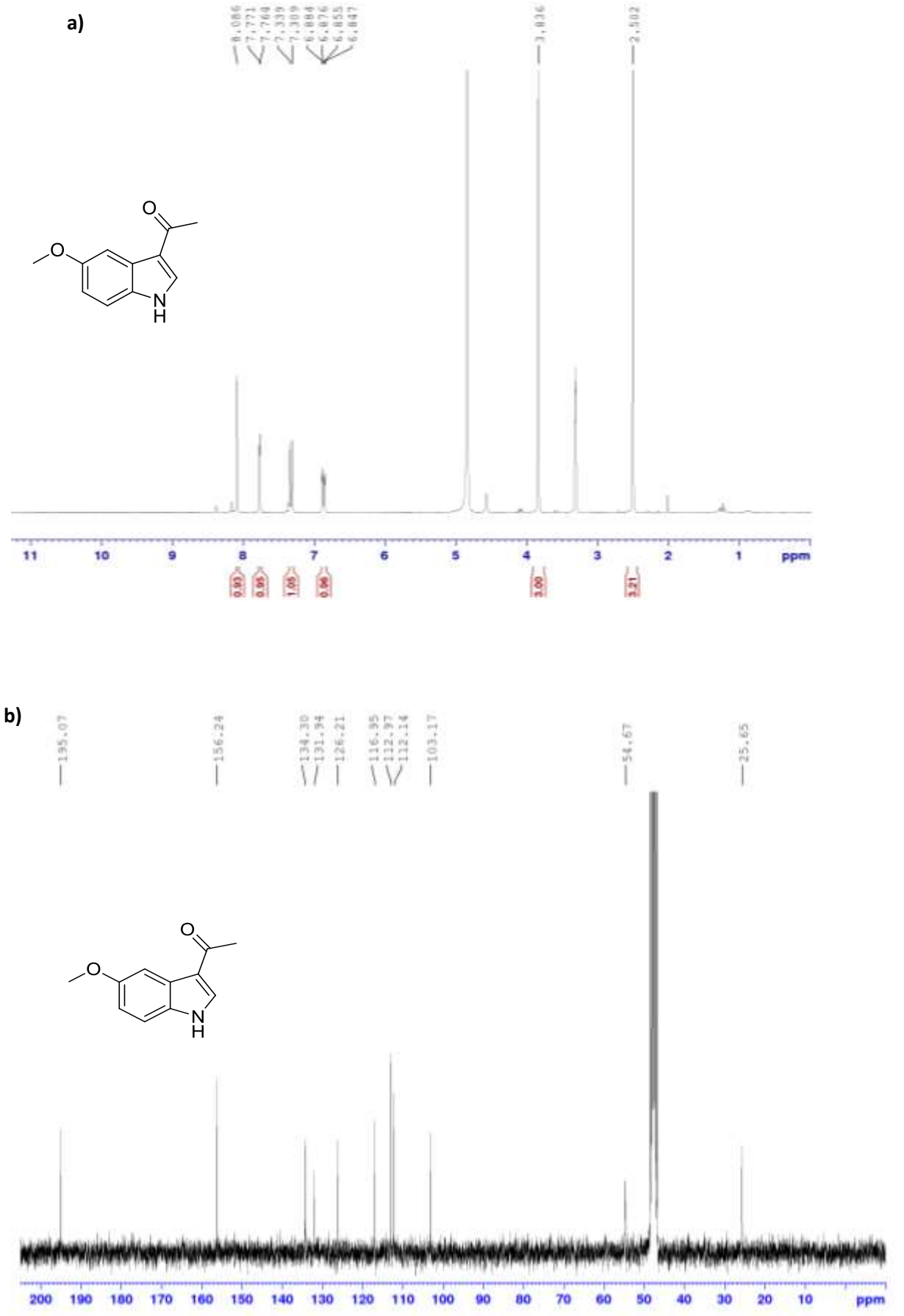

Fig 3.3 a) ^{1}H-NMR and b) ^{13}C-NMR spectra of **3.13**.

3.2.5 Synthesis of α-brominated 3-acetylindoles (3.15 – 3.20)

Having synthesised 3-acetylindoles, we employed the bromination method adapted by Veale *et al.* using $CuBr_2$ as the brominating agent, ethyl acetate and chloroform as solvent to attain α-mono brominated intermediates (**Scheme 3.6**).[128] Chloroform was reported to inhibit a second bromination occurring. Generally, di-bromination was reported to occur when starting material and mono-brominated intermediate levels were almost equivalent.[128] We therefore monitored reaction progress by TLC, stopping the reaction when di-bromination was observed. The reaction times varied considerably depending on the nature of the 3-acetylindole, from 30 min to an excess of 6 h, which was seemingly idiosyncratic to the starting materials.

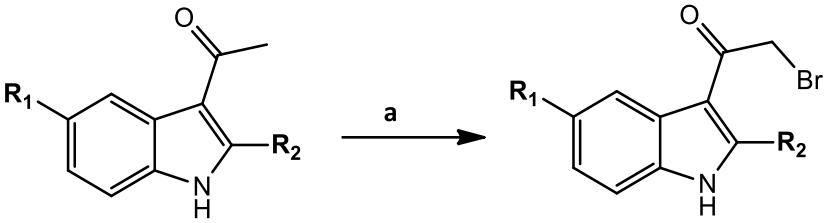

3.8: R_1 = CN, R_2 = H
3.10: R_1 = Cl, R_2 = H
3.11: R_1 = CH_3, R_2 = H
3.12: R_1 = H, R_2 = CH_3
3.13: R_1 = OCH_3, R_2 = H
3.14: R_1 = H, R_2 = H

3.15: R_1 = CN, R_2 = H
3.16: R_1 = Cl, R_2 = H, 30%
3.17: R_1 = CH_3, R_2 = H, 19%
3.18: R_1 = H, R_2 = CH_3, 44%
3.19: R_1 = OCH_3, R_2 = H, 37%
3.20: R_1 = H, R_2 = H, 17%

Scheme 3.6 Synthesis of α-brominated 3-acetylindoles.

a) $CuBr_2$, $CHCl_3$, EtOAc, 6 h, 75 ^oC

Purification of compound **3.15** via column chromatography was not successful, co-elution of the mono-brominated intermediate and reaction substrate **3.8** was observed repeatedly (TLC plate showed two distinct spots with significantly different retention factors - RF). We therefore resolved to proceed with **3.15** as an impure mixture which, as a consequence, hampered the accurate calculation of product yields in subsequent reactions. Generally, reaction yields for compounds **3.16** – **3.20** were quite low in accordance with the literature.[128] However, quenching of the reaction prior to the

formation of the undesired di-brominated product, meant that unreacted 3-acetylindole could be recovered and re-reacted to generate more α-bromoketone.

*3.2.5.1 Characterisation of compounds **3.15** – **3.20***

The successful bromination of compounds **3.15** – **3.20** was confirmed by NMR analysis. For example, the methyl signal at 2.50 ppm belonging to the 3-acetyl group initially observed in compound **3.13** was no longer present. Instead, we observed a new signal at 4.51 ppm of the ^{1}H-NMR spectrum of the corresponding compound **3.19**, integrating for two protons, and characteristic of a methylene group (**Fig 3.4**). Compounds **3.15** – **3.20** showed this characteristic exchange of the methyl signal for a new methylene signal. **3.16** and **3.20** were comparable to literature.[115] We then proceeded to the final step of synthesis using the α-brominated compounds.

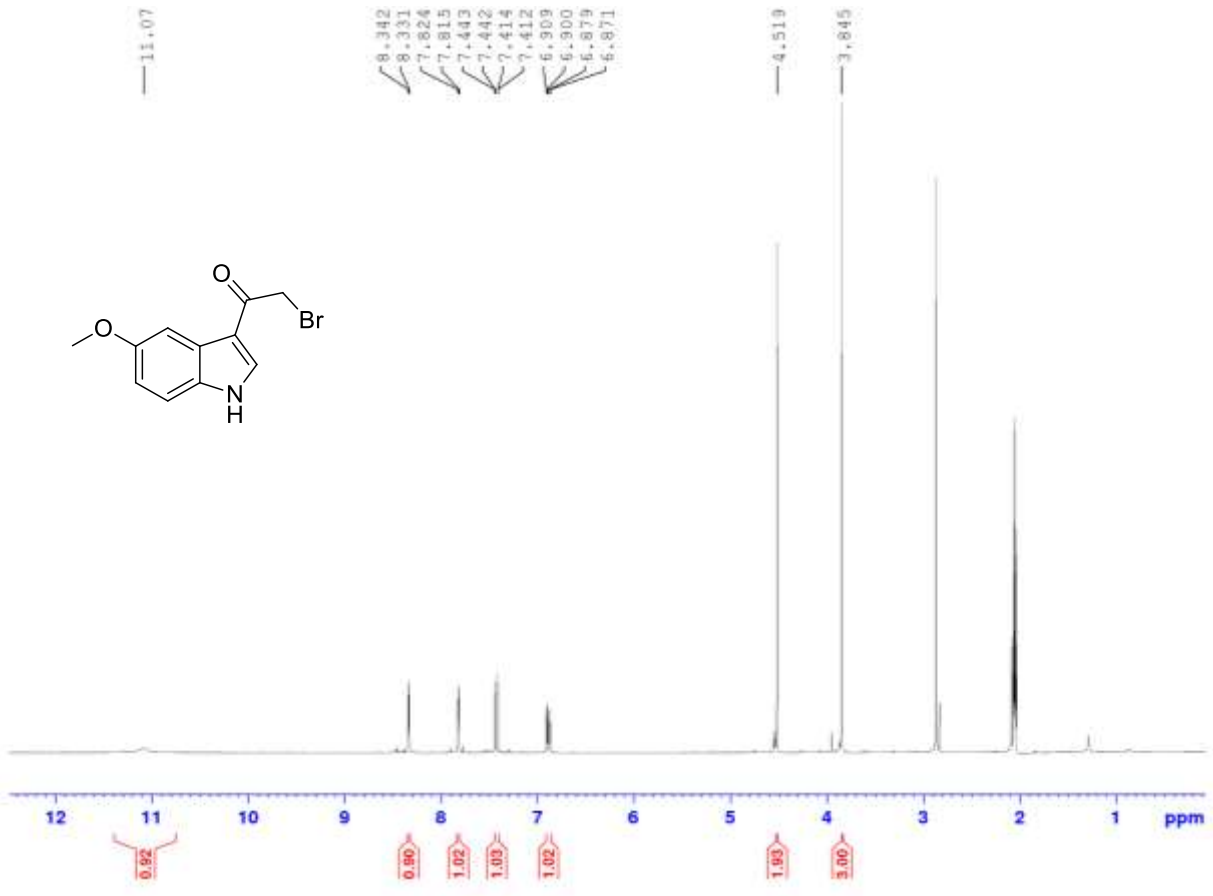

Fig 3.4 ^{1}H-NMR spectrum of **3.19**.

3.2.6 Synthesis of indolyl-3-ethanone-α-thioethers

The final step of this synthetic procedure was the synthesis of indolyl-3-ethanone-α-thioethers, we therefore employed the coupling reaction previously used in our lab to access the desired final products (**Scheme 3.7**). Based on syntheses by He e*t al.*[129] and Black *et al.*[130], the polar aprotic acetone was used as the reaction solvent in the presence of K_2CO_3 as a base to facilitate the nucleophilic displacement of α-bromoketone with a relevant nucleophile.

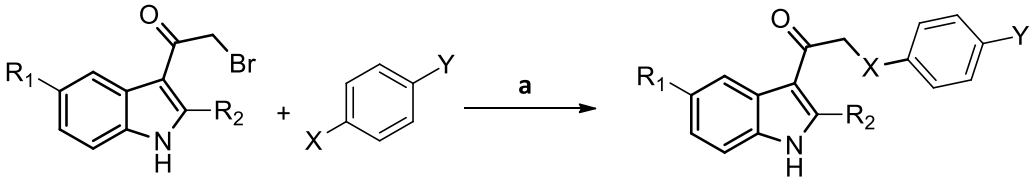

R_1 = CN, Cl, OCH_3, CH_3 X = S, O

R_2 = H, CH_3 Y = Br, NO_2

Scheme 3.7 General synthesis of indolyl-3-ethanone-α-thioethers.

a) K_2CO_3, Acetone, 5 h, 60 ^oC

To verify synthesis of final coupled compounds and for full characterisation, ^{1}H-NMR and ^{13}C-NMR analyses along with 2D spectra, HSQC, HMBC and COSY were attained. High resolution mass spectrometry, infrared spectrometry and melting point analyses were also conducted.

3.2.6.1 Synthesis of 3-(2-((4-bromophenyl)thio)acetyl)-1*H*-indole-5-carbonitrile (3.21)

Using 4-bromothiophenol as the nucleophile with 3-(2-bromoacetyl)-1*H*-indole-5-carbonitrile (**3.15**), we synthesised our first desired compound **3.21** (**Scheme 3.8**). However, the reaction yielded disappointingly low amounts of product. We repeated the synthesis to attain adequate amounts for compound characterisation and biological studies. Following purification we were able to recover the acetylated indole (**3.8**) whilst **3.15** was completely used up. The reaction had to be run for elongated time periods of 24 – 36 h, monitoring product formation and reaction completion by TLC. Low yields were likely attributed to the use of a crude reaction mixture, a trend maintained in later syntheses.

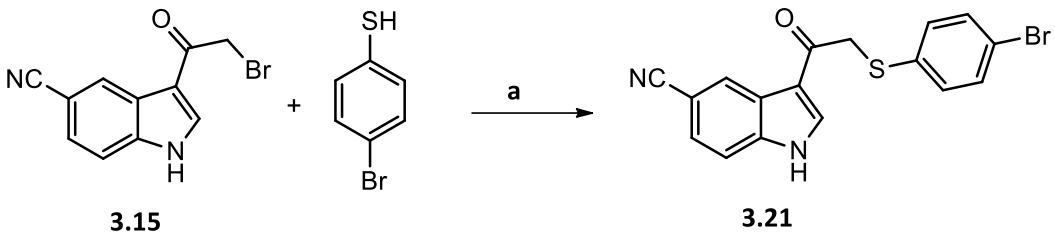

Scheme 3.8 Synthesis of 3-(2-((4-bromophenyl)thio)acetyl)-1*H*-indole-5-carbonitrile.

a) K_2CO_3, Acetone, 24 - 36 h, 60 ^oC

*3.2.6.1.1 Characterisation of compound **3.21***

The successful coupling to form **3.21** was verified by NMR analysis. We observed signals that integrated for a total of eleven protons on the ^{1}H-NMR spectrum for compound **3.21** (**Fig 3.5**). The methylene signal had shifted from 4.71 ppm in **3.15** to 4.52 ppm in **3.21**. Characteristic of a para-substituted phenyl ring, two signals integrating for two protons each were sighted at 7.48 – 7.46 ppm and 7.34 – 7.32 ppm. HMBC was used to assess arrangement of atoms in chemical space, confirming synthesis of **3.21**.

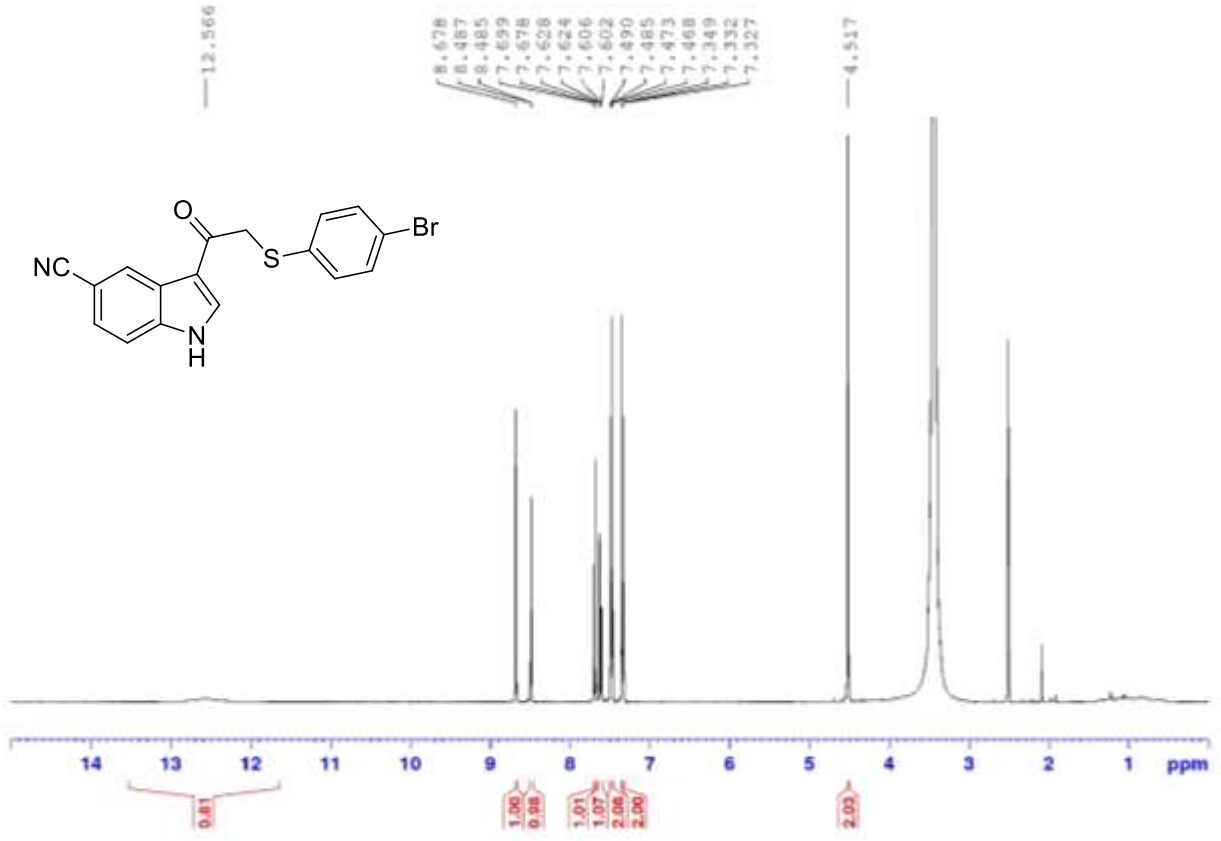

Fig 3.5 ^{1}H-NMR spectrum of **3.21**.

Following sparing solubility in DMSO, compound **3.21** further suffered from low solubility in biological medium, thus affecting its biological activity. We therefore sought to increase the solubility of compounds in our library to allow for biological testing.

Prior studies in our lab, utilising compounds **3.22** and **3.23** revealed that the ether bridge containing **3.22** was slightly less active against *P. falciparum* compared to **3.23**.[131] However, the oxygen atom rendered the molecule less lipophilic than its sulfur containing analogue due to its increased polarity and capacity to form hydrogen bonds compared to sulfur.[132–134] Accordingly, we thought it prudent to explore oxygen containing analogues, which feature a nitro group on the phenyl ring.

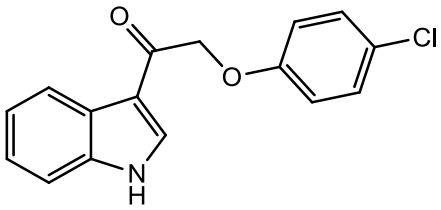

3.22: IC_{50} = 1.8 μM; clogP = 3.6

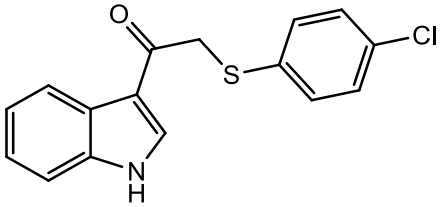

3.23: IC_{50} = 1.4 μM; clogP = 4.3

3.2.6.2 Synthesis of indolyl-3-ethanone-α-ethers (3.24 – 3.26)

Scheme 3.9 shows the synthesis of oxygen containing analogues **3.24** – **3.26**.

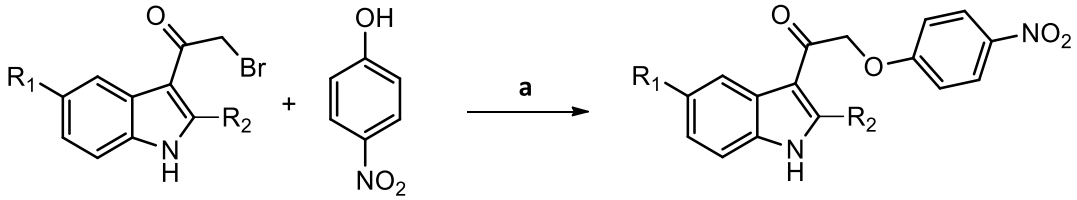

3.15: R_1 = CN, R_2 = H
3.17: R_1 = CH_3, R_2 = H
3.18: R_1 = H, R_2 = CH_3

3.24: R_1 = CN, R_2 = H
3.25: R_1 = CH_3, R_2 = H, 82%
3.26: R_1 = H, R_2 = CH_3, 98%

Scheme 3.9 Synthesis of indolyl-3-ethanone-α-ethers.
a) K_2CO_3, Acetone, 5 h, 60 °C

Compared to **Scheme 3.8**, yields were generally higher while reaction times were shorter.

3.2.6.2.1 Characterisation of compounds 3.24 – 3.26

Characteristic para substituted phenyl signals integrating for two protons each were observed in the ^{1}H-NMR spectra of **3.25** at 8.21 – 8.19 ppm and 7.18 – 7.15 ppm respectively (**Fig 3.6**). A change in chemical environment was observed with the methylene signal shifting from 4.47 ppm in **3.17** to 5.52 ppm in **3.25**. Compounds **3.24** and **3.26** showed similar characteristic signals and a methylene shift confirming coupling to 4-nitrophenol.

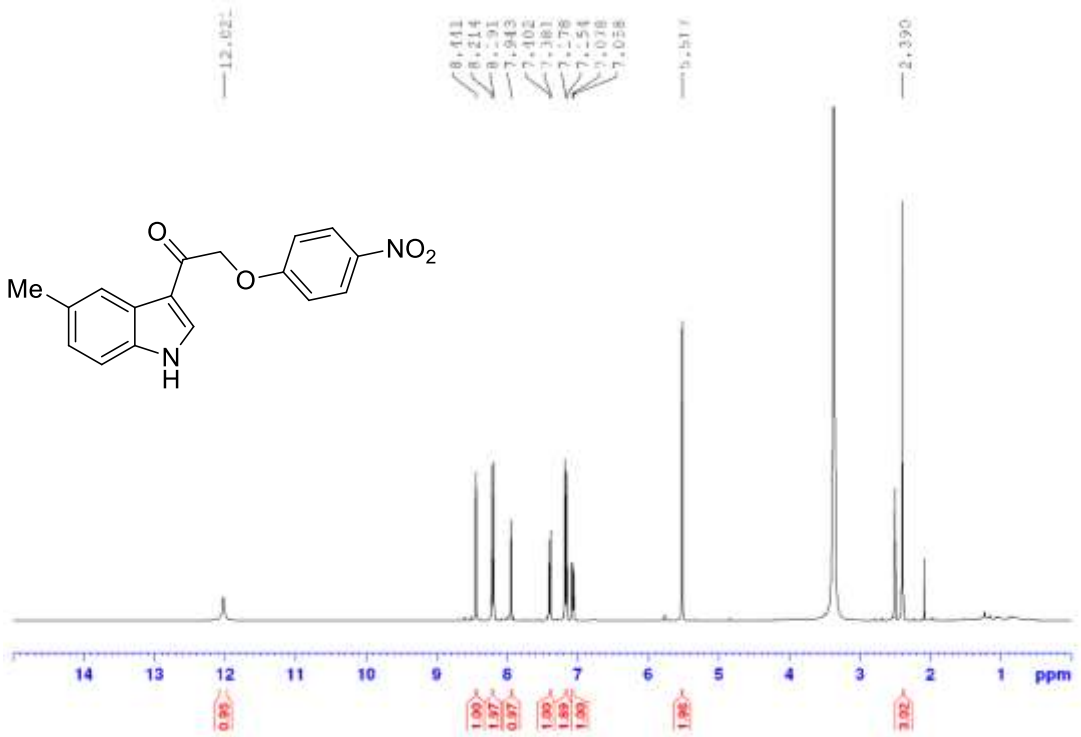

Fig 3.6 ^{1}H-NMR spectrum of **3.25**.

3.2.6.3 Synthesis of indolyl-3-ethanone-α-thioethers (3.27 – 3.31)

Compounds **3.15** – **3.19** were coupled to the nucleophile 4-nitrothiophenol (**Scheme 3.10**). The observed reaction yields were comparatively lower than for the 4-nitrophenol coupled compounds **3.24** – **3.26**.

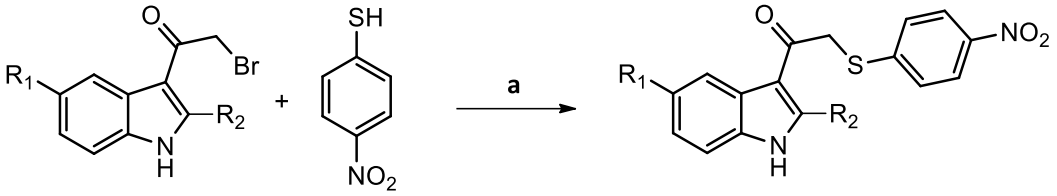

3.15: R_1 = CN, R_2 = H
3.16: R_1 = Cl, R_2 = H
3.17: R_1 = CH_3, R_2 = H
3.18: R_1 = H, R_2 = CH_3
3.19: R_1 = OCH_3, R_2 = H

3.27: R_1 = CN, R_2 = H
3.28: R_1 = Cl, R_2 = H, 46%
3.29: R_1 = CH_3, R_2 = H, 62%
3.30: R_1 = H, R_2 = CH_3, 69%
3.31: R_1 = OCH_3, R_2 = H, 87%

Scheme 3.10 Synthesis of indolyl-3-ethanone-α-thioethers.

a) K_2CO_3, Acetone, 5 h, 60 ^oC

The NMR analyses of these compounds showed similar characteristics observed with **3.24** – **3.26**.

3.2.6.4 Synthesis of 2-(4-(1*H*-tetrazol-5-yl)phenoxy)-1-(1*H*-indol-3-yl)ethanone (3.32)

As a result of the synthesis of tetrazole containing compounds (discussed in **Chapter 4**), we had access to 4-(1*H*-tetrazol-5-yl)phenol, which we employed as a nucleophile for the interest of probing size limitations of the binding pocket and possible interactions that would occur with the acidic tetrazole moiety when coupled to **3.20** (**Scheme 3.11**).

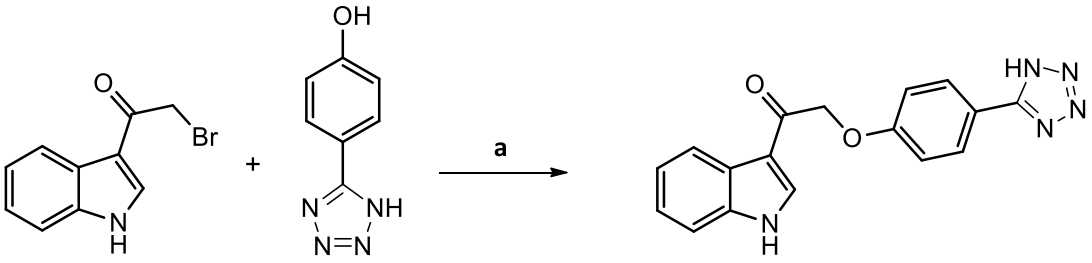

3.20

3.32, 20%

Scheme 3.11 Synthesis of 2-(4-(1*H*-tetrazol-5-yl)phenoxy)-1-(1*H*-indol-3-yl)ethanone.

a) K_2CO_3, Acetone, 5 h, 60 ^oC

*3.2.6.4.1 Characterisation of **3.32***

The ^{1}H-NMR spectrum of **3.32** was consistent to that of compounds **3.24** – **3.26**, with a shift in the methylene signal from 4.65 ppm in **3.20** to 6.27 ppm in **3.32** (**Fig 3.7a**). We identified the signal 165.8

ppm in the ^{13}C-NMR spectrum, representing the quaternary carbon on the tetrazole moiety (**Fig 3.7b**).

Using HSQC and HMBC we were able to confirm the successful formation of compound **3.32**.

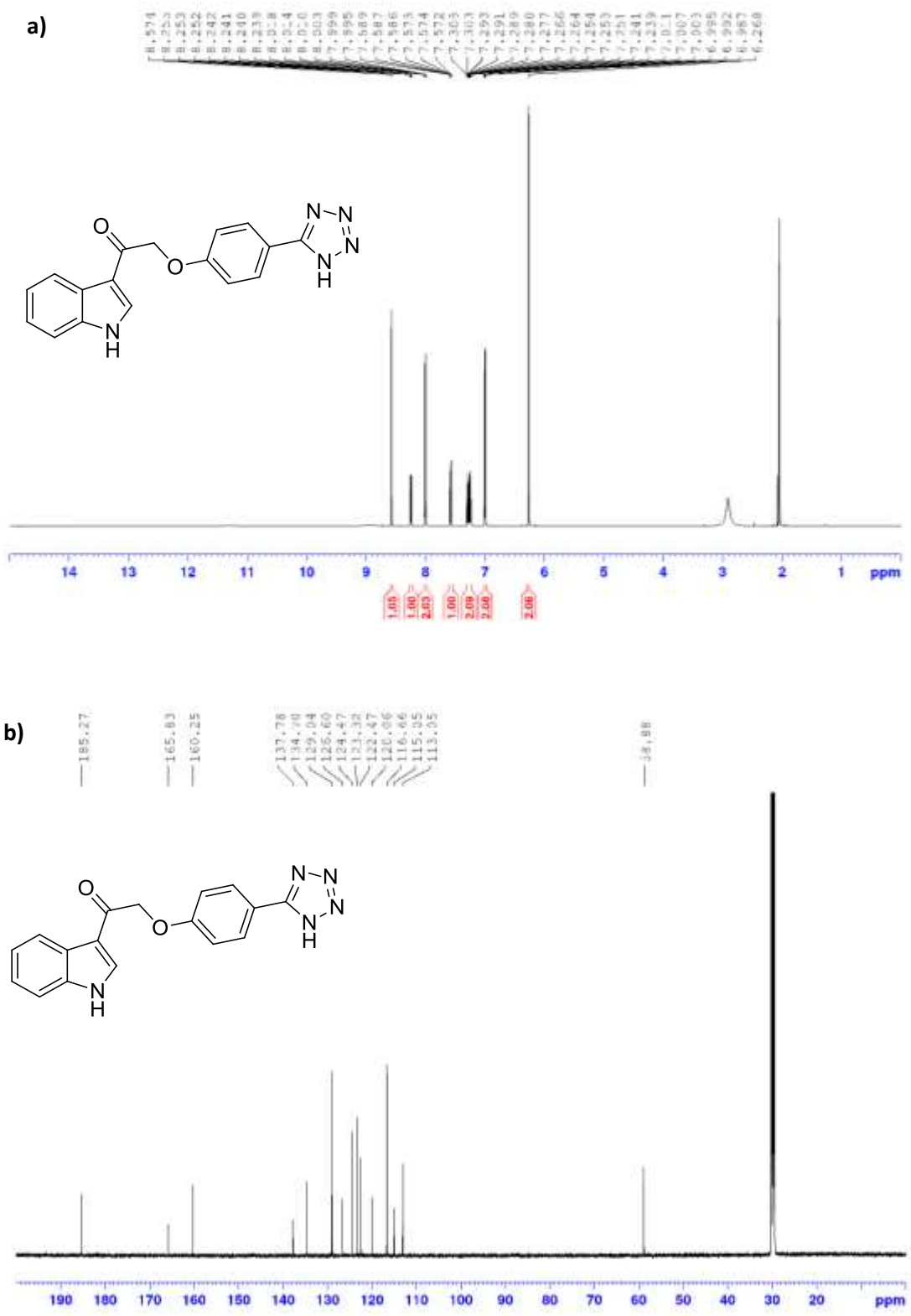

Fig 3.7 a) ^{1}H-NMR and b) ^{13}C-NMR spectra of **3.32**.

3.3 Biological assay results

Compounds **3.21** and **3.24** – **3.32** were screened for viability against *P. falciparum* 3D7 strain at 20 µM concentration using the Markwalter assay that detects *Plasmodium* lactate dehydrogenase (*P*LDH).[135] Makler and Hinrichs found that the activity of *P*LDH enzyme correlated to the number of parasites present in an analyte. In the assay, the activity of *P*LDH results in the reduction of the yellow dye, nitroblue tetrazolium (NBT) to formazan which is blue in colour, propelled by phenazine ethosulfate (PES) and reduced 3-acetylpyridine-adenine dinucleotide (APADH).[136] Compounds **3.25** – **3.32** reduced parasite cell viability below 25%, and were submitted for dose dependant assessment. In addition, mammalian cytotoxicity was assessed against a HeLa cell line at a single concentration. This assay indicated that there was no significant reduction in cell viability at 20 µM, indicating that these compounds show low toxicity (**Table 3.1**). clogP values were obtained using Swiss ADME, a free online source from the Swiss Institute of Bioinformatics.[137,138]

Compound **3.28** exhibited the highest anti-plasmodial activity amongst the compounds synthesised for this project, with no significant toxicity to HeLa cells. A higher pIC_{50} value was observed for **3.28** compared to the *p*-bromothiophenol containing **2.47**, suggesting that the *p*-NO_2 is important for enhanced biological activity. The clogP values also suggest that **3.28** is more hydrophilic than **2.47** which would increase its solubility, an important parameter in drug design.

While **3.21**, which was tested as a suspension was found to be inactive, its nitro containing analogue **3.27** displayed moderate activity. This data suggested that the electron withdrawing nitrile bioisostere reduced anti-plasmodial activity compared to **2.74**. To understand further the nature of the 5-substituent required to enhance activity we looked at compounds **4.29** and **3.31** possessing electron donating and hydrophobic methyl and methoxy groups. These compounds showed improved anti-plasmodial activity compared to **3.27**. Though inferior to the pIC_{50} values of **3.28** and CQ, the activity of compound **3.31** was comparable to that of **2.47** suggesting a hydrophobic interaction is important in this region, and the electron withdrawing nature of the chlorine substituent is less important.

Table 3.1 Bioassay results of compounds **3.21** and **3.24** – **3.32** against *P. falciparum* 3D7.

Compound #	Structure	*P. falciparum* 3D7		HeLa Toxicity (% cell viability)	clogP
		IC_{50} (μM)	pIC_{50} (M)		
3.21	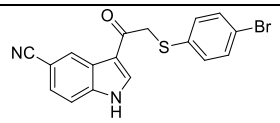	inactive-	-	105	3.90
3.24	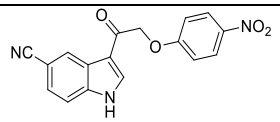	inactive	-	107	2.12
3.25	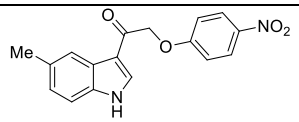	0.868	6.06	86	2.53
3.26	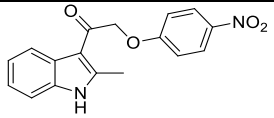	2.181	5.66	79	2.52
3.27	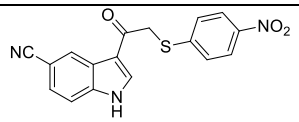	0.536	6.27	97	2.62
3.28	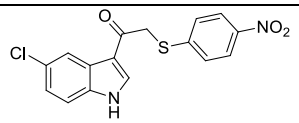	0.037	7.44	85	3.41
3.29	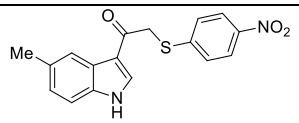	0.248	6.61	100	3.04
3.30	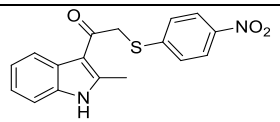	1.369	5.86	107	3.04
3.31	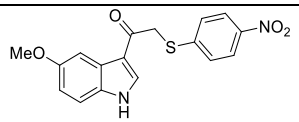	0.129	6.89	102	2.67
3.32	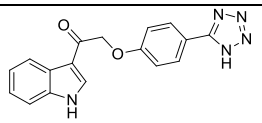	8.28	5.08	79	2.34
		Reference compounds			
2.46	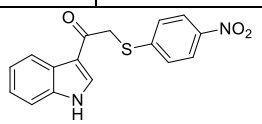	0.24	6.62		3.4
2.47	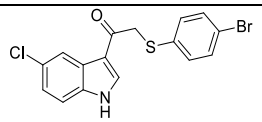	0.09	7.05		5.1
CQ		0.024	7.61		

3.30 with a 2-methyl substituent was less active against *Plasmodium* compared to compound **2.46**. We suspected that the methyl group was constricting the bond rotation about C-3 or might have formed somewhat of hydrophobic interactions, which possibly restricted the compound adjusting to a conformation that allows maximum interaction with the binding pocket.

As anticipated, the clogP values of **3.25** and **3.26** were lower than for analogue compounds **3.29** and **3.30** owing to the more electronegative oxygen in the ether bridge than the sulfur. The trade-off for the increased hydrophilicity was a declined anti-plasmodial activity. Synonymous with the ether bridge containing **3.25** and **3.26**, compound **3.32** had a markedly lower anti-plasmodial activity. This suggested that a sulfur atom is a critical element of the pharmacophore.

3.4 Conclusions

In this chapter we set out to synthesise indolyl-3-ethanone-α-thioethers to further understand the SAR and nature of the putative target binding pocket of this series of compounds. We employed the Friedel-Crafts acetylation and α-bromination described by Veale *et al.* and despite the low yields and repeat syntheses to attain viable amounts of α-brominated analogues, we managed to access the desired compounds (**3.21** and **3.24** – **3.32**) using the coupling reaction adapted from the synthetic methods by He *et al*. and Black *et al*.[129,130]

Despite its low solubility in assay medium, compound **3.21** was assayed as a suspension and found inactive against the malaria parasites. *p*-Nitrophenol analogues were synthesised, improving solubility and further exhibiting activity against *P. falciparum* 3D7 (**3.25** and **3.26**). Similar to **3.21**, compound **3.24** was inactive with % viability against parasitaemia >100%.

Having synthesised the *p*-nitrothiophenol coupled analogues, we identified most active of the series, compound **3.28**, though with a relatively lower pIC_{50} to CQ, **3.28** was more active against *Plasmodium* compared to **2.47**. Observing the activities of **3.28** and **2.47** we can also conclude that the interaction

between the target site and *p*-NO_2 enhances anti-plasmodial activity, superior to the *p*-Br containing thiophenol.

Compared to 5-chloro, the bioisosteric 5-methyl, 5-cyano and 5-methoxy analogues were less active against *P. falciparum* 3D7, suggesting the possible formation of an important halogen bond between the 5-chloro substituent and the binding pocket, enhancing biological activity. Furthermore we observed the comparable activity of compounds **3.29** and **3.31** suggesting that the electron donating C-5 substituents form hydrophobic interactions with the target site also tolerating slight increases in substituent size (**3.31**). This finding attracts further C-5 study using 5-NO_2, 5-NH_2 and isopropyl substituents as examples.

Compound **3.30** also showed us the possibility of hydrophobic interactions forming with C-2 substituents which could restrict the conformational fitting of the compound into the binding pocket, suggesting an unsubstituted C-2 to be important for activity.

With the information gleaned from this project, compound **3.28** presents an opportunity for further investigations and optimisation of this series of privileged indole based compounds to yield a potent lead compound.

Chapter 4: Tetrazoles

4.1 General overview

The tetrazole ring is an electron rich five-membered heterocycle with one carbon atom and four nitrogen atoms. The compound has two unsaturated bonds and can exist in two tautomeric forms (**4.1a** and **4.1b**).[139] The tetrazole ring facilitates numerous interactions such as hydrogen bonds, coordination bonds, hydrophobic interactions and π-stacking interactions with biological macromolecules eliciting a wide array of pharmaceutically important biological activities.[140] Owing to its combined lipophilic acidic nature, tetrazoles have found application as a bioisostere of carboxylic acid, amide and related heterocycles, resulting in improved compound pharmacokinetic profiles.[140,141]

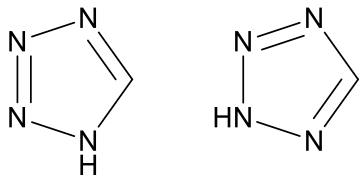

4.1a **4.1b**

Tetrazoles and their derivatives have been identified as antibacterial, anti-inflammatory, analgesic, anticancer, antiviral, herbicidal, anti-proliferative, anticonvulsant, anti-parasitic and hypoglycaemic agents. We will continue to look at some of these derivatives and their application in medicinal chemistry.

4.2 Antifungal agents

The triazole compound, TAK-456 (**4.2**) containing a postion-1 substituted tetrazole, was found to exhibit potent antifungal activity against major opportunistic fungi of the *Candida* and *Aspergillus* species. TAK-456 exhibited superior *in vitro* activity against *C. albicans, C. krusei, C. parapsilosis, C. neoformans, C. tropicalis, C. glabrata, A. niger, A. fumigatus and A. flavus* compared to fluconazole (**4.3**). The activities of TAK-456 were comparable to the reference azole drugs, itraconazole (**4.4**) and

voriconazole (**4.5**), with the exception of *C. glabrata*. TAK-456 also exhibited an effective *in vivo* activity against fluconazole resistant strains of *C. albicans* whilst showing efficacy against *A. fumigatus* comparable to itraconazole and voriconazole.[142] With observed *in vivo* and *in vitro* activities, toxicity similar or less to the azoles antifungal agents, TAK-456 presents a potent clinical drug candidate in treatment of fungal infections.[142]

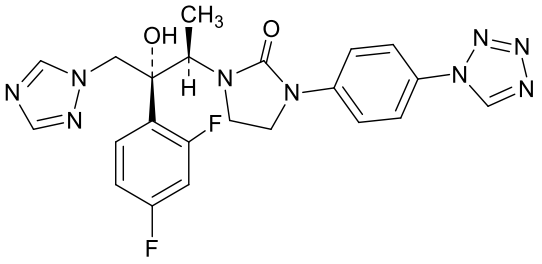

4.2 TAK-456

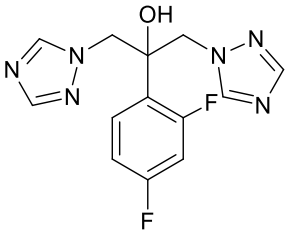

4.3 Fluconazole

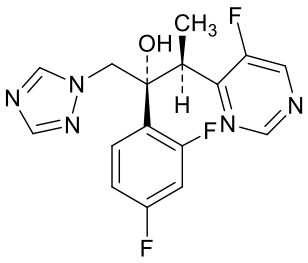

4.5 Voriconazole

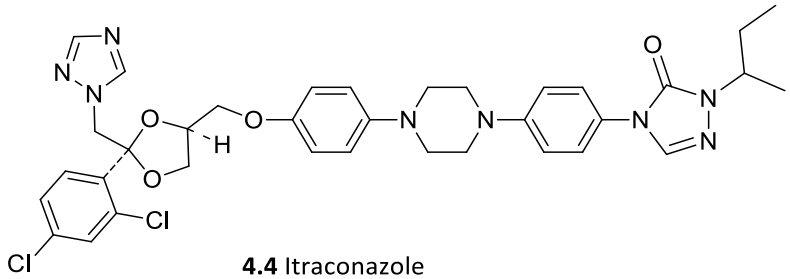

4.4 Itraconazole

Hayashii *et al.* further developed an injectable salt of TAK-456, the water soluble prodrug TAK-457 (**4.6**) which was also found potent against pulmonary fungal infections caused by *A. fumigatus* with an activity comparable to the injectable amphotericin B. The development of the injectable, TAK-457, encourages research into new and effective, non-toxic antifungal injectable agents using the prodrug approach.[143]

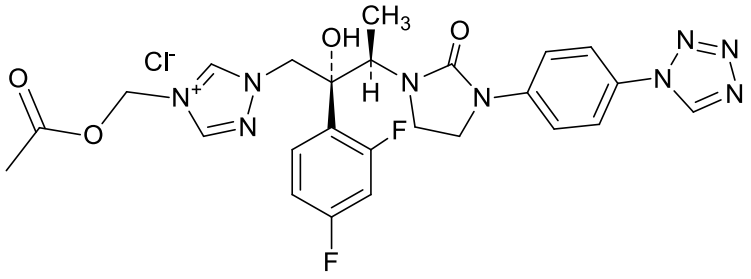

4.6 TAK-457

4.3 Antimicrobial agents

Ceftezole (**4.7**) and cefazolin (**4.8**) are ß-lactam antibiotics that contain a tetrazole moiety. The two compounds are analogues of cephalosporin C, belonging to the 1st generation of cephalosporins first developed in the 1960s and still widely used as injectable antibiotics.[144–146] Cefazolin exhibited bactericidal activity against gram positive and gram negative bacteria killing isolates of *E.coli*, klebsiella, *H. influenza*, *S. aureus* with no bactericidal activity against *P. aeruginosa*. The bactericidal activity of cefazolin was comparable to that of cefalothin (**4.9**), another 1st generation cephalosporin, but with cefazolin exerting less injection pain on administration.[145,147,148] Studies showed that ceftezole had a broad spectrum activity against gram negative and gram positive bacteria, similar to that of cefazolin with the exception of *P.aeruginosa, S. marcescens, P. vulgaris and P. morganii*.[146]

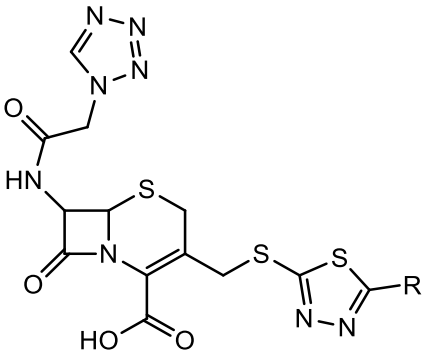

4.7 Ceftezole: R = H
4.8 Cefazolin: R = CH_3

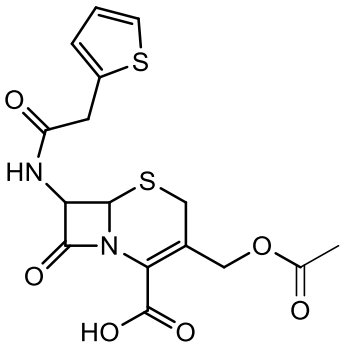

4.9 Cefalothin

Cefamandole (**4.10**) and cefmetazole (**4.11**) are semisynthetic antibiotics which represent tetrazole containing 2nd generation cephalosporins, with an additional 2-methyl substituent on the tetrazole compared to the previously discussed cefazolin and ceftezole compounds. Cefamandole exhibited superior activity compared to cefazolin and cefalothin against gram negative bacteria, though slightly less active against gram positive bacteria compared to cefalothin. Cefamandole was found active against *H. influenza,* methicillin resistant *S.* aureus with resistance studies showing that, compared to

cefazolin and cephalothin, cefamandole was less susceptible to hydrolysis by ß-lactamase enzymes.[149–151]

Cefmetazole also exhibited superior activity compared to cefazolin and cefalothin against gram negative bacteria, particularly the anaerobic *Bacteroides fragilis*.[152,153] Though when compared to the 2nd generation cephalosporin, cefoxitin (**4.12**), cefmetazole was found to be less effective against the *Bacteroides* group.[153] Though more potent and having a longer half-life, cefmetazole had a narrower spectrum of antibacterial activity than cefoxitin, acting against methicillin susceptible *Staphylococcus spp.*, *H. influenza* and *Neisseria spp.* Similar to cefoxitin, cefmetazole was stable against hydrolysis by ß-lactamase enzymes.[154]

Much like the 1st generation cephalosporins, cefamandole and cefmetazole drugs were inactive against *P. aeruginosa* and enterococci.[144,154]

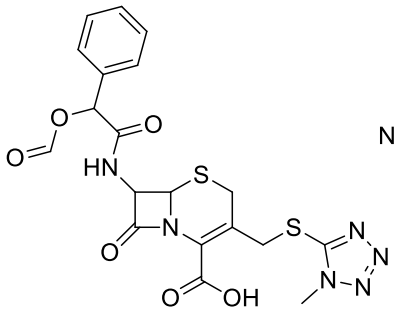

4.10 Cefamandole

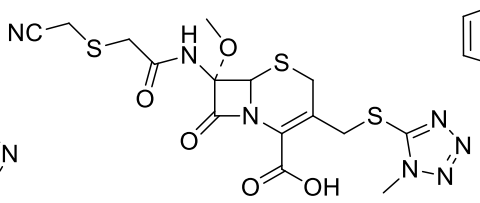

4.11 Cefmetazole

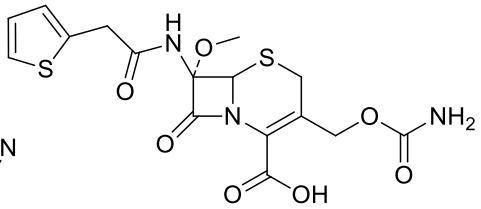

4.12 Cefoxitin

Latamoxef/moxalactam (**4.13**) is a 3rd generation cephalosporin with a six membered ring fused to a sulfur containing ß-lactam instead of an oxygen. The compound was found to exhibit antibacterial activity against *Enterobacteriacae* at concentrations much lower than those of cefoxitin and cefamandole. Furthermore, latamoxef was found active against *P. aeruginosa* but owing to limited effectiveness could not be indicated as a monotherapy drug for *P. aeruginosa* infections. Latamoxef was very active against *Klebsiella, Serratia marcescens* and *E.coli* but, against *Staphylococcus spp.*

latamoxef was less effective in killing off tested isolates as compared to cefamandole and cefalothin.[155–157]

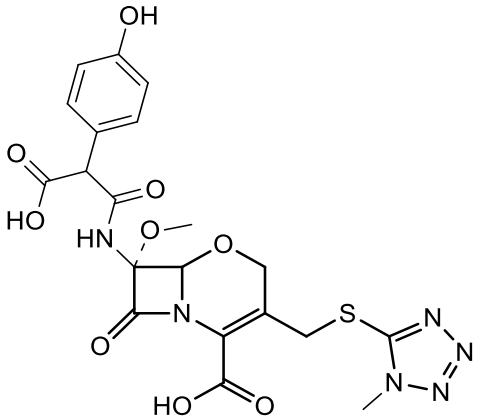

4.13 Latamoxef (moxalactam)

A new oxazolidinone derivative, DA-7867 (**4.14**) containing a 1-methyl-tetrazolyl-substituted pyridine ring was synthesised in the search for new antimicrobial agents. Studies were conducted using the approved antibacterial drug linezolid (**4.15**) as a reference against a range of gram positive bacterial strains. Results indicated that DA-7867 was superior to linezolid both *in vitro* and *in vivo* against methicillin resistant *S. aureus,* vancomycin resistant enterococci, penicillin resistant *Streptococcus pneumoniae*, *Haemophilus influenza* and *Moraxella catarrhalis*. Though the mechanism of action of DA-7867 has not been determined, the compound presents a potential drug candidate for further clinical studies.[158–160]

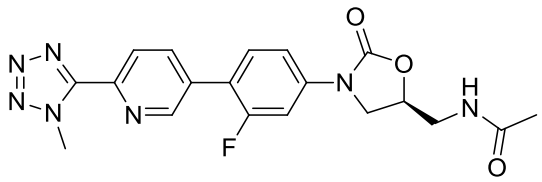

4.14 DA-7867

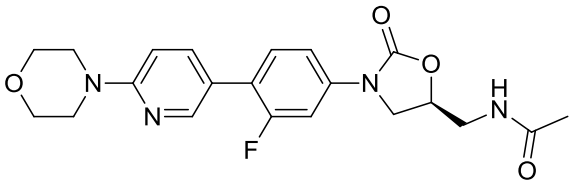

4.15 Lizenolid

Owing to the on-going studies of linezolid against *Mycobacterium tuberculosis*, DA-7867 was also tested against the bacteria with results showing superior activity than linelozid.[161] Linezolid has shown effective clearance of mycobacteria after designated treatment periods without the resurgence of

infection one year after treatment termination, however this is coupled to high dose related adverse effects in XDR TB test patients. The development of new oxazolidinone derivatives presents possible potent TB treatment candidates aimed to have safer side effect profiles compared to lizenolid.[162,163]

Clinical studies for DA-7867 have however been hindered by its limited solubility *in vivo.* This drawback saw the development of torezolid (**4.16**) and its sodium phosphate containing prodrug, **4.17**, that possessed an increased drug solubility profile and improved availability for *in vivo* tissue absorption.[164] In antibacterial studies, torezolid exhibited a superior potency against methicillin resistant *S. aureus*, vancomycin resistant enterococci, penicillin resistant *Streptococcus pneumoniae*, *Haemophilus influenza*, *Moraxella catarrhalis* and *Mycobacteruim tuberculosis* compared to linezolid.[165,166] Although the potency of torezolid was lower than that of DA-7867[166], the improved pharmacokinetic profile of its prodrug prompted clinical studies to be performed on the compound as a potential antimicrobial drug candidate.[164]

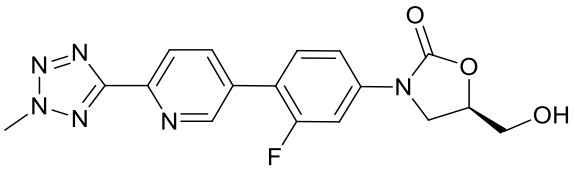

4.16 Torezolid

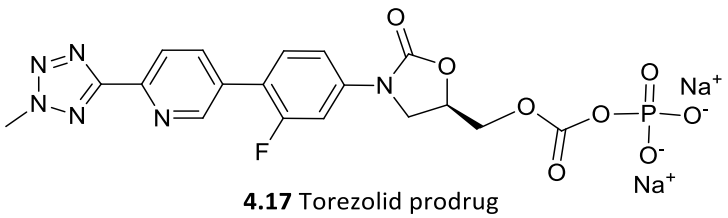

4.17 Torezolid prodrug

4.4 Antiviral agents

In the search for new effective anti-retroviral therapies owing to mutations in human immunodeficiency virus-1 (HIV-1) and treatment related toxicity, 7-(2*H*-tetrazol-5-yl)-1*H*-indole (**4.18**) was synthesised based on the drug candidate BMS-488043 (**4.19**) which had been found active against HIV-1 and safe for administration in human.[167] HIV-1 gains entry to infected host cells when the gp120 protein surface subunit of the viral envelope attaches to a CD4 receptor on the host cell surface. A conformational change in gp120 follows this attachment, leading to the gp120 protein binding to chemokine co-receptors which allows the viral transmembrane protein gp41 to puncture through the

host cell membrane. Fusion of viral and host cells occur, resulting in the release of viral genetic material into the host cell. The entry process of HIV-1 offers a multi-target pathway for drugs known as entry inhibitors to be developed, including attachment inhibitors.[168–170]

7-(2*H*-tetrazol-5-yl)-1*H*-indole was found to be potent at nanomolar concentrations, inhibiting HIV-1 cells attaching to CD4 cells. The major drawback of **4.18** was an almost negligible *in vivo* oral bioavailability which prompted the synthesis of substituted tetrazole prodrug analogues **4.20** and **4.21** containing *N*-acetoxymethyl and *N*-methyl respectively. Both prodrugs were found to be comparable in potency with **4.18**, maintaining a low cytotoxicity with highly improved oral bioavailability. Prodrug **4.20** showed higher plasma concentration of active drug compared to **4.21**. This study revealed that substitutions on the tetrazole ring with specific groups can improve the pharmacokinetic profile of these drugs and therefore allow further development of more potent HIV-1 entry inhibitors.[167]

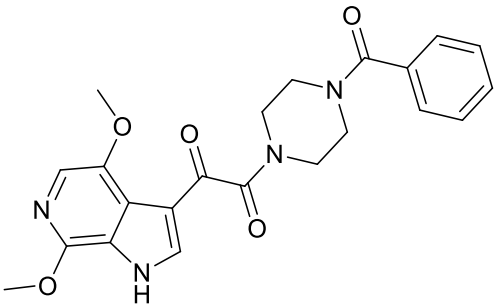

4.19 BMS-488043

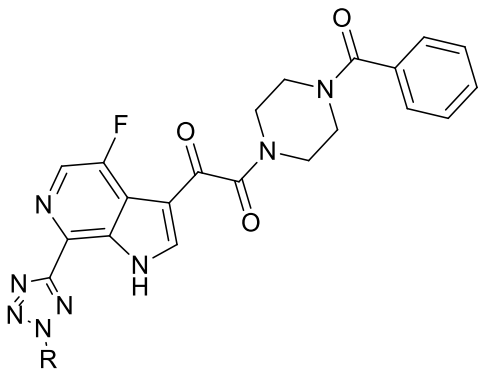

4.18: R = H
4.20: R = CH_2OCOCH_3
4.21: R = CH_3

Chang *et al.* synthesised a series of pyridylimidazolidinone derivatives based on the lead compound DBPR103 (**4.22**). The synthesised compounds were tested *in vitro* against isolated strains of the picornavirus genus and human enterovirus 71 (EV71).[171] EV71 infection has been identified as the cause of foot, hand and mouth disease in children along with neurologic complications including brainstem encephalitis, aseptic meningitis, and acute flaccid paralysis.[172,173] Compounds **4.23**, **4.24**, **4.25a** – **b**, **4.26a** – **b** exhibited strong activity against the viral strains with **4.23**, **4.25a** and **4.26b**

showing the highest activity. To determine the spectrum of activity of compounds **4.23**, **4.25a** and **4.26b**, further assays were conducted on picornavirus genera including rhinoviruses, echoviruses, coxsackieviruses and genotypes A, B and C of enterovirus strains. Results showed that compounds **4.23**, **4.25a** and **4.26b** are more active than the lead compound **4.22**, with no evident cytotoxicity, and hence presenting these compounds as viable drug candidates for further evaluation. This study also reveals important groups that enhance antiviral activity, that is, the heterocyclic biosiosteres of 4-chlorophenyl in **4.23**, the oxadiazole in **4.25a** and the metabolically stable tetrazole in **4.26b**.[171]

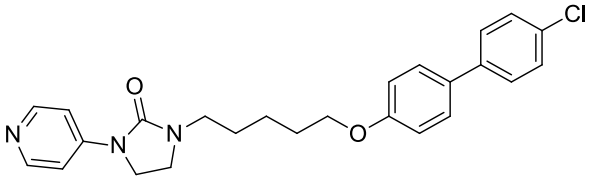

4.22 DBPR103

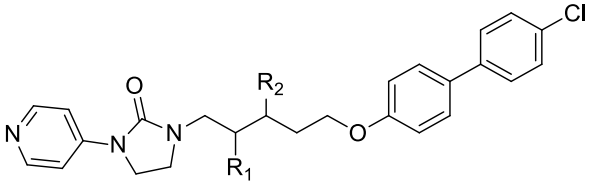

4.23: $R_1 = H$, $R_2 = CH_3$
4.24: $R_1 = CH_3$, $R_2 = H$

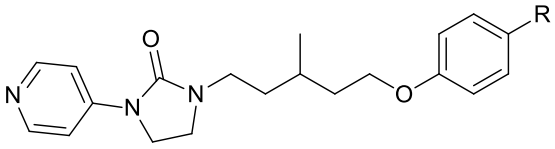

4.25a: R =

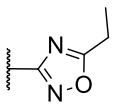

4.25b: R =

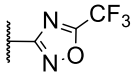

4.26a: R =

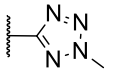

4.26b: R =

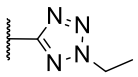

The WHO reports that the influenza virus is a contagious infection that has been observed to cause seasonal epidemics in animal and human populations. The virus is of 3 main types, A, B and C of which antigenic mutations in virus strains of type A and B have been the main cause of eruptions and pandemics experienced worldwide thus far. The avian strains, H1N1 and H5N1 are examples of type A influenza viruses that have previously caused a worldwide pandemic. The WHO recommends the prevention of infection by vaccinating individuals in risk groups and treating already infected individuals timeously to reduce complications and death.[174,175]

The drugs amantadine (**4.27**) and rimantadine (**4.28**) are adamantane (**4.29**) derivatives used in the treatment of type A influenza viruses not type B. There is need to develop broad acting antiviral agents for both type A and B viruses. The adamantine derivatives block the release of viral RNA into infected cells by inhibiting the viral transmembrane protein, M2. Adamantane derivative drug resistant strains with substituted amino acids in the M2 protein have emerged and rapidly spread, prompting the need for new, effective antiviral agents with a broad spectrum activity.[176] Zarubaev *et al.* synthesised a library of azolo-adamantane compounds which were tested against the highly rimantadine resistant virus strain A/Puerto Rico/8/34. Compounds **4.30** – **4.33** were found to inhibit the tested viral strain more potently than rimantadine, thought to be due to a higher affinity of the adamantyl-tetrazole compounds to M2 protein or possibly, a different binding site. The prospect of azolo-adamantane derivatives binding to a target site other than M2 protein, would encourage the identification of this target for the evelopment of more potent agents as drug candidates in antiviral treatment. These compounds would avert the already existing adamantane-derivative drug resistance.[177]

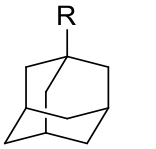

4.27: R = NH_2
4.28: R = $CH(NH_2)CH_3$
4.29: R = H

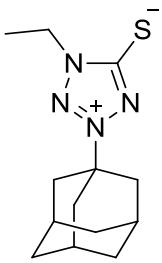

4.30

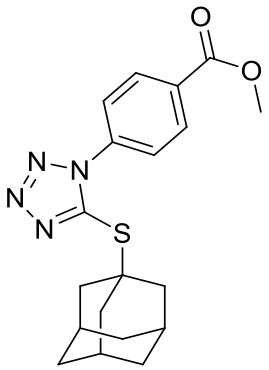

4.31

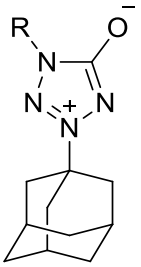

4.32: R = CH_2CH_3
4.33: R = 4-$(CH_3OOC)CH_3$

4.5 Anticancer agents

Bhaskar and Mohite synthesised a small library of 1,5-disubstituted tetrazole containing compounds which were tested *in vitro* against 60 lines of human cancer cell types including breast, prostate, kidney, ovary, brain, colon, leukemia, melanoma and lung cancer. The tested compounds **4.34a** – **c**

and **4.35a** – **e** were found to be selective growth inhibitors of cancer cells. Compounds **4.34a** and **4.35c** were selective to CNS cancer, compounds **4.34b**, **4.34c**, **4.35b** and **4.35e** to renal cancer while **4.35a** and **4.35d** to ovarian cancer. The anticancer activity of these compounds was found to be related to the nature of the postion-1 substituent on the tetrazole ring. Accordingly, compound **4.35b** was found to be most active amongst the synthesised compounds, exhibiting a selective % growth of ovarian cancer cells (SK-OV-3 cell line) of 34.94%. These compounds, simple in their structure, require further investigation to describe and improve the anticancer activity observed.[178]

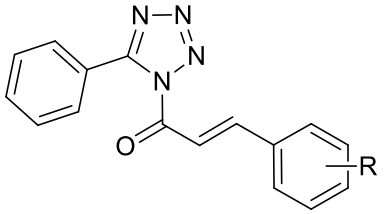

4.34a: R = *o*-Cl
4.34b: R = *p*-Cl
4.34c: R = *p*-Br

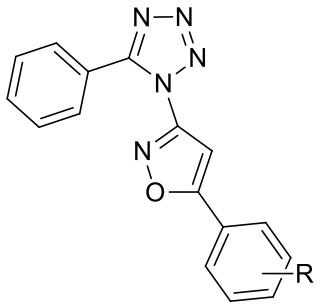

4.35a: R = *o*-Cl
4.35b: R = *p*-Cl
4.35c: R = *p*-Br
4.35d: R = *p*-OCH_3
4.35e: R = *m*-NO_2

Protein arginine deiminases (PADs) are calcium dependent enzymes that convert arginine residues to citrulline. Isozymes PAD1, -2, -3, -4 are found in humans and have been identified as drug targets owing to their yet to be understood dysregulated expression in certain disease conditions. PAD4 has been found associated to inflammatory diseases where citrullinated proteins are recognised and attacked by auto-antibodies such as the rheumatoid factor, promoting disease progression. Overexpression of PAD4 has been found in various malignant cancer patients (but not in benign cancers), rheumatoid arthritis, multiple sclerosis and ulcerative colitis. As a known transcriptional corepressor of the tumour suppressor protein, p53, overexpression of PAD4 is believed to propagate tumorigenesis and disrupt apoptosis.[179–181] The PADs as drug targets present an opportunity to develop inhibitors with clinical significance. Subramanian *et al.* synthesised tetrazole analogues of the PAD inhibitor Cl-amidine (**4.36**) to improve the pharmacological profile of the compound. Owing to the peptide structure of Cl-amidine and its derivatives, proteolysis is an imminent challenge, hence the attempt by Subramanian *et al.* to synthesise more stable, potent and selective PAD inhibitors. The

anti-proliferative potency of the synthesised compounds was tested against the rapid growing human osteosarcoma U20S cell line at 20 µM concentrations. Compounds **4.37a** and **4.37b** were found more active against the cancer cells than Cl-amidine with compound **4.37a** having a superior activity, completely inhibiting tumour cell growth. Compound **4.37b** showed higher selectivity for PAD2 over PAD4 and also exhibited better *in vitro* stability compared to Cl-amidine and **4.37a**. This study further elucidates the viability of PAD inhibitors as potential drugs in chemotherapy and the need for continued investigations.[182]

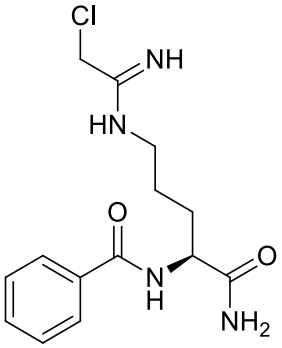

4.36

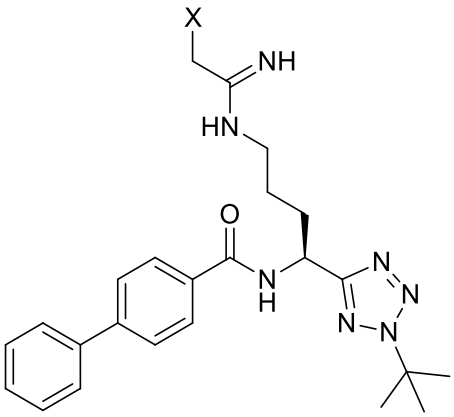

4.37a: X = Cl
4.37b: X = F

Marked by its anti-proliferative activity of inhibiting tubulin polymerisation into microtubules during cell division, the naturally occurring combrestatin A-4 (**4.38**) is active against a variety of cancer cell lines including overexpressing P-glycoprotein multidrug resistant cell lines.[183] The SAR of combrestatin A-4 linked its anti-proliferative activity to the essential presence of a trimethoxy substituted A-ring and cis configured double bond bridge to a *p*-methoxy substituted B-ring.[184,185] The issue with combrestatin A-4 is the isomerisation of its active cis- double bond configuration to the less active, more stable trans- configuration during storage and metabolism. A series of 1,5-diaryl-1,2,4-triazoles was synthesised in response to the loss of activity by combrestatin A-4. Compound **4.39** from the series of potent inhibitors of tumour growth was found to be the most active.[186] This result encouraged Romagnoli *et al.* to develop the bioisosteric series of 1,5-diaryl substituted 1,2,3,4-tetrazoles. The synthesised compounds were tested against cancerous HeLa, A549, HL-60, Jurkat,

MCF-7 and HT-29 cell lines.[183] Jedhe *et al.* also synthesised a range of combrestatin-A4 analogues containing hydroxyl moieties on rings A and B intended to form stabilising hydrogen bonds with a central 1,5-disubstituted tetrazole. HeLa, A549, H1299 cell lines and breast adenocarcinoma MCF-7 growth inhibiting activity was tested.[187] Both studies achieved the cis- double bond stabilisation. Compounds **4.40**, **4.41** and its regioisomer **4.42,** synthesised by Romagnoli *et al.* were found to be most active of the tetrazole containing series. In comparison to compounds **4.38** and **4.39**, compound **4.41** exhibited superior inhibition of tubulin polymerisation. When tested against A-549-T12, a paclitaxel (**4.43**) resistant cell line, compounds **4.40** – **4.42** were relatively more active implying their usefulness in treating cancers resistant to other anti-tubulin agents such as paclitaxel. Further *in vivo* studies using human colon adenocarcinoma xenografts showed results of the potent **4.41** reducing tumour volume by 66% compared to the 43.7% of compound **4.38** with no apparent toxicity. This study presents **4.41** as a potential anti-tubulin agent requiring further investigation for use in cancer treatment.[183]

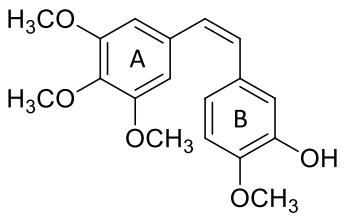

4.38 Combrestatin A-4

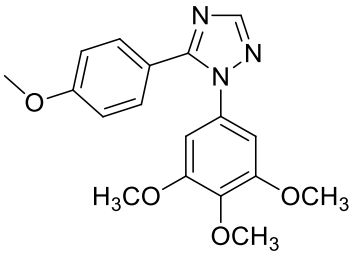

4.39

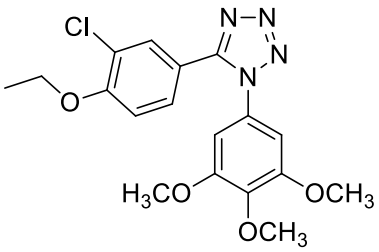

4.40

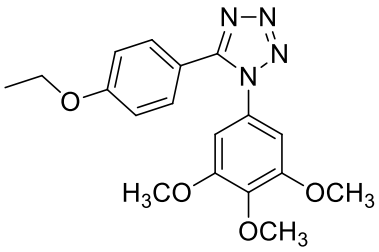

4.41

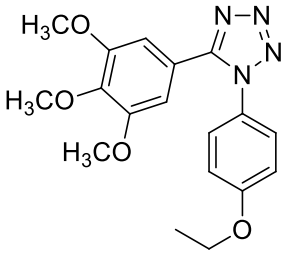

4.42

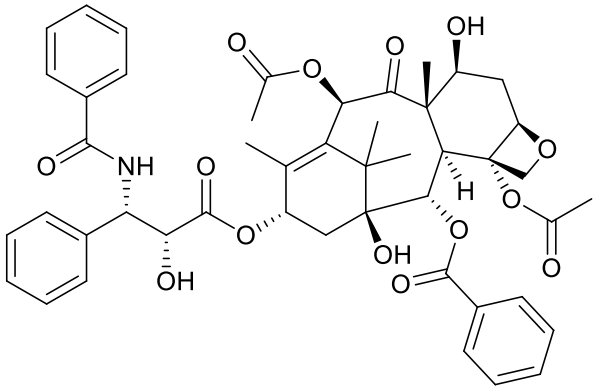

4.43 Paclitaxel

Compounds **4.44** and **4.45,** synthesised by *Jedhe at al.* were the most active from the series, though with showing less anti-proliferative activity compared to compound **4.41**. The anti-tubulin inhibition of compound **4.45** with an *o*-hydroxyl and *m*-NH_2 on ring B was however superior to that of compound **4.44** with an *o*-hydroxyl and *m*-hydroxyl, showing the importance of the *m*-NH_2 for inhibition. Notwithstanding the achieved synthesis of compounds with stabilising hydrogen bonds, the anticipated improvement in cancer cell growth inhibition and anti-tubulin activity was not realised.[187]

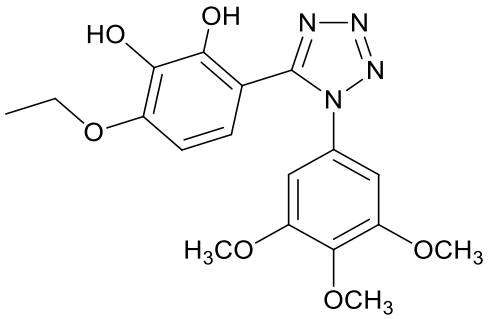

4.44

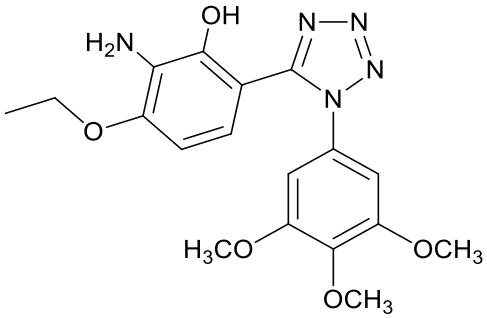

4.45

Arshad *et al.* synthesised a series of tetrazolohydrazone compounds targeting specific proteins linked to breast cancer and aimed at lowering the cytotoxic effects of therapy. Breast cancer cells responsive to hormone treatment, i.e. estrogen receptor (ER) positive MCF-7 cell line and cancer cells non-responsive to hormone treatment, i.e. ER negative MDA-MB-231 and ZR-75 cell lines were used in this study. Compounds **4.46** – **4.48** selectively inhibited the growth of ER positive MCF-7 cancer cells while

compound **4.49** selectively inhibited the growth of ER negative cancer cells. The growth of cancerous cell lines was retarded by 10-30% compared to untreated cells. The selectivity of the compounds to breast cancer cell lines was verified by gene tests of which one test showed the increase in CD44 gene expression causing poor disease prognosis and metastasis when MCF-7 is treated with the tetrazolohydrazones. This study probes and encourages investigation into specific cancer types and the identification of related proteins as potential targets of chemotherapy, possibly reducing the cytotoxic effects observed with non-specific drug treatment.[188]

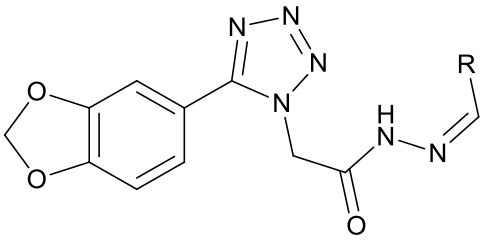

4.46: R = 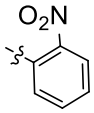

4.47: R = 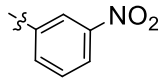

4.48: R = 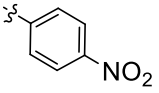

4.49: R = 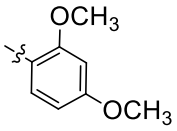

4.6 Hypotensive agents

In hypertension treatment, the renin-angiotensin aldosterone system (RAAS) is a drug targeted pathway that regulates extracellular fluid balance and arterial pressure. **Fig 4.1** shows the angiotensin converting enzyme mediated conversion of angiotensin I to angiotensin II (AII), which subsequently binds non-specifically to angiotensin type 1 and type 2 receptors (AT_1R and AT_2R). AT_1R exerts most RAAS effects inclusive of vasoconstriction and stimulating the release of aldosterone which promotes the reabsorption of sodium and water into the blood circulation, increasing blood pressure.[189–191]

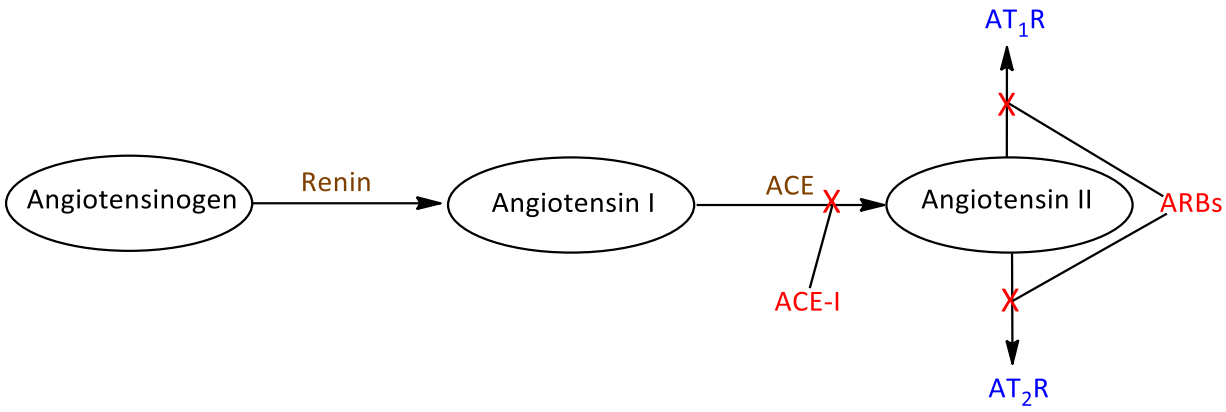

Fig 4.1 Angiotensin II formation and pathway inhibition points.

Accordingly, ACE inhibiting drugs (ACE-I) such as captopril and enalapril are used in the management of high blood pressure owing to their vasodilatory effect and capacity to lower the sodium and water reabsorption by inhibiting aldosterone release. ACE inhibition has been found to also potentiate bradykinin action causing an unwanted dry cough and angioedema. This has encouraged research into the synthesis of angiotensin receptor blockers (ARBs) to avoid the side effects caused by ACE inhibition. Losartan (**4.50**), irbesartan (**4.51**) and valsartan (**4.52**) are examples of tetrazole containing ARBs that have been developed and are clinically used to block AII target sites.[192–194]

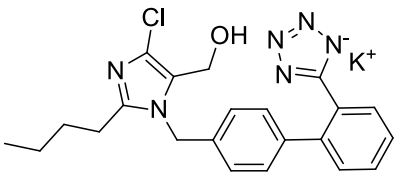

4.50 Losartan

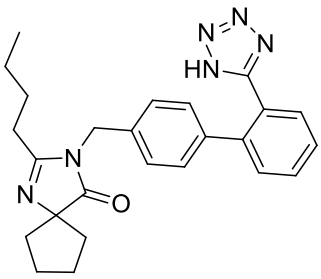

4.51 Irbesartan

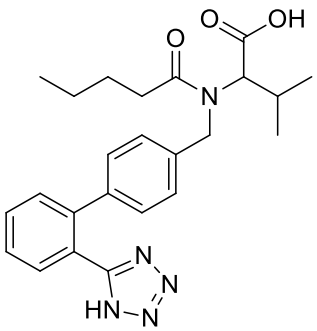

4.52 Valsartan

4.7 Leukotriene inhibitors

Some tetrazole containing compounds have been found to exhibit anti-leukotriene function acting as antagonists of the pro-inflammatory mediators, leukotrienes (LTs). LTs released from mast cells by allergenic stimulation, have been found associated with inflammatory and immune body responses inclusive of allergic rhinitis, asthma and pulmonary airway obstructive conditions. Leukotriene B_4 (LTB_4) represents one of two classes of LTs that promotes inflammation of cell tissue via neutrophil action whilst the second class called the cysteinyl LTs (CysLTs) cause smooth muscle contraction. The combined action of these two signalling molecules can therefore cause airway obstruction by bronchoconstriction and inflammation in asthmatic patients via LT G-coupled protein receptors.[195,196] LT receptors are distributed around the body in tissues including the lungs, spleen, small intestines, placenta, brain, heart and lymph nodes.[197]

Pranlukast (**4.53**) is a selective $CysLT_1$ receptor antagonist that inhibits LT agonistic bronchoconstriction and also preventing the stimulation of eosinophil modulated inflammation. This drug is used in asthma patients to prevent acute attacks.[198] Pranlukast development is marked by a series of structural modifications through compound FPL 55712 (**4.54**) which contains a carboxylic acid that conferred the compound's anti-leukotriene activity.[199] The carboxylic acid was bioisosterically replaced with metabolism-resistant tetrazole forming the compound tomelukast (**4.55**) with an improved pharmacokinetic profile hence more bioavailable *in vivo*.[141,199] Clinical trials for tomelukast were performed, during which toxicology studies showed tomelukast to be hepatotoxic, enlarging the liver of test rats.[200] This urged further structural optimisation to avert toxicity leading to the synthesis of the more potent pranlukast with an improved safety profile.

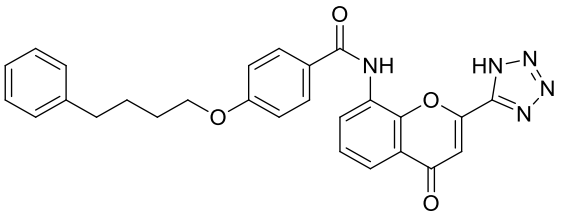

4.53 Pranlukast

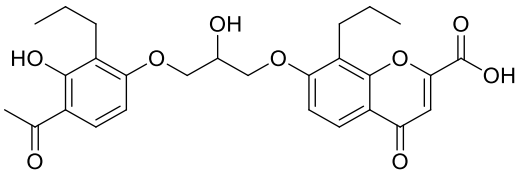

4.54 FPL-55712

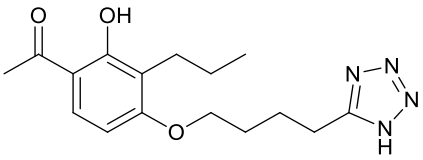

4.55 Tomelukast

4.8 Chemical tagging

An interesting study by Otsuki *et al.* disclosed that 5-sulfonyl tetrazoles can be used in chemical tagging of small bioactive compounds to identify and allow further elaboration of molecular targets. Probe molecules are used in chemical tagging, comprising of a ligand that binds to the target protein, a tagging function which links the probe to the target protein, and a tag that will act as a marker for detection. In this study, cyclosporine A which binds to the known receptor cyclophilin A[201] was used as the ligand, biotin as the tag and owing to the highly reactive nature of the electrophilic sulfonyl group, 5-sulfonyl tetrazole was used as the tagging function (**Fig 4.2**). Studies detected the biotin tag on the target receptor, cyclophilin A. Nucleophilic groups on the target protein were therefore thought to attack the electrophile hence forming a bond[202] with the tagging function. This study plays an important role in advancing medicinal chemistry, presenting a simple assembly of a 5-sulfonyl tetrazole containing probe for use in drug target identification.[203]

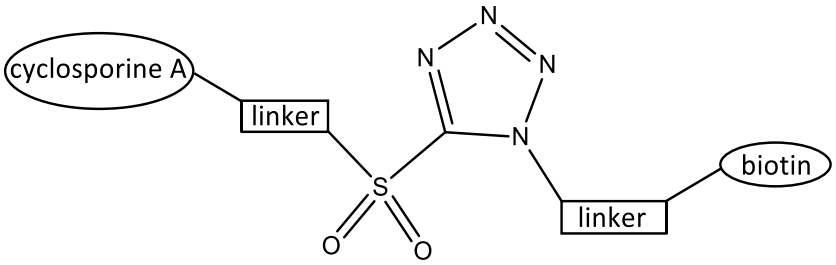

Fig 4.2 Composition of a probe molecule.

4.9 Rationale of project

The simple structure of the tetrazole moiety and its application in medicinal chemistry in combination with other pharmacophores prompted our investigation into its possible application in targeted treatment of breast cancer. Women of sub-Saharan Africa have been predominantly plagued by cancer of the breasts but particularly in this project we will focus on triple negative breast cancer (TNBC). Genetic profiling studies of TNBC revealed gene expression dependent tumour subtypes which largely affects the efficacy of administered cancer drug therapies. TNBC is non-responsive to hormone treatment, expressing tumours void of estrogen receptor (ER), progesterone receptor (PR) and human epidermal growth factor receptor 2 (HER2).[204,205] Due to the absence of effective drug treatment, there is a dire need for the identification of new drug targets and development of effective TNBC treatment.

Heat shock protein 90 (HSP90) and heat shock protein 70 (HSP70) are chaperone proteins that facilitate correct folding of polypeptide chains and protein complexation preventing aggregation with other proteins. Therefore, these chaperones are critical for cancer cell survival, ensuring that mutated and overexpressed oncoproteins correctly fold and are protected from degradation.[206] Heat shock protein organising protein (HOP) is a co-chaperone that mediates HSP70 and HSP90 interactions forming a complex that facilitates the effective transfer of client proteins between the two chaperones[207] (**Fig 4.3**). The tetratricopeptide repeat domains (TPR) of HOP feature regions rich in basic amino acids (referred to as the carboxylate clamp) which coordinate the binding of HSP90 and 70 through selective salt bridge interactions with acid rich MEEVD (HSP90) or GPTIEEVD (HSP70) peptides present on the chaperones.[208]

We postulated that the disruption of this protein-protein interaction (PPI) would impede chaperone protein assembly, arrest HSP function and lead to the degradation of essential oncogenic client proteins, ultimately leading to cancer cell death.

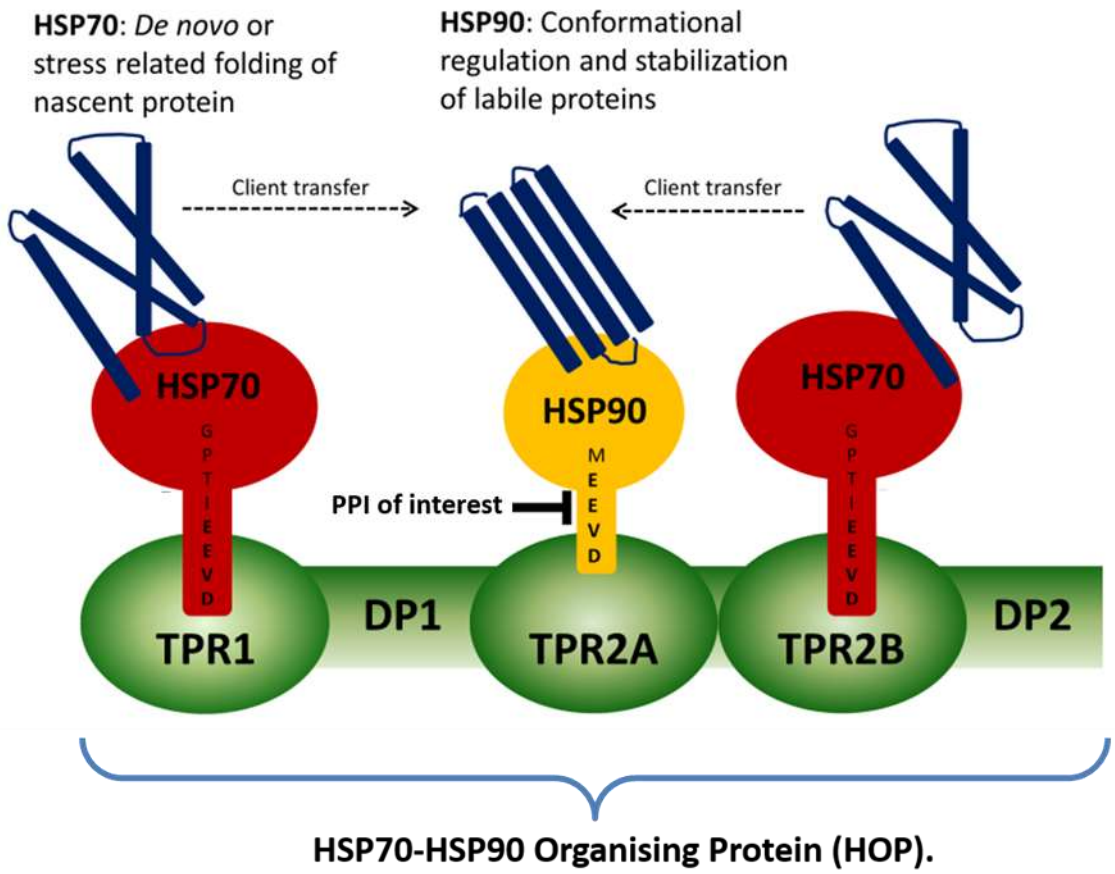

Fig 4.3 Interaction of client protein transferring HOP with chaperones HSP70 and HSP90 during chaperone mediated protein folding.

Previous work conducted in our laboratory identified a small cohort of acid and tetrazole containing fragments (e.g. **4.56** – **4.58**) which bound to the carboxylate clamp of the HOP TPR2A domain. Furthermore, these fragments have displayed weak biological activity against breast cancer cell lines.

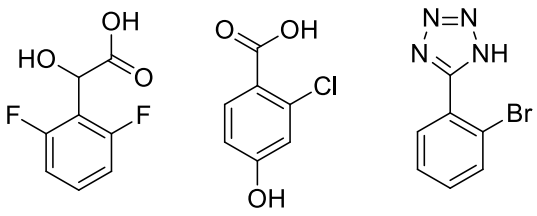

4.56 **4.57** **4.58**

Accordingly, as part of the fragment elaboration phase of this project, we sought to incorporate and combine structural elements of these fragments in order to elucidate an SAR and begin to improve on the anticancer activity of these compounds. We therefore aimed at synthesising a de-halogenated mandelic acid fragment (**4.59**), bioisosteric phenyl tetrazole fragments (**4.60** – **4.61**) and di-halogenated benzyl tetrazole fragments (**4.62** – **4.65**) as analogues of **4.56** – **4.58**.

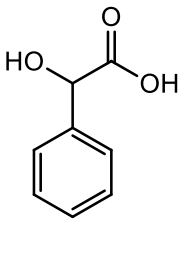

4.59

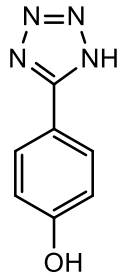

4.60

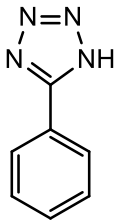

4.61

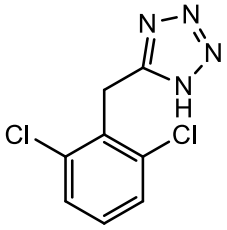

4.62

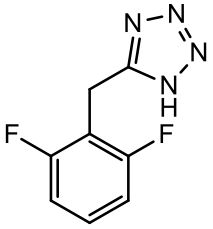

4.63

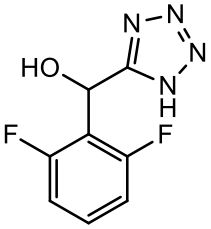

4.64

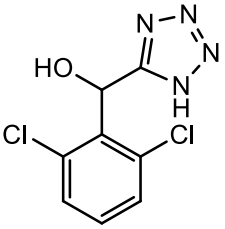

4.65

For the purposes of this project we reasoned the synthetic outline as depicted in **Fig 4.4.** We were particularly interested in utilising the nitrile moiety, which can be derived via dehydration of an amide.[209] Subsequent nitrile hydrolysis would generate an acid[210] (**4.59**) or undergo a 1,3-dipolar cycloaddition to form a tetrazole[211] (**4.60** – **4.65**). We will discuss further the synthetic methods employed from literature to generate the desired fragments.

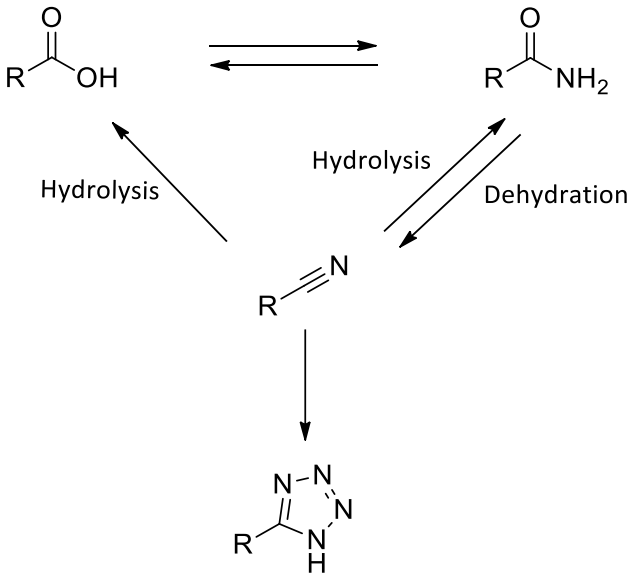

Fig 4.4 Proposed synthetic outline of tetrazole and acid fragments.

4.10 Synthesis of tetrazole and acid fragments (4.59 – 4.60)

In this section we will describe fragment synthesis, discuss the results obtained and characterisation processes used.

4.10.1 Synthesis of 2-hydroxy-2-phenylacetic acid (4.59)

To attain fragment **4.59**, also known as mandelic acid, we hydrolysed the nitrile of commercially available mandelonitrile (**4.66**) using hydrochloric acid to generate a carboxylic acid as depicted in **Scheme 4.1**.

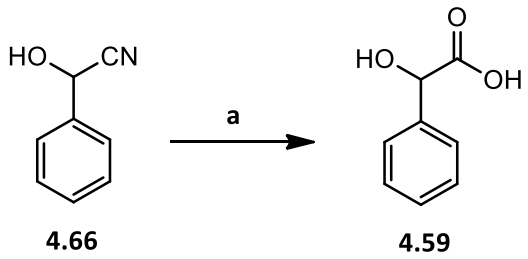

Scheme 4.1 Synthesis of 2-hydroxy-2-phenylacetic acid/mandelic acid (**4.59**).

a) 32% HCl, 16 h at rt then 4 h in reflux

This reaction proceeded smoothly, resulting in the desired product at a low but acceptable yield of 49%.

*4.10.1.1 Characterisation of **4.59***

We confirmed the synthesis of the compound using NMR-analysis and High Res MS. We observed on the ^{1}H-NMR spectrum a singlet signal at 5.13 ppm integrating for one proton, characteristic of the methine proton at **a** (**Fig 4.5a**). The characteristic phenyl signals were present in the aromatic region. We further observed the absence of the characteristic nitrile signal initially present in the ^{13}C-NMR spectrum of mandelonitrile, sighting a new signal at 174.7 ppm, characteristic of the carbonyl group (**Fig 4.5b**). **Fig 4.5c** further confirmed the formation of the α-hydroxy acid at *m/z* 175.0060 $[M+Na]^{+}$, signal representative of a sodium adduct of **4.59**. Obtained results are consistent with reported analyses.[212]

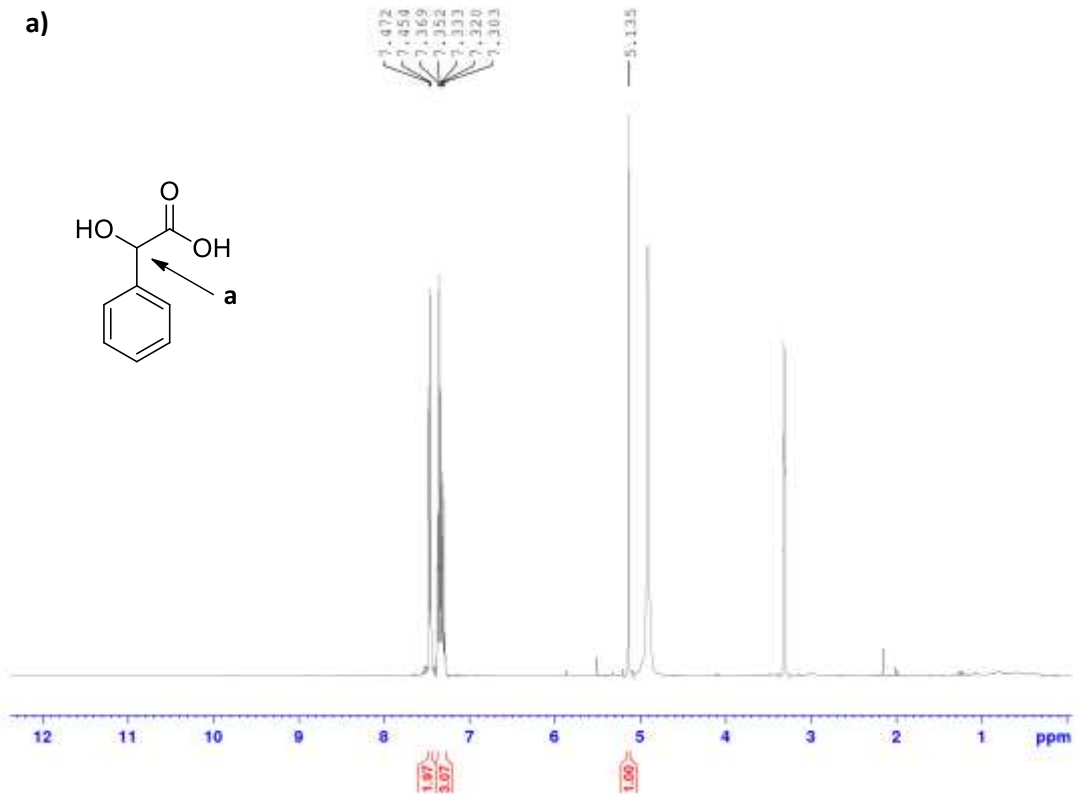

Fig 4.5a ^{1}H-NMR spectrum of **4.59**.

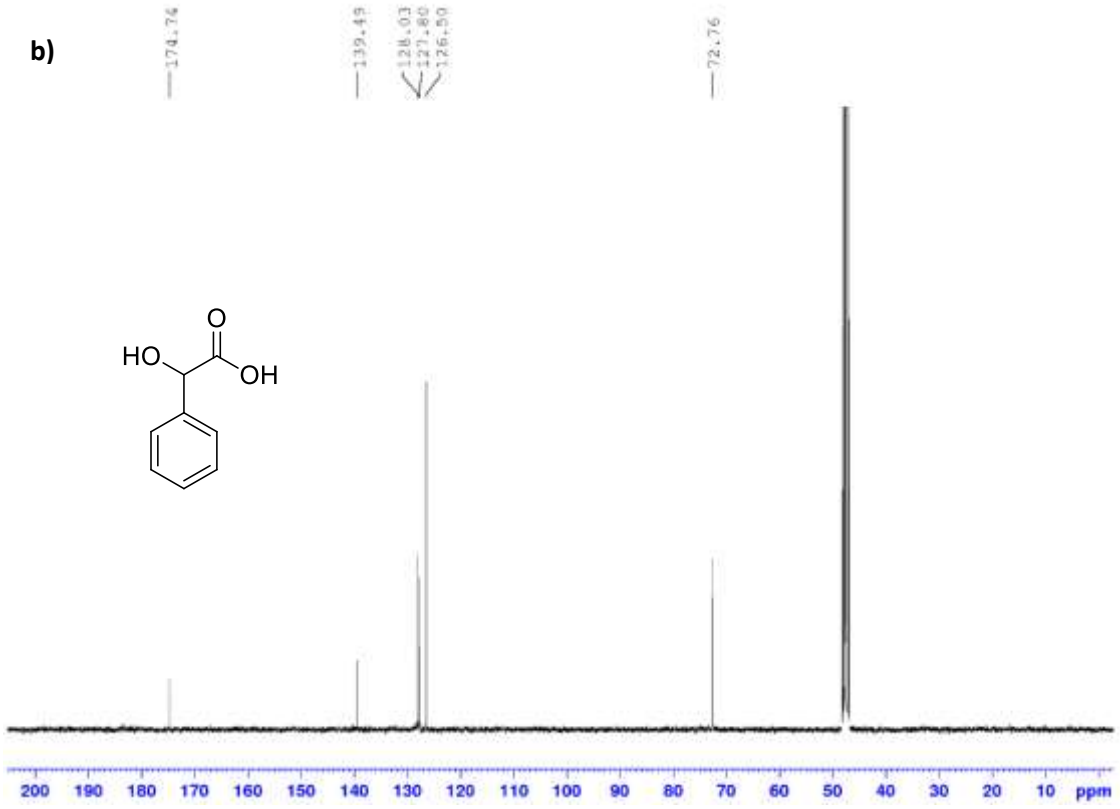

Fig 4.5b ^{13}C-NMR spectrum of **4.59**.

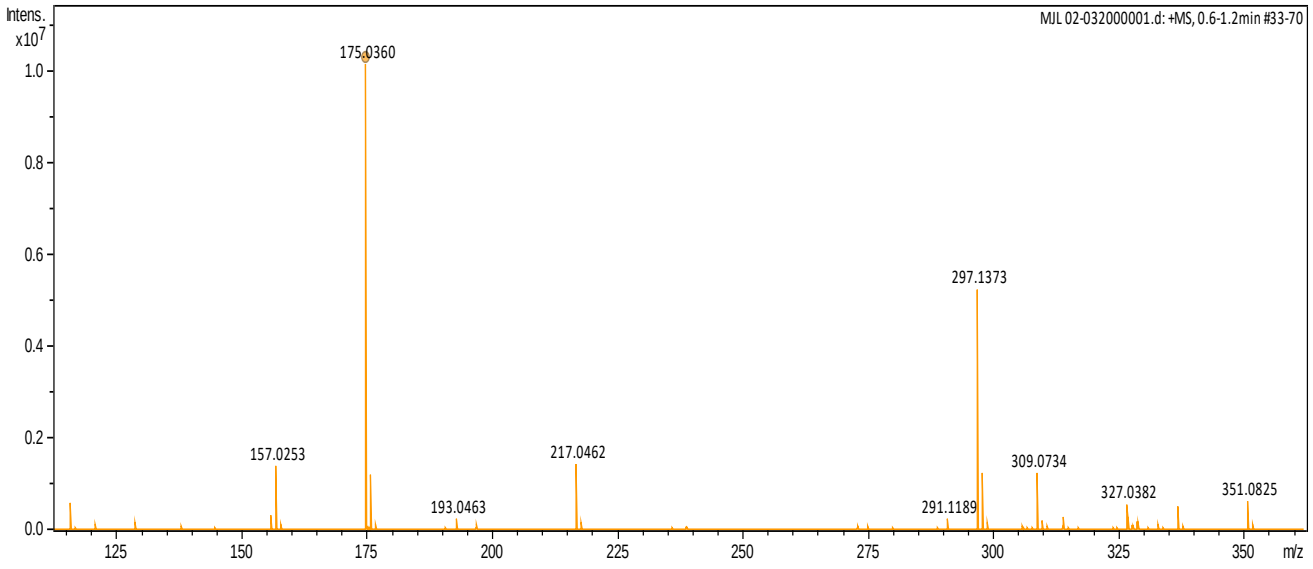

Fig 4.5c High resolution Mass Spectrum of **4.59**.

4.10.2 Synthesis of tetrazole fragments 4.60 – 4.63

To attain these compounds, we employed the 1,3-cycloaddition method outlined by Mohite *et al.* which generates $^{-}N_3$ ions *in situ* utilising ammonium chloride and inorganic NaN_3 with several commercially available nitriles.[213] Anhydrous solvent was used in this reaction so as to restrict the formation of hydrazoic acid during the reaction.[214]

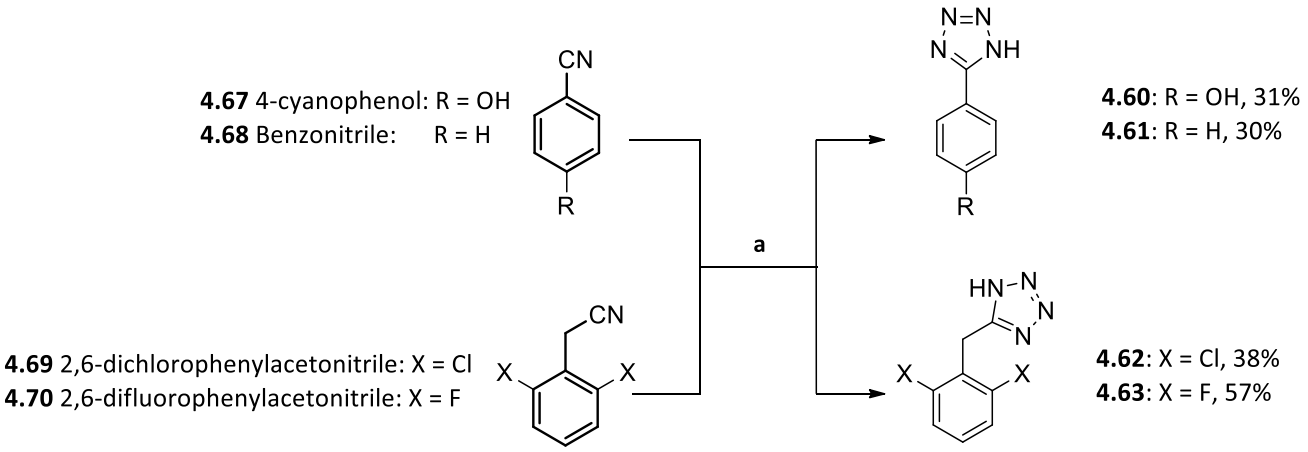

Scheme 4.2 Synthesis of **4.60** - **4.63**.

a) NaN_3, NH_4Cl, *N,N*-dimethylformamide, 7 h, 125 ^{o}C, N_2

Reactions yielding **4.61** – **4.63**, proceeded to completion with no residual starting material after 7 h under an inert nitrogenous atmosphere. We observed higher reaction yields for 1,3-dihalogenated phenyl rings. We suspected that the halogens electron withdrawing nature increased the polarity of the nitrile, thereby encouraging 1,3-cycloaddition to commence. Unlike the other fragments, **4.60** was afforded at 31% yield after 48 h reaction time, with a 30% residue of the initial starting material. The effect of the electron donating OH on the *p*-substituted phenyl is thought to cause this marked difference.

4.10.2.1 Characterisation of 4.60 and 4.61

NMR analysis confirmed synthesis of these fragments. The signals of the phenyl ring protons were identified in the aromatic region of the ^{1}H-NMR spectrum of **4.60** (**Fig 4.6a**). We observed the characteristic tetrazole carbon signal on the ^{13}C-NMR spectrum of **4.60** (**Fig 4.6b**) at 155.4 ppm,

confirming successful 1,3-cycloaddition. The spectra of fragment **4.61** was also consistent with observed characteristic signals. Both fragment results were comparable with published analyses.[215,216]

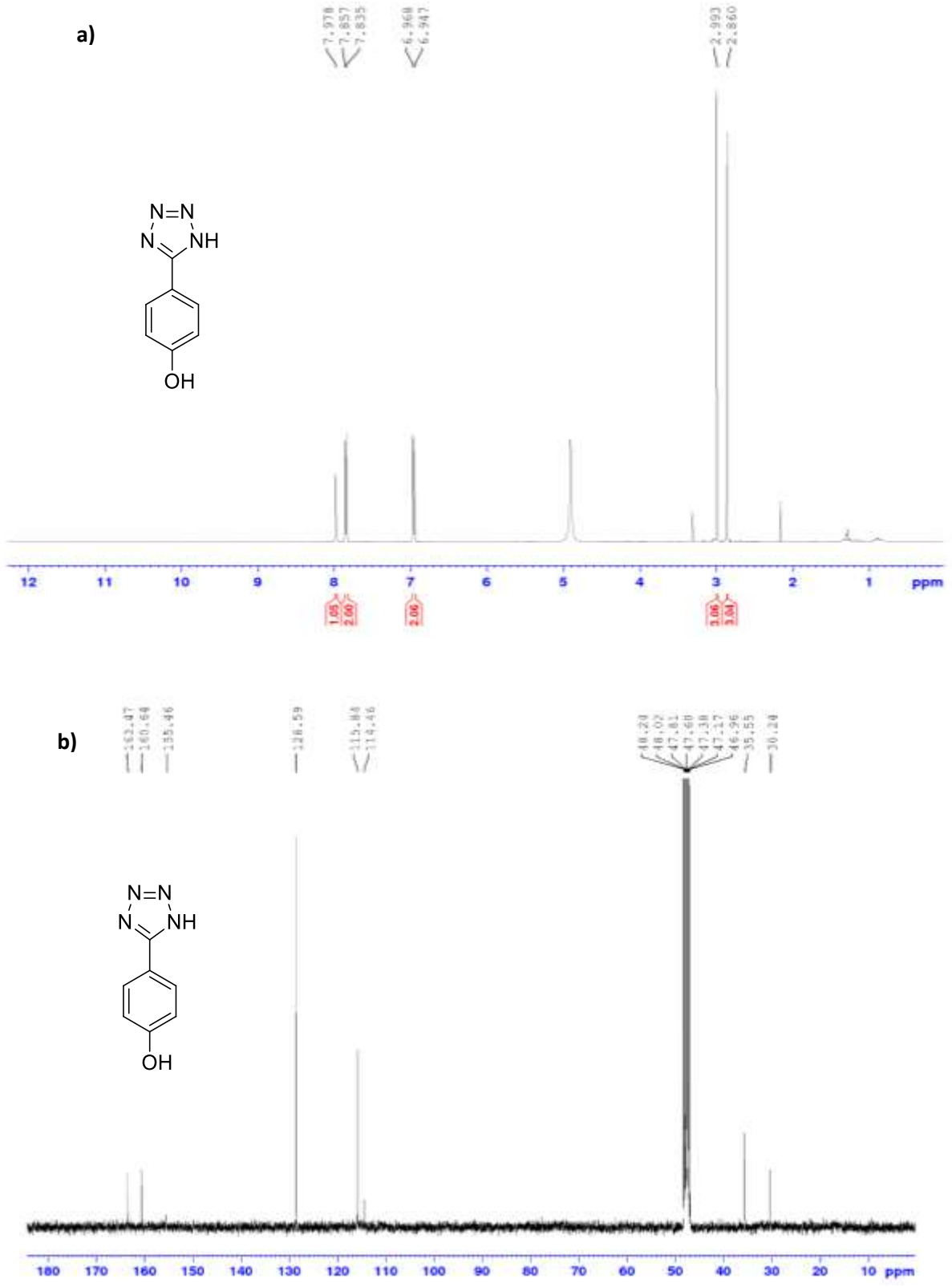

Fig 4.6 a) ^{1}H-NMR and b) ^{13}C-NMR spectra of **4.60**.

An interesting feature of note in **Fig 4.6a** are the signals at 7.97 ppm, 2.99 ppm and 2.86 ppm indicating the presence of a DMF molecule post extraction and purification of the fragment. With studies reporting capacity of the DMF molecule to form hydrogen bonds with polar molecules[217,218], we thought that DMF forms the same interactions with the *p*-hydroxyl group and the NH-group on the tetrazole.

*4.10.2.2 Characterisation of **4.62** and **4.63***

To confirm synthesis of these fragments, NMR-analysis and High Res MS was conducted. An important feature observed from the ^{1}H-NMR spectra of **4.62** compared to the starting material was the up-field shift of the methylene signal to 4.52 ppm (**Fig 4.7a**). The phenyl proton signals were present in the aromatic region. We noted the absence of the characteristic nitrile signal from the ^{13}C-NMR spectrum, sighting a new signal at 154.2 ppm, characteristic of the tetrazole carbon (**Fig 4.7b**). **Fig 4.7c** showed the mass of **4.62** at *m/z* 229.0033 (calcd for $C_8H_7N_4{}^{35}Cl_2$ $[M+H]^+$. Fragment **4.63** displayed similar characteristic NMR signals and the mass spectrum correlated with the predicted molecular formula.

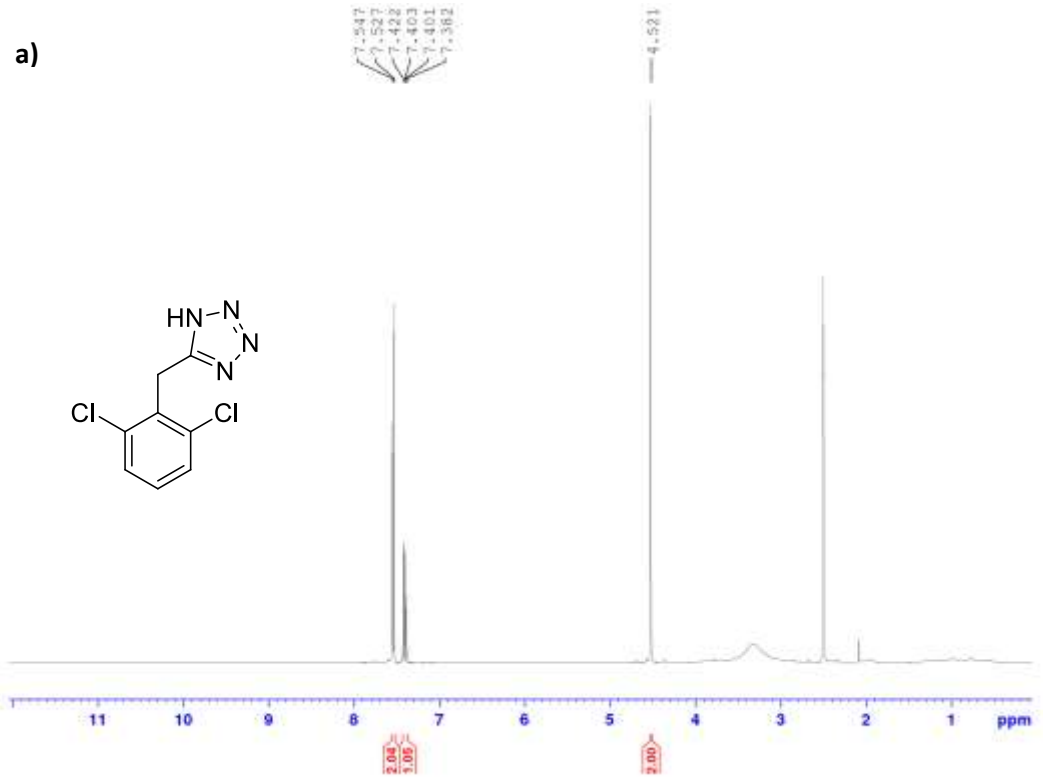

Fig 4.7a ^{1}H-NMR spectrum of **4.62**.

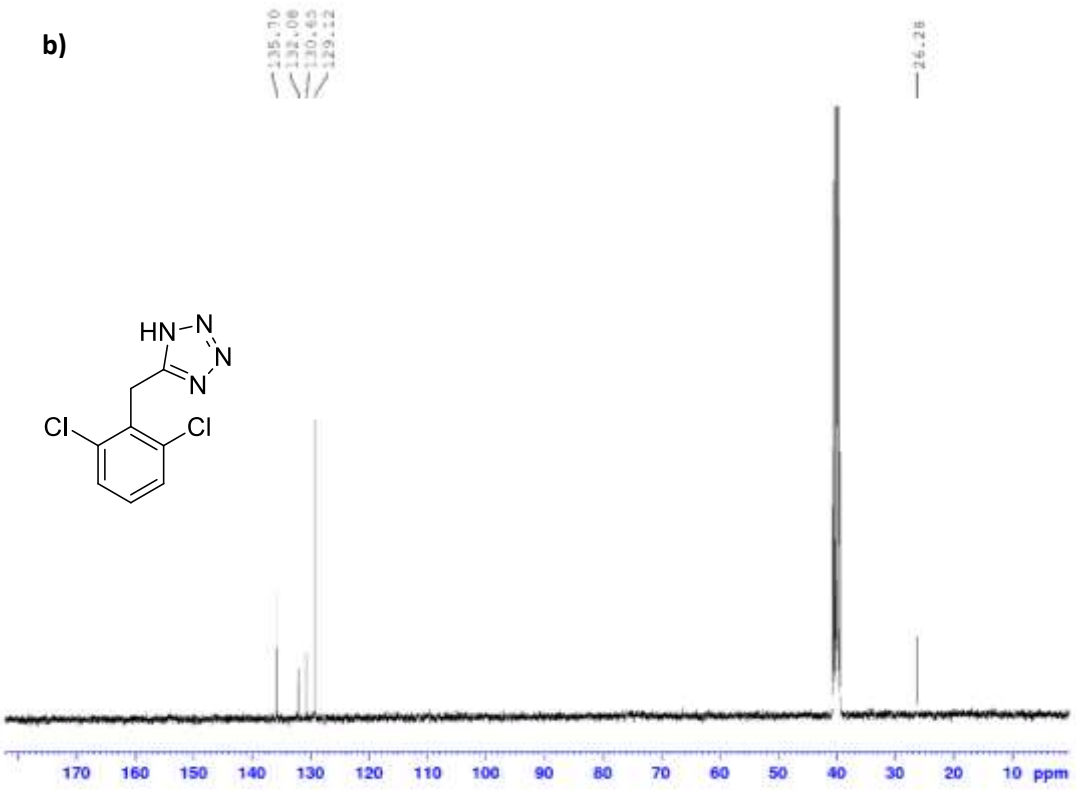

Fig 4.7b ^{13}C-NMR spectrum of **4.62**.

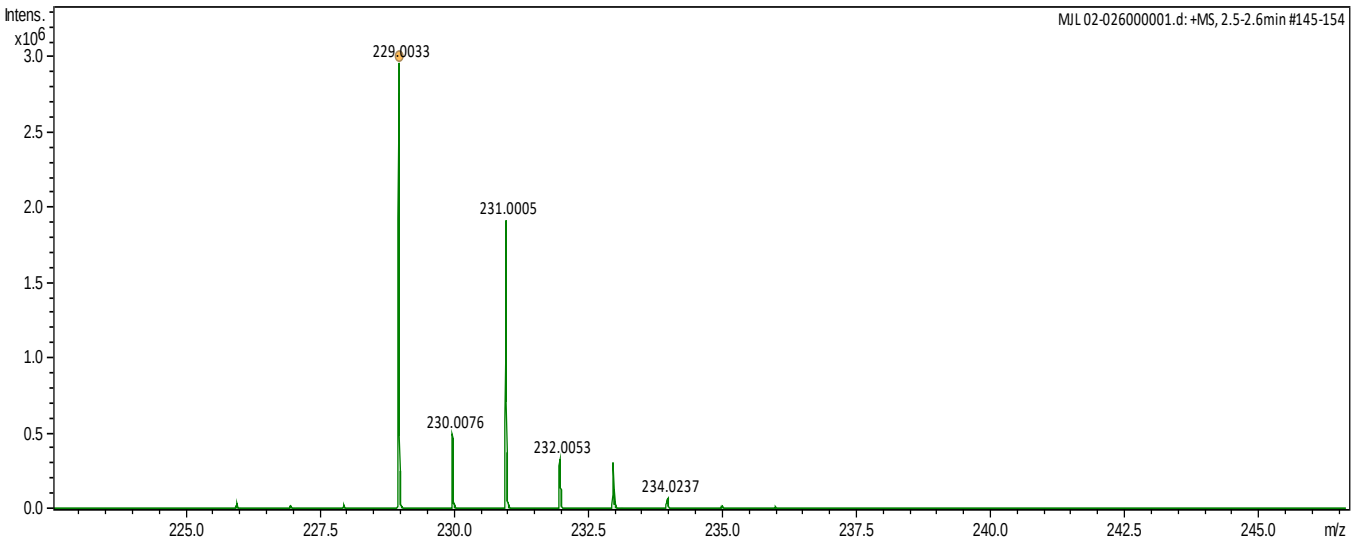

Fig 4.7c High resolution Mass Spectrum of **4.62**.

4.10.3 Synthesis of intermediate fragments 4.71 and 4.72

To access fragments **4.64** and **4.65**, we first had to attain the respective dichloro- and difluoro-substituted derivatives of mandelonitrile (**4.71** and **4.72**) from the corresponding aldehyde precursors (**4.73** and **4.74**). Suzuki *et al.* describes a $ZnCl_2$ catalysed nucleophilic substitution that utilises TMSCN as the source of nucleophilic CN^- ions in the fairly inert solvent, dichloromethane.[219] Following the successful trial reaction using benzaldehyde (**4.75**) to form mandelonitrile, the method was applied on the aldehyde precursors using anhydrous $ZnBr_2$ as the catalyst due to its availability (**Scheme 4.3**).

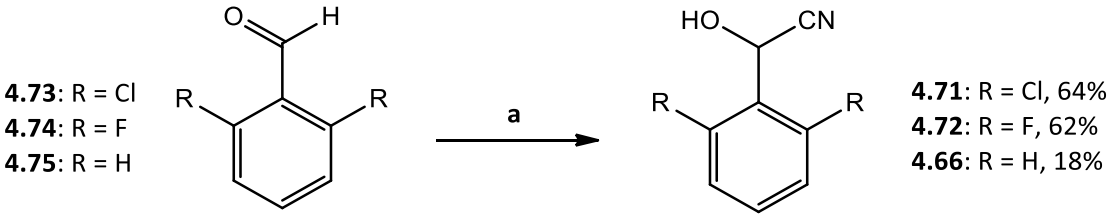

Scheme 4.3 Synthesis of intermediate fragments **4.71** and **4.72**.

a) TMSCN, $ZnBr_2$, Dichloromethane, 4 h, rt, N_2

The reaction yields were above 60% for **4.71** and **4.72**. Mandelonitrile (**4.66**) yield was quite poor at 18%. This difference in yield is thought to be the result of the electron deficient phenyl ring owing to the presence of halogen di-substitution discussed in **4.10.2**.

4.10.3.1 Characterisation of 4.71 and 4.72

NMR analysis was performed, confirming synthesis of compounds. We observed a signal at 6.26 ppm on the ^{1}H-NMR spectrum of **4.71,** characteristic of the methine proton at **a** (**Fig 4.8a**). We further observed a carbon signal at 118.8 ppm on the ^{13}C-NMR spectrum, characteristic of the nitrile (**Fig 4.8b**).Similar characteristic signals were observed on the NMR spectra of fragment **4.72**.

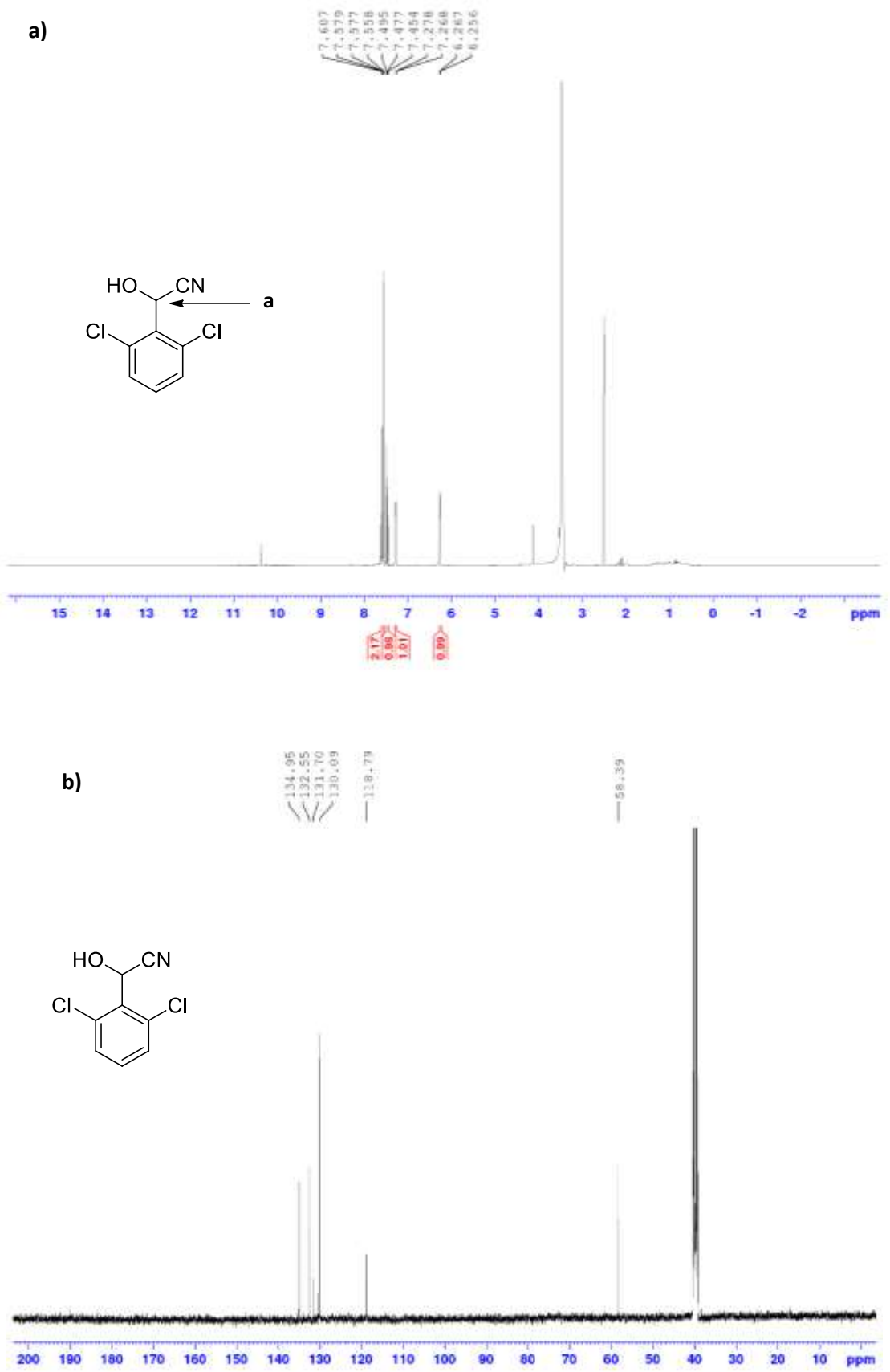

Fig 4.8 a) ^{1}H-NMR and b) ^{13}C-NMR spectra of **4.71**.

4.10.4 Synthesis of fragments 4.64 and 4.65

To access these compounds, we employed the synthetic method described in **4.10.2** to **4.71** and **4.72**. The reactions were unfortunately unsuccessful in affording us the desired fragments. We therefore thought that the presence of the electron donating α-hydroxyl group restricted 1,3-cycloaddition, possibly due to a stable delocalised system of electrons formed with the nitrile.

Though unable to complete synthesis of fragments **4.64** and **4.65** we propose the 1,3-cycloaddition described by Aureggi and Sedelmeier as a potential synthetic route to afford us these fragments. The method utilises diethyl aluminium chloride as a catalyst, activating NaN_3 in an aprotic medium such as toluene and ultimately converting a nitrile into a tetrazole.[220]

4.11 Conclusions

In this chapter we described the applications of tetrazoles in medicinal chemistry. We went on to focus particularly on TNBC and the need for drug treatment specific to cancerous cells and identification of new drug targets for effective treatment. Under the premises of fragment based drug discovery we aimed at synthesising fragments **4.59** – **4.65** as analogues of **4.56** – **4.58** previously prepared in our lab and found to exhibit weak biological activity against cancer cell lines. Fragments **4.59** – **4.63** were successfully synthesised and are currently being characterised for TNBC activity. The results of which will enable us to further describe the SAR of these fragments allowing continued structural optimisation to enhance the binding activity of fragments to the targeted PPI of the HOP complex.

Unfortunately, we were unable to complete the synthesis of fragments **4.64** and **4.65** though having attained the nitrile intermediates (**4.71** and **4.72**) from their corresponding aldehydes.

Chapter 5: Experimental Data

1D and 2D NMR spectra were obtained using either a Bruker Fourier 300 MHz, 400 MHz or 600 MHz Avance II spectrometer. Chemical shifts are reported in ppm with residual reference solvents resonances as follows: Acetone-d_6 δ_H 2.05, δ_C 29.8, 206.2; CD_3OD δ_H 3.31, δ_C 49.0; DMSO δ_H 2.50, δ_C 39.5 ppm.[221] High resolution mass spectrometry was performed on a Waters Synapt G2 TOF instrument with an ESI source. IR spectra were obtained using a Perkin Elmer Spectrum 100 FTIR. Melting points were determined using a Reichert hot stage microscope (Protea Holding Ltd.). Flash column chromatography was performed using Kieselgel 60 (230–400 mesh) silica gel. Distilled solvents were used.

5.1 Synthesis of 1*H*-indole-5-carbonitrile (3.5)

To a stirring mixture of CuI (80 mg, 0.41 mmol) and anhydrous *N,N*-DMF (20 ml) in a 2-neck round bottom flask under a nitrogenous atmosphere was added 5-iodoindole (500 mg, 2.05 mmol), PPh_3 (107 mg, 0.41 mmol) and CuCN (552 mg, 6.17 mmol). Reaction was ran for 24 h at 140 °C. Reaction mixture was allowed to cool. EtOAc was used to extract the organic material, washing with saturated NaCl solution. The extract was dried with anhydrous $MgSO_4$ before concentrating *in vacuo*. Purified compound was attained by flash column chromatography (Hexane: EtOAc, 7:3).

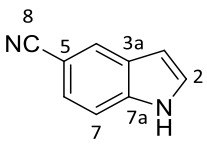

1*H*-indole-5-carbonitrile[124] (**3.5**); brown amorphous solid; yield 77%; IR (cm^{-1}) 3400, 2224, 1610, 1414, 769, 732; ^{1}H NMR (DMSO, 300 MHz): δ_H 11.65 (1H, brs, NH-1), 8.08 (1H, dd, *J* = 1.6, 0.7 Hz, H-4), 7.57 – 7.54 (2H, m, H-2, H-7), 7.41 (1H, dd, *J* = 8.4, 1.6 Hz, H-6), 6.58 (1H, dd, *J* = 3.2, 0.7 Hz, H-3); ^{13}C NMR (DMSO, 75 MHz): δ_C 137.6 (q_C, C-7a), 128.1 (CH, C-2), 127.4 (q_C, C-3a), 125.7 (CH, C-4), 123.7 (CH, C-6), 120.8 (CN, C-8), 112.7 (CH, C-7), 102.1 (CH, C-3), 100.9 (q_C, C-5) ppm.

5.2 General procedure for the synthesis of 3-acetyindoles (3.8 – 3.12)

To a stirring solution of indole (1 eq) and anhydrous DCM (7.5 ml) under nitrogen at 0 °C was added $SnCl_4$ (1.2 eq) after which the ice bath was removed. After 30 min of stirring acetyl chloride (1.2 eq) was added followed by nitromethane (4.5 ml). The reaction was allowed to proceed for 4 h before quenching with ice. Organic material was extracted with EtOAc, washing with saturated NaCl solution. The extract was dried over $MgSO_4$ before concentrating *in vacuo*. Flash column chromatography was performed to purify the compound (varying proportions of Hexane: EtOAc).

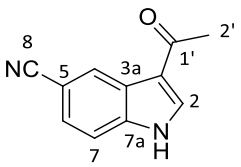

3-acetyl-1*H*-indole-5-carbonitrile (**3.8**); cream amorphous solid; yield 46%; IR (cm^{-1}) 3109, 2220, 1739, 1628, 1615, 1444, 1376, 805, 655; ^1H NMR (DMSO, 300 MHz): δ_H 12.40 (1H, brs, NH-1), 8.52 (1H, dd, *J* = 1.6, 0.8 Hz, H-4), 8.51 (1H, s, H-2), 7.65 (1H, dd, *J* = 8.5, 0.8 Hz, H-7), 7.58 (1H, dd, *J* = 8.5, 1.6 Hz, H-6), 2.48 (3H, s, H-2'); ^{13}C NMR (DMSO, 75 MHz): δ_C 192.9 (CO, C-1'), 138.5 (q_C, C-7a), 136.6 (CH, C-4), 126.3 (CH, C-2), 125.7 (CH, C-6), 125.0 (q_C, C-5), 120.2 (CN, C-8), 116.9 (q_C, C-3), 113.7 (CH, C-7), 103.9 (q_C, C-3a), 27.3 (CH_3, C-2') ppm.

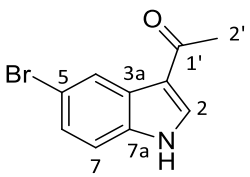

1-(5-bromo-1*H*-indol-3-yl)ethanone[116] (**3.9**); yield 69%; ^1H NMR (CD_3OD, 300 MHz): δ_H 8.37 (1H, s, H-2), 8.18 (1H, s, H-4), 7.36 – 7.34 (1H, m, H-6, H-7), 2.50 (3H, s, H-2'); ^{13}C NMR (DMSO, 75 MHz): δ_C 135.7 (q_C, C-3a), 135.1 (CH, C-4), 127.1 (q_C, C-7a), 125.7 (CH, C-6), 124.0 (CH, C-2), 116.5 (q_C, C-3), 115.2 (q_C, C-5), 113.1 (CH, C-7), 22.8 (CH_3, C-2') ppm.

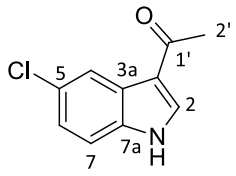

1-(5-chloro-1*H*-indol-3-yl)ethanone (**3.10**); cream amorphous solid; yield 45%; IR (cm^{-1}) 3155, 2923, 1716, 1626, 1522, 1427, 940, 892, 793, 631; ^{1}H NMR (DMSO, 400 MHz): δ_H 12.10 (1H, brs, NH-1), 8.38 (1H, d, *J* = 3.1 Hz, H-2), 8.14 (1H, d, *J* = 2.1 Hz, H-4), 7.49 (1H, d, *J* = 8.6 Hz, H-7), 7.22 (1H, dd, *J* = 8.6, 2.1 Hz, H-6), 2.45 (3H, s, H-2'); ^{13}C NMR (DMSO, 100 MHz): δ_C 193.2 (CO, C-1'), 136.2 (CH, C-2), 135.6 (q_C, C-7a), 126.9 (q_C, C-5), 126.8 (q_C, C-3a), 123.2 (CH, C-6), 120.8 (CH, C-4), 116.8 (q_C, C-3), 114.2 (CH, C-7), 27.6 (CH_3, C-2') ppm.

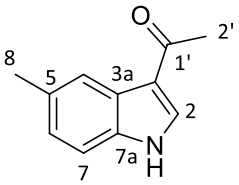

1-(5-methyl-1*H*-indol-3-yl)ethanone (**3.11**); brown amorphous solid; yield 19%; IR (cm^{-1}) 3132, 2918, 1621, 1431, 1374, 943, 798, 757; ^{1}H NMR (DMSO, 300 MHz): δ_H 11.77 (1H, brs, NH-1), 8.22 (1H, s, H-2), 7.98 (1H, m, H-4), 7.34 (1H, d, *J* = 8.3 Hz, H-7), 7.02 (1H, dd, *J* = 8.3, 1.6 Hz, H-6), 2.42 (3H, s, H-2'), 2.39 (3H, s, H-8); ^{13}C NMR (DMSO, 75 MHz): δ_C 193.0 (CO, C-1'), 135.3 (q_C, C-7a), 134.6 (CH, C-2), 130.7 (q_C, C-5), 126.0 (q_C, C-3a), 124.5 (CH, C-6), 121.4 (CH, C-4), 117.0 (q_C, C-3), 112.1 (CH, C-7), 27.6 (CH_3, C-2'), 21.7 (CH_3, C-8) ppm.

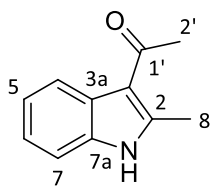

1-(2-methyl-1*H*-indol-3-yl)ethanone (**3.12**); brown amorphous solid; yield 30%; IR (cm^{-1}) 3162, 3050, 2970, 1609, 1528, 1444, 1413, 1390, 969, 905, 739; ^{1}H NMR (DMSO, 400 MHz): δ_H 11.81 (1H, brs, NH-1), 8.02 – 8.00 (1H, m, H-4), 7.37 – 7.35 (1H, m, H-7), 7.14 – 7.11 (2H, m, H-5, H-6), 2.67 (3H, s, H-8), 2.51 (3H, s, H-2'); ^{13}C NMR (DMSO, 100 MHz): δ_C 193.5 (CO, C-1'), 144.6 (q_C, C-2), 135.1 (q_C, C-7a), 127.3 (q_C, C-3a), 122.2 (CH, C-6), 121.7 (CH, C-5), 121.0 (CH, C-4), 113.9 (q_C, C-3), 111.6 (CH, C-7), 31.3 (CH_3, C-2'), 15.4 (CH_3, C-8) ppm.

5.3 Synthesis of 1-(5-methoxy-1*H*-indol-3-yl)ethanone (3.13)

To a stirring mixture of CuI (484 mg, 2 eq) in anhydrous *N,N*-DMF (15 ml) was added 1-(5-bromo-1*H*-indol-3-yl)ethanone (**3.9**, 250 mg, 1 eq). Sodium methoxide [sodium (362 mg, 15 eq), absolute methanol (10 ml)] was then added and the reaction allowed to proceed for 6 h under reflux. Reaction mixture was allowed to cool before filtering and concentrating *in vacuo*. 10% NaOH (30 ml) was added and extraction with EtOAc performed. The mixture was dried over $MgSO_4$ then purified by flash column chromatography (DCM: EtOAc, 4:1).

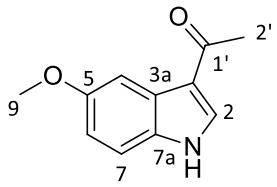

1-(5-methoxy-1*H*-indol-3-yl)ethanone (**3.13**); brown amorphous solid; yield 20%; IR (cm^{-1}) 3150, 2934, 1613, 1518, 1427, 804, 652, 587; ^1H NMR (CD_3OD, 300 MHz): δ_H 8.08 (1H, s, H-2), 7.77 (1H, d, *J* = 2.4 Hz, H-4), 7.32 (1H, d, *J* = 8.9 Hz, H-7), 6.86 (1H, dd, *J* = 8.9, 2.4 Hz, H-6), 3.83 (3H, s, H-9), 2.50 (3H, s, H-2'); ^{13}C NMR (CD_3OD, 75 MHz): δ_C 195.0 (CO, C-1'), 156.2 (q_C, C-5), 134.3 (CH, C-2), 131.9 (q_C, C-7a), 126.2 (q_C, C-3a), 116.9 (q_C, C-3), 112.9 (CH, C-6), 112.1 (CH, C-7), 103.1 (CH, C-4), 54.6 (CH_3, C-9), 25.6 (CH_3, C-2') ppm.

5.4 General procedure for the synthesis of α-brominated 3-acetylindoles (3.15 – 3.20)

3-acetylindole (1 eq) in $CHCl_3$ (20 ml) was added to a stirring mixture of $CuBr_2$ (1.8 eq) in EtOAc (15 ml) under reflux. Reaction progressed at 75 °C, monitored by TLC observing for di-bromination. Reaction mixture was allowed to cool prior to washing with saturated NaCl solution and drying over $MgSO_4$. Following *in vacuo* concentration of crude product, purification was performed using flash column chromatography.

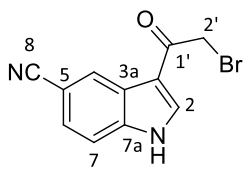

3-(2-bromoacetyl)-1*H*-indole-5-carbonitrile (**3.15**); cream amorphous solid; Inseparable mixture from 3-acetyl-1H-indole-5-carbonitrile (**3.8**), taken forward into next step without further purification.

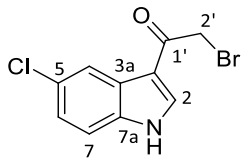

2-bromo-1-(5-chloro-1*H*-indol-3-yl)ethanone[115] (**3.16**); cream amorphous solid; yield 30%; IR (cm^{-1}) 3167, 2933, 1709, 1633, 1515, 1426, 1386, 806, 758, 626, 583; ^{1}H NMR (DMSO, 300 MHz): δ_H 12.31 (1H, brs, NH-1), 8.53 (1H, d, *J* = 3.0 Hz, H-2), 8.12 (1H, d, *J* = 2.1 Hz, H-4), 7.53 (1H, d, *J* = 8.6 Hz, H-7), 7.26 (1H, dd, *J* = 8.6, 2.1 Hz, H-6), 4.66 (2H, s, H-2'); ^{13}C NMR (DMSO, 75 MHz): δ_C 186.9 (CO, C-1'), 137.0 (CH, C-2), 135.7 (q_C, C-7a), 127.4 (q_C, C-5), 127.1 (q_C, C-3a), 123.7 (CH, C-6), 120.8 (CH, C-4), 114.5 (CH, C-7), 113.6 (q_C, C-3), 33.9 (CH_2, C-2') ppm.

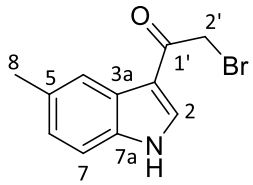

2-bromo-1-(5-methyl-1*H*-indol-3-yl)ethanone (**3.17**); orange amorphous solid; yield 19%; IR (cm^{-1}) 3185, 2919, 1643, 1514, 1430, 1365, 801, 761, 672; ^{1}H NMR (CH_3OD, 300 MHz): δ_H 8.21 (1H, s, H-2), 8.03 (1H, s, H-4), 7.34 (1H, d, *J* = 8.3 Hz, H-7), 7.09 (1H, d, *J* = 8.3 Hz, H-6), 4.47 (2H, s, H-2'), 2.45 (3H, s, H-8); ^{13}C NMR (CH_3OD, 75 MHz): δ_C 188.0 (CO, C-1'), 135.4 (q_C, C-7a), 134.6 (CH, C-2), 131.9 (q_C, C-5), 126.0 (q_C, C-3a), 124.8 (CH, C-6), 121.2 (CH, C-4), 113.6 (q_C, C-3), 111.3 (CH, C-7), 31.1 (CH_2, C-2'), 20.4 (CH_3, C-8) ppm.

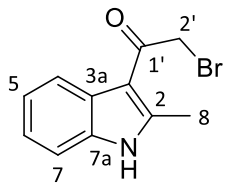

2-bromo-1-(2-methyl-1*H*-indol-3-yl)ethanone (**3.18**); brown amorphous solid; yield 44%; IR (cm^{-1}) 3302, 3114, 2946, 1715, 1624, 1454, 1411, 980, 890, 757, 589; ^{1}H NMR (CD_3OD, 300 MHz): δ_H 7.97 – 7.94 (1H, m, H-4), 7.38 – 7.34 (1H, m, H-7), 7.21 – 7.17 (2H, m, H-5, H-6), 4.51 (2H, s, H-2'), 2.74 (3H, s, H-8); ^{13}C NMR (CD_3OD, 75 MHz): δ_C 188.1 (q_C, C-1'), 146.6 (q_C, C-2), 135.3 (q_C, C-7a), 126.6 (q_C, C-3a), 122.2 (CH, C-6), 121.8 (CH, C-5), 120.5 (CH, C-4), 110.9 (q_C, C-3), 34.4 (CH_2, C-2'), 14.0 (CH_3, C-8) ppm.

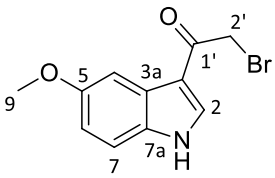

2-bromo-1-(5-methoxy-1*H*-indol-3-yl)ethanone (**3.19**); cream amorphous solid; yield 37.1%; IR (cm^{-1}) 3186, 2928, 1639, 1514, 1426, 1029, 951, 920, 886, 743, 670; ^{1}H NMR (Acetone-d_6, 300 MHz): δ_H 11.07 (1H, brs, NH-1), 8.34 (1H, d, *J* = 3.3 Hz, H-2), 7.82 (1H, d, *J* = 2.6 Hz, H-4), 7.43 (1H, d, *J* = 8.9 Hz, H-7), 6.89 (1H, dd, *J* = 8.9, 2.6 Hz, H-6), 4.51 (2H, s, H-2'), 3.84 (3H, s, H-9); ^{13}C NMR (Acetone-d_6, 75 MHz): δ_C 186.1 (q_C, C-1'), 156.4 (q_C, C-5), 134.0 (CH, C-2), 131.8 (q_C, C-7a), 126.9 (q_C, C-3a), 114.1 (q_C, C-3), 113.5 (CH, C-6), 112.8 (CH, C-7), 103.2 (CH, C-4), 54.9 (CH_3, C-9), 32.2 (CH_2, C-2') ppm.

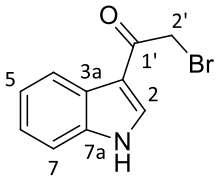

2-bromo-1-(1*H*-indol-3-yl)ethanone (**3.20**); yellow amorphous solid; yield 17%; IR (cm^{-1}) 1729, 1625, 1517, 1426, 1388, 1236, 745, 678; ^{1}H NMR (DMSO, 400 MHz): δ_H 12.15 (1H, s, NH-1), 8.48 (1H, d, *J* = 3.2 Hz, H-2), 8.16 – 8.14 (1H, m, H-4), 7.51 – 7.49 (1H, m, H-7), 7.26 – 7.21 (2H, m, H-5, H-6), 4.65 (2H, s, H-2'); ^{13}C NMR (DMSO, 100 MHz): δ_C 186.9 (CO, C-1'), 137.2 (q_C, C-7a), 135.8 (CH, C-2), 125.9 (q_C, C-3a), 123.7 (CH, C-4), 122.6 (CH, C-6), 121.7 (CH, C-5), 114.0 (q_C, C-3), 112.8 (CH, C-7), 34.0 (CH_2, C-2') ppm.

5.5 General procedure for the synthesis of compounds 3.21 and 3.24 – 3.32

A relevant nucleophile (2 eq) was added to a stirring mixture of α-brominated 3-acetylindole (1 eq) and K_2CO_3 (2 eq) in acetone. The reaction was stopped after 5 h at 60 ° C, save for **3.21** that reacted for 36 h. The acetone was removed *in vacuo* before extracting the organic material with EtOAc and washing with saturated NaCl solution. Flash column chromatography was used to purify compounds followed by crystallisation from EtOAc, washing with cold $CHCl_3$.

NB: Yields for compounds **3.21**, **3.24** and **3.27** could not be accurately calculated owing to the use of impure **3.15**.

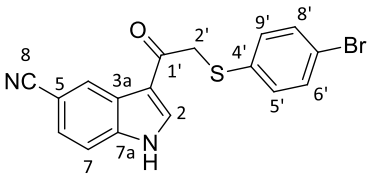

3-(2-((4-bromophenyl)thio)acetyl)-1*H*-indole-5-carbonitrile (**3.21**); cream amorphous solid; mp 242 – 246 °C; IR (cm^{-1}) 3133, 2931, 2221, 1784, 1615, 1523, 1440, 1373, 805, 784, 637; ^{1}H NMR (DMSO, 400 MHz): δ_H 12.56 (1H, brs, NH-1), 8.67 (1H, s, H-2), 8.48 (1H, brs, H-4), 7.68 (1H, d, *J* = 8.4 Hz, H-7), 7.61 (1H, dd, *J* = 8.4, 1.5 Hz, H-6), 7.48 – 7.46 (2H, m, H-6', H-8'), 7.34 – 7.32 (2H, m, H-5', H-9'), 4.52 (2H, s, H-2'); ^{13}C NMR (DMSO, 100 MHz): δ_C 189.2 (CO, C-1'), 138.5 (q_C, C-7a), 137.2 (CH, C-2), 135.8 (q_C, C-4'), 131.7 (CH, C-6', C-8'), 130.0 (CH, C-5', C-9'), 126.2 (CH, C-4), 126.0 (CH, C-6), 125.2 (q_C, C-3a), 120.0 (CN, C-8), 118.7 (q_C, C-7'), 115.1 (q_C, C-3), 113.9 (CH, C-7), 104.3 (q_C, C-5), 39.6***** (CH_2, C-2') ppm.

*****resolved by HSQC

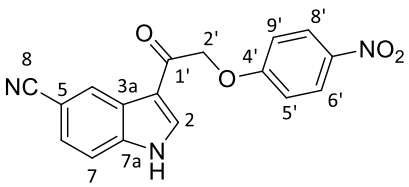

3-(2-(4-nitrophenoxy)acetyl)-1*H*-indole-5-carbonitrile (**3.24**); cream amorphous solid; mp 254 – 256 °C; IR (cm^{-1}) 3180, 3116, 2994, 2216, 1729, 1657, 1505, 1430, 1344, 1261, 1239, 945, 779; ^{1}H NMR (DMSO, 400 MHz): δ_H 8.63 (1H, s, H-2), 8.46 (1H, d, *J* = 1.4 Hz, H-4), 8.18 (2H, m, H-6', H-8'), 7.70 (1H, d, *J* = 8.5 Hz, H-7), 7.61 (1H, dd, *J* = 8.5, 1.4 Hz, H-6), 7.16 (2H, m, H-5', H-9'), 5.54 (2H, s, H-2'); ^{13}C NMR (DMSO, 100 MHz): δ_C 189.1 (CO, C-1'), 164.0 (q_C, C-4'), 141.5 (q_C, C-7'), 138.7 (q_C, C-7a), 136.9 (CH, C-2), 126.7 (CH, C-4), 126.6 (CH, C-6), 126.3 (CH, C-6', C-8'), 125.5 (q_C, C-3a), 120.5 (CN, C-8), 115.7 (CH, C-5', C-9'), 114.4 (CH, C-7), 113.7 (q_C, C-3), 104.8 (q_C, C-5), 70.8 (CH_2, C-2') ppm; HRESMS *m/z* 320.0676 (calcd for $C_{17}H_{10}N_3O_4$ $[M+H]^-$ 320.0671).

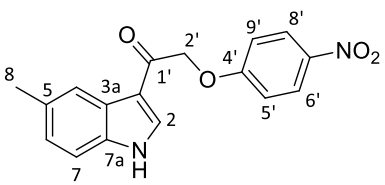

1-(5-methyl-1*H*-indol-3-yl)-2-(4-nitrophenoxy)ethanone (**3.25**); orange crystalline solid; yield 82%; mp 235 – 237 °C; IR (cm^{-1}) 3253, 2920, 2854, 1709, 1650, 1591, 1422, 1339, 1251, 1234, 820, 750, 689; ^{1}H NMR (DMSO, 400 MHz): δ_H 12.02 (1H, brs, NH-1), 8.44 (1H, s, H-2), 8.21 – 8.19 (2H, m, H-6', H-

8'), 7.94 (1H, s, H-4), 7.39 (1H, d, *J* = 8.3 Hz, H-7), 7.18 – 7.15 (2H, m, H-5', H9'), 7.07 (1H, d, *J* = 8.3 Hz, H-6), 5.52 (2H, s, H-2'), 2.39 (3H, s, H-8); ^{13}C NMR (DMSO, 100 MHz): δ_C 188.6 (CO, C-1'), 164.2 (q_C, C-4'), 141.4 (q_C, C-7'), 135.2 (q_C, C-7a), 134.5 (CH, C-2), 131.4 (q_C, C-5), 126.2 (CH, C-6', C-8'), 126.1 (q_C, C-3a), 125.1 (CH, C-6), 121.3 (CH, C-4), 115.7 (CH, C-5', C-9'), 113.2 (q_C, C-3), 112.4 (CH, C-7), 70.7 (CH_2, C-2'), 21.7 (CH_3, C-8) ppm; HRESMS *m/z* 311.1025 (cald for $C_{17}H_{15}N_2O_4$ $[M+H]^+$ 311.1032).

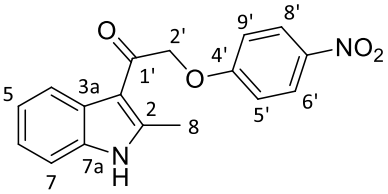

1-(2-methyl-1*H*-indol-3-yl)-2-(4-nitrophenoxy)ethanone (**3.26**); yellow amorphous solid; yield 98%; mp 217 – 219 °C; IR (cm^{-1}) 3274, 2923, 1637, 1590, 1508, 1457, 1333, 1250, 974, 838, 740; ^{1}H NMR (Acetone-d_6, 600 MHz): δ_H 11.08 (1H, brs, NH-1), 8.22 – 8.20 (2H, m, H-6', H-8'), 8.06 – 8.04 (1H, m, H-4), 7.45 – 7.43 (1H, m, H-7), 7.21 – 7.19 (2H, m, H-5, H-6), 7.19 – 7.17 (2H, m, H-5', H-9'), 5.56 (2H, s, H-2'), 2.81 (3H, s, H-8); ^{13}C NMR (Acetone-d_6, 150 MHz): δ_C 188.3 (CO, C-1'), 164.2 (q_C, C-4'), 145.0 (q_C, C-2), 141.4 (q_C, C-7'), 135.3 (q_C, C-7a), 126.7 (q_C, C-3a), 125.5 (CH, C-6', C-8'), 122.3 (CH, C-5), 121.9 (CH, C-5), 121.0 (CH, C-4), 115.1 (CH, C-5', C-9'), 111.4 (CH, C-7), 111.3 (q_C, C-3), 72.3 (CH_2, C-2'), 14.6 (CH_3, C-8) ppm; HRESMS *m/z* 311.1026 (cald for $C_{17}H_{15}N_2O_4$ $[M+H]^+$ 311.1032).

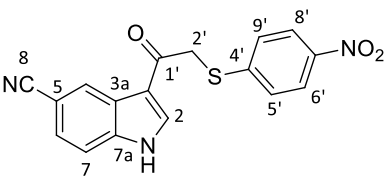

3-(2-((4-nitrophenyl)thio)acetyl)-1*H*-indole-5-carbonitrile (**3.27**); yellow amorphous solid; mp 226 – 230 °C; IR (cm^{-1}) 3182, 2920, 2219, 1637, 1580, 1513, 1434, 1335, 843, 742; ^{1}H NMR (Acetone-d_6, 300 MHz): δ_H 11.65 (1H, brs, NH-1), 8.71 (1H, s, H-2), 8.64 (1H, d, *J* = 1.4 Hz, H-4), 8.16 – 8.13 (2H, m, H-6', H-8'), 7.75 (1H, d, *J* = 8.6 Hz, H-7), 7.65 – 7.62 (2H, m, H-5', H-9'), 7.59 (1H, dd, *J* = 8.*6*, 1.4 Hz, H-6), 4.72 (2H, s, H-2'); ^{13}C NMR (DMSO, 100 MHz): δ_C 188.8 (CO, C-1'), 147.7 (q_C, C-4'), 145.0 (q_C, C-7'), 138.9 (q_C, C-7a), 137.9 (CH, C-2), 126.9 (CH, C-5', C-9'), 126.6 (CH, C-4), 126.5 (CH, C-6), 125.0 (q_C, C-3a), 124.3 (CH, C-6', C-8'), 120.4 (CN, C-8), 115.5 (q_C, C-3) 114.4 (CH, C-7), 104.8 (q_C, C-5), 39.3***** (CH_2, C-2') ppm; HRESMS *m/z* 336.0454 (calcd for $C_{17}H_{10}N_3O_3S$ $[M+H]^-$ 336.0443).

*****resolved by HSQC

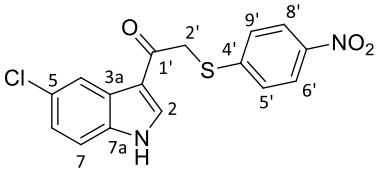

1-(5-chloro-1*H*-indol-3-yl)-2-((4-nitrophenyl)thio)ethanone (**3.28**); yellow amorphous solid; yield 46%; mp 249 – 252 °C; IR (cm^{-1}) 3170, 3121, 2922, 1713, 1637, 1577, 1507, 1424, 1329, 843, 739, 680; ^{1}H NMR (Acetone-d_6, 600 MHz): δ_H 11.37 (1H, brs, NH-1), 8.59 (1H, d, *J* = 2.4 Hz, H-2), 8.28 (1H, d, *J* = 2.1 Hz, H-4), 8.16 – 8.13 (2H, m, H-5', H-9'), 7.64 – 7.61 (2H, m, H-6', H-8'), 7.57 (1H, d, *J* = 8.7 Hz, H-7), 7.27 (1H, dd, *J* = 8.7, 2.1 Hz, H-6), 4.69 (2H, s, H-2'); ^{13}C NMR (Acetone-d_6, 150 MHz): δ_C 188.7 (CO, C-1'), 148.3 (q_C, C-4'), 145.9 (q_C, C-7'), 136.0 (CH, C-2), 135.8 (q_C, C-7a), 128.5 (q_C, C-5), 127.9 (q_C, C-3a), 127.3 (CH, C-6', C-8'), 124.5 (CH, C-5', C-9'), 124.3 (CH, C-6), 121.9 (CH, C-4), 115.9 (q_C, C-3), 114.5 (CH, C-7), 39.9 (CH_2, C-2') ppm; HRESMS *m/z* 347.0255 (calcd for $C_{16}H_{12}N_2O_3S^{35}Cl$ $[M+H]^+$ 347.0257).

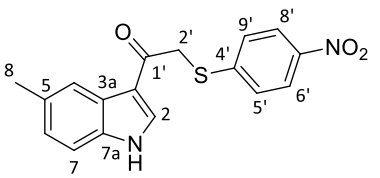

1-(5-methyl-1*H*-indol-3-yl)-2-((4-nitrophenyl)thio)ethanone (**3.29**); yellow amorphous solid; yield 62%; mp 218 – 221 °C; IR (cm^{-1}) 3139, 3112, 2914, 1703, 1611, 1502, 1431, 1338, 960, 800, 739; ^{1}H NMR (DMSO, 400 MHz): δ_H 12.02 (1H, brs, NH-1), 8.52 (1H, m, H-2), 8.14 – 8.11 (2H, m, H-6', H-8'), 7.95 (1H, s, H-4), 7.60 – 7.56 (2H, m, H-5', H-9'), 7.37 (1H, dd, *J* = 8.1, 3.3 Hz, H-7), 7.05 (1H, d, *J* = 8.1, 3.3 Hz, H-6), 4.70 (2H, s, H-2'), 2.39 (3H, s, H-8); ^{13}C NMR (DMSO, 100 MHz): δ_C 188.3 (CO, C-1'), 148.1 (q_C, C-4'), 144.9 (q_C, C-7'), 135.6 (CH, C-2), 135.4 (q_C, C-7a), 131.4 (q_C, C-5), 126.8 (CH, C-5', C-9'), 126.1 (q_C, C-3a), 125.0 (CH, C-6), 124.2 (CH, C-6', C-8'), 121.4 (CH, C-4), 114.9 (q_C, C-3), 112.4 (CH, C-7), 39.2 (CH_2, C-2'), 21.8 (CH_3, C-8) ppm; HRESMS *m/z* 327.0798 (calcd for $C_{17}H_{15}N_2O_3S$ $[M+H]^+$ 327.0803).

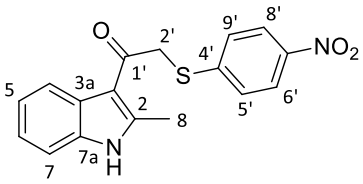

1-(2-methyl-1*H*-indol-3-yl)-2-((4-nitrophenyl)thio)ethanone (**3.30**); orange amorphous solid; yield 69%; mp 215 – 218 °C; IR (cm^{-1}) 3288, 2906, 1732, 1610, 1500, 1455, 1416, 1332, 980, 832, 738, 715; ^{1}H NMR (DMSO, 400 MHz): δ_H 12.05 (1H, brs, NH-1), 8.15 – 8.12 (2H, m, H-6', H-8'), 8.06 – 8.02 (1H, m, H-4), 7.55 – 7.52 (2H, m, H-5', H-9'), 7.41 – 7.39 (1H, m, H-7), 7.19 – 7.16 (2H, m, H-5, H-6), 4.80 (2H, s, H-2'), 2.76 (3H, s, H-8); ^{13}C NMR (DMSO, 100 MHz): δ_C 187.7 (CO, C-1'), 147.8 (q_C, C-4'), 145.6 (q_C, C-2), 144.3 (q_C, C-7'), 134.8 (q_C, C-7a), 126.7 (q_C, C-3a), 126.5 (CH, C-5', C-9'), 123.8 (CH, C-6', C-8'), 122.2 (CH, C-6), 121.8 (CH, C-5), 120.8 (CH, C-4), 111.9 (q_C, C-3), 111.4 (CH, C-7), 42.4 (CH_2, C-2'), 15.3 (CH_3, C-8) ppm; HRESMS *m/z* 327.0801 (calcd for $C_{17}H_{15}N_2O_3S$ $[M+H]^+$ 327.0803).

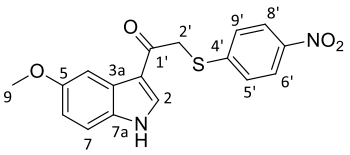

1-(5-methoxy-1*H*-indol-3-yl)-2-((4-nitrophenyl)thio)ethanone (**3.31**); yellow crystalline solid; yield 87%; mp 218 – 223 °C; IR (cm^{-1}) 3165, 2928, 1735, 1610, 1501, 1427, 1337, 1275, 842, 798, 739; ^{1}H NMR (DMSO, 400 MHz): δ_H 12.05 (1H, brs, NH-1), 8.53 (1H, d, *J* = 3.3 Hz, H-2), 8.14 – 8.12 (2H, m, H-6', H-8'), 7.63 (1H, d, *J* = 2.4 Hz, H-4), 7.59 – 7.57 (2H, m, H-5', H-9'), 7.39 (1H, d, *J* = 8.8 Hz, H-7), 6.86 (1H, dd, *J* = 8.8, 2.4 Hz, H-6), 4.70 (2H, s, H-2'), 3.76 (3H, s, H-9); ^{13}C NMR (DMSO, 100 MHz): δ_C 188.3 (CO, C-1'), 156.2 (q_C, C-5), 148.1 (q_C, C-4'), 144.9 (q_C, C-7'), 135.7 (CH, C-2), 131.8 (q_C, C-7a), 126.8 (CH, C-5', C-9'), 126.7 (q_C, C-3a), 124.2 (CH, C-6', C-8'), 115.1 (q_C, C-3), 113.5 (q_C, C-7), 113.4 (CH, C-6), 103.3 (CH, C-4), 55.7 (CH_3, C-9), 39.1 (CH_2, C-2') ppm; HRESMS *m/z* 343.0744 (calcd for $C_{17}H_{15}N_2O_4S$ $[M+H]^+$ 343.0753).

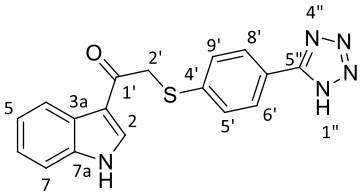

2-(4-(1*H*-tetrazol-5-yl)phenoxy)-1-(1*H*-indol-3-yl)ethanone (**3.32**); white needle-like crystalline solid; yield 20%; mp 225 – 230 °C; IR (cm^{-1}) 3473, 3307, 2957, 2737, 1640, 1617, 1595, 1523, 1442, 1379, 1244, 1141, 836, 759; ^{1}H NMR (Acetone-d_6, 600 MHz): δ_H 8.57 (1H, s, H-2), 8.26 – 8.24 (1H, m, H-4), 8.02 – 7.99 (2H, m, H-6', H-8'), 7.59 – 7.57 (1H, m, H-7), 7.31 – 7.23 (2H, m, H-5, H-6), 7.01 – 6.99 (2H, m, H-5', H-9'), 6.27 (2H, s, H-2'); ^{13}C NMR (Acetone-d_6, 100 MHz): δ_C 185.2 (CO, C-1'), 165.8 (q_C, C-5''), 160.2 (q_C, C-4'), 137.8 (q_C, C-7a), 134.8 (CH, C-2), 129.0 (CH, C-6', C-8'), 126.6 (q_C, C-3a), 124.5 (CH, C-6), 123.3 (CH, C-5), 122.5 (CH, C-4), 120.1 (q_C, C-7'), 116.7 (CH, C-5', C-9'), 115.0 (q_C, C-3), 113.0 (CH, C-7), 58.1 (CH_2, C-2') ppm; HRESMS *m/z* 320.1142 (calcd for $C_{17}H_{14}N_5O_2$ $[M+H]^+$ 320.1147).

5.5 Synthesis of mandelic acid (4.59)

32% HCl solution (5 ml) was added with mandelonitrile (**4.66**, 200 mg, 1.50 mmol) into a round bottom flask and stirred for 16 h at room temperature. Following this, the mixture was refluxed for 4 h before cooling and extracting the organic material with EtOAc. $MgSO_4$ was used to dry the crude mixture prior to concentration under high vacuum. The mixture was purified by flash column chromatography (Hexane: EtOAc, 4:1).

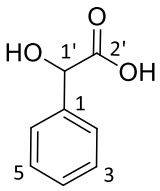

Mandelic acid[212] (**4.59**); cream amorphous solid; yield 49%; IR (cm^{-1}) 3445, 2904, 2618, 1714, 1456, 1239, 1189, 1061, 933, 871, 725, 692; ^{1}H NMR (CD_3OD, 400 MHz): δ_H 7.46 (2H, d, *J* = 7.1 Hz, H-2, H-6), 7.37 – 7.30 (3H, m, H-3, H-4, H-5), 5.13 (1H, s, H-1'); ^{13}C NMR (CD_3OD, 100 MHz): δ_C 174.7 (CO, C-2'), 139.5 (q_C, C-1), 128.0 (CH, C-3, C-5), 127.8 (CH, C-4), 126.5 (CH, C-2, C-6), 72.7 (CH, C-1') ppm; HRESMS *m/z* 175.0360 (calcd for $C_8H_8O_3Na$ $[M+Na]^+$ 175.0371).

5.6 General procedure for the synthesis of tetrazoles (4.60 – 4.63)

To a stirring mixture of a nitrile (1 eq) in anhydrous *N,N*-DMF (2 ml) was added NaN_3 (1 eq) and acetyl chloride (1 eq) under a nitrogenous atmosphere. The reaction proceeded for 7 h at 125 °C, save for **3.60** with a 48 h reaction time. Reaction mixture was allowed to cool before adding 1M NaOH (10 ml) and allowing the mixture to stir for a further 30 min. The pH of the resultant mixture was adjusted to 1 using 32% HCl solution. The organic material was extracted with EtOAc prior to drying over $MgSO_4$. Compounds were purified using flash column chromatography (Hexane: EtOAc, 1:1) followed by crystallisation from EtOAc and washing with $CHCl_3$.

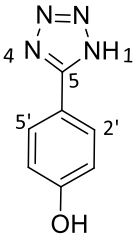

4-(1*H*-tetrazol-5-yl)phenol[216] (**4.60**); white crystalline solid; yield 31%; IR (cm^{-1}) 3414, 2843, 2620, 1614, 1599, 1415, 1279, 1249, 1079, 830, 751; ^1H NMR (CD_3OD, 400 MHz): δ_H 7.84 (2H, d, *J* = 8.7 Hz, H-2', H-6'), 6.95 (2H, d, *J* = 8.7 Hz, H-3', H-5'); ^{13}C NMR (CD_3OD, 100 MHz): δ_C 160.6 (q_C, C-4'), *155.4 (q_C, C-5), 128.6 (CH, C-2', C-6'), 115.8 (CH, C-3', C-5'), 114.4 (q_C, C-1') ppm.

*resolved by HMBC

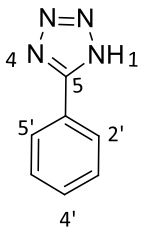

5-phenyl-1*H*-tetrazole[215] (**4.61**); white crystalline solid; yield 30%; IR (cm^{-1}) 1608, 1563, 1485, 987, 684; ^1H NMR (CD_3OD, 400 MHz): δ_H 8.03 – 8.01 (2H, m, H-2', H-6'), 7.60 – 7.58 (3H, m, H-3', H-4', H-5'); ^{13}C NMR (CD_3OD, 100 MHz): δ_C 156.0 (q_C, C-5), 131.2 (CH, C-4'), 129.1 (CH, C-3', C-5'), 126.8 (CH, C-2', C-6'), 123.9 (q_C, C-1') ppm.

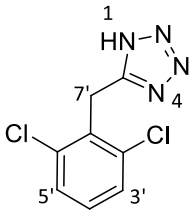

5-(2,6-dichlorobenzyl)-1*H*-tetrazole (**4.62**); colourless crystalline solid; yield 38%; IR (cm^{-1}) 2978, 2618, 1564, 1436, 920 ,764; ^{1}H NMR (DMSO, 400 MHz): δ_H 7.54 (2H, d, *J* = 8.0 Hz, H-3', H-5'), 7.40 (1H, dd, *J* = 8.4, 7.5 Hz, H-4'), 4.52 (2H, s, H-7'); ^{13}C NMR (DMSO, 100 MHz): δ_C *154.2 (q_C, C-5), 135.7 (q_C, C-2', C-6'), 132.0 (q_C, C-1'), 130.6 (CH, C-4'), 129.1 (CH, C-3', C-5'), 26.3 (CH_2, C-7') ppm; HRESMS *m/z* 229.0033 (calcd for $C_8H_7N_4{}^{35}Cl_2$ $[M+H]^+$ 229.0048).

*resolved by HMBC

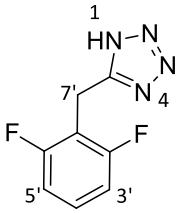

5-(2,6-difluorobenzyl)-1*H*-tetrazole (**4.63**); cream needle-like crystalline solid; yield 57.8%; IR (cm^{-1}) 3001, 2865, 1626, 1589, 1469, 1442, 1190, 1007, 776; ^{1}H NMR (CD_3OD, 300 MHz): δ_H 7.44 – 7.34 (1H, m, H-4'), 7.07 – 6.99 (2H, m, H-3', H-5'), 4.37 (2H, s, H-7'); ^{13}C NMR (CD_3OD, 75 MHz): δ_C 163.0 (q_C, C-2', C-6'), 159.7 (q_C, C-5), 154.5 (q_C, C-1'), 129.8 (CH, C-4), 111.2 (CH, C-3', C-5'), 16.4 (CH_2, C-7') ppm; HRESMS *m/z* 197.0753 (calcd for $C_8H_7N_4F_2$ $[M+H]^+$ 197.0639).

5.7 General procedure for the synthesis of phenyl nitriles (4.66 and 4.71 – 4.72)

To a charged 2-neck round bottom flask with a nitrogen stream was added anhydrous $ZnBr_2$ (1.5 eq). Appropriate aldehyde (**4.73** – **4.74**, 1 eq) and anhydrous DCM (5 ml) were added and the mixture stirred to homogeneity. TMSCN (1.3 eq) was then added and reaction was allowed to stir for 4 h at room temperature. Afterwards, 9 ml of HCl: Methanol (1:2) was added and reaction mixture stirred for a further 1 h before extracting the organic material with EtOAc, washing with water. $MgSO_4$ was used to dry the extract prior to concentration *in vacuo*. Purification was done using flash column chromatography (Hexane: EtOAc, 9:1).

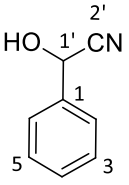

2-hydroxy-2-phenylacetonitrile[212] (**4.66**); yellow oil; yield 18%; ^{1}H NMR (DMSO, 400 MHz): δ_H 7.51 – 7.38 (5H, m, H-2, H-6), 5.76 – 5.74 (1H, d, *J* = 5.1 Hz, H-1'); ^{13}C NMR (DMSO, 100 MHz): δ_C 137.7 (q_C, C-1), 129.3 (CH, C-2, C-6), 129.2 (CH, C-4), 126.8 (CH, C-3, C-5), 121.0 (CN, C-2'), 62.2 (CH, C-1') ppm.

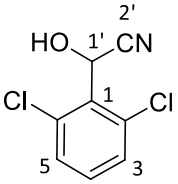

2-(2,6-dichlorophenyl)-2-hydroxyacetonitrile (**4.71**); yellow amorphous solid; yield 64%; IR (cm^{-1}) 3378, 2935, 2259, 1564, 1437, 1039, 830, 782, 766; ^{1}H NMR (DMSO, 400 MHz): δ_H 7.61 – 7.56 (2H, m, H-3, H-5), 7.47 (1H, dd, *J* = 8.9, 7.1 Hz, H-4), 7.27 (1H, d, *J* = 4.3 Hz, OH), 6.26 (1H, d, *J* = 4.3 Hz, H-1'); ^{13}C NMR (DMSO, 100 MHz): δ_C 134.9 (q_C, C-2, C-6), 132.5 (CH, C-4), 131.7 (q_C, C-1), 130.1 (CH, C-3, C-5), 118.8 (CN, C-2'), 58.4 (CH, C-1') ppm.

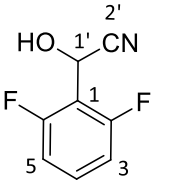

2-(2,6-difluorophenyl)-2-hydroxyacetonitrile (**4.72**); yellow crystalline solid; yield 62%; IR (cm^{-1}) 3383, 2923, 2259, 1624, 1473, 1236, 1039, 929, 784; ^{1}H NMR (DMSO, 400 MHz): δ_H 7.60 – 7.52 (1H, m, OH), 7.24 – 7.18 (3H, m, H-3, H-4, H-5), 5.93 (1H, d, *J* = 5.8 Hz, H-1'); ^{13}C NMR (DMSO, 100 MHz): δ_C 161.7 (q_C, C-2, C-6), 159.2 (q_C, C-1) 133.0 (CH, C-4), 119.3 (CN, C-2'), 112.8 (CH, C-3, C-5), 52.4 (CH, C-1') ppm.

References

(1) Hay, S. I.; Guerra, C. A.; Gething, P. W.; Patil, A. P.; Tatem, A. J.; Noor, A. M.; Kabaria, C. W.; Manh, B. H.; Elyazar, I. R. F.; Brooker, S.; Smith, D. L.; Moyeed, R. A.; Snow, R. W. *PLoS Med.* **2009**, *6*, 286–302.

(2) Kim, Y.; Schneider, K. A. *Nat. Educ. Knowl.* **2013**, *4*, 6.

(3) de Koning-Ward, T. F.; Dixon, M. W. A.; Tilley, L.; Gilson, P. R. *Nat. Rev. Microbiol.* **2016**, *14*, 494–507.

(4) Sherman, I. W. *Microbiol. Rev.* **1979**, *43*, 453–495.

(5) Bray, R. S.; Garnham, P. C. C. *Br. Med. Bull.* **1982**, *38*, 117–122.

(6) Soulard, V.; Bosson-Vanga, H.; Lorthiois, A.; Roucher, C.; Franetich, J.-F.; Zanghi, G.; Bordessoulles, M.; Tefit, M.; Thellier, M.; Morosan, S.; Le Naour, G.; Capron, F.; Suemizu, H.; Snounou, G.; Moreno-Sabater, A.; Dominique, M. *Nat. Commun.* **2015**, *6*, 1–9.

(7) Genome Research Limited. What is malaria https://www.yourgenome.org/facts/what-is-malaria (accessed Nov 4, 2017).

(8) Skeet, J. *Nurs. Times* **2005**, *101*, 43–45.

(9) Institute of Medicine (US) Committee on the Economics of Antimalarial Drugs. In *Saving Lives, Buying Time: Economics of Malaria Drugs in an Age of Resistance*; Arrow, K. J., Panosian, C., Gelband, H., Eds.; National Academic Press (US), 2004.

(10) Blumberg, L. H. *South African Med. J.* **2015**, *105*, 175–178.

(11) Lines, J. *Trop. Med. Int. Heal.* **1996**, *1*, 616–632.

(12) Cuervo-Parra, J. A.; Cortés, T. R.; Lepe-Ramirez, M. In *Insecticides Resistance*; Trdan, S., Ed.; 2016.

(13) Tene, B. F.; Poupardin, R.; Costantini, C.; Awono-Ambene, P.; Wondji, C. S.; Ranson, H.; Antonio-Nkondjio, C. *PLoS One* **2013**, e61408.

(14) Raghavendra, K.; Barik, T. K.; Reddy, B. P. N.; Sharma, P.; Dash, A. P. *Parasitol. Res.* **2011**, *108*, 757–779.

(15) Kasner, E.; Hunter, C. A.; Ph, D.; Kariko, K.; Ph, D. *Int. J. Antimicrob. Agents* **2013**, *70*, 646–656.

(16) White, N. J. *J. Clin. Invest.* **2004**, *113*, 1084–1092.

(17) Trape, J. F. *Am. J. Trop. Med. Hyg.* **2001**, *64*, 12–17.

(18) Ursos, L. M. B.; Roepe, P. D. *Med. Res. Rev.* **2002**, *22*, 465–491.

(19) Frosch, A. E. P.; Venkatesan, M.; Laufer, M. K. *Malar. J.* **2011**, *10*, 1–10.

(20) Gatton, M. L.; Martin, L. B.; Cheng, Q. *Antimicrob. Agents Chemother.* **2004**, *48*, 2116–2123.

(21) Basco, L. K.; Tahar, R.; Ringwald, P. *Antimicrob. Agents Chemother.* **1998**, *42*, 1811–1814.

(22) Mbugi, E. V; Mutayoba, B. M.; Malisa, A. L.; Balthazary, S. T.; Nyambo, T. B.; Mshinda, H. *Malar. J.* **2006**, *5*, 1–11.

(23) Matondo, S. I.; Temba, G. S.; Kavishe, A. A.; Kauki, J. S.; Kalinga, A.; van Zwetselaar, M.; Reyburn, H.; Kavishe, R. A. *Malar. J.* **2014**, *13*, 1–7.

(24) Bosman, A.; Mendis, K. N. *Am. J. Trop. Med. Hyg.* **2007**, *77*, 193–197.

(25) WHO. *Antimalarial drug combination therapy*; Geneva, 2001.

(26) White, N. *Philos. Trans. R. Soc. B* **1999**, *354*, 739–749.

(27) Ashley, E. A.; Dhorda, M.; Fairhurst, R. M.; Amaratunga, C.; Lim, P.; Suon, S.; Sreng, S.; Anderson, J. M.; Mao, S.; Sam, B.; Sopha, C.; Chuor, C. M.; Nguon, C.; Sovannaroth, S.; Pukrittayakamee, S.; Jittamala, P.; Chotivanich, K.; Chutasmit, K.; Suchatsoonthorn, C.; Runcharoen, R.; Hien, T. T.; Thuy-Nhien, N. T.; Thanh, N. V.; Phu, N. H.; Htut, Y.; Han, K.-T.;

Aye, K. H.; Mokuolu, O. A.; Olaosebikan, R. R.; Folaranmi, O. O.; Mayxay, M.; Khanthavong, M.; Hongvanthong, B.; Newton, P. N.; Onyamboko, M. A.; Fanello, C. I.; Tshefu, A. K.; Mishra, N.; Valecha, N.; Phyo, A. P.; Nosten, F.; Yi, P.; Tripura, R.; Borrmann, S.; Bashraheil, M.; Peshu, J.; Faiz, M. A.; Ghose, A.; Hossain, M. A.; Samad, R.; Rahman, M. R.; Hasan, M. M.; Islam, A.; Miotto, O.; Amato, R.; MacInnis, B.; Stalker, J.; Kwiatkowski, D. P.; Bozdech, Z.; Jeeyapant, A.; Cheah, P. Y.; Sakulthaew, T.; Chalk, J.; Intharabut, B.; Silamut, K.; Lee, S. J.; Vihokhern, B.; Kunasol, C.; Imwong, M.; Tarning, J.; Taylor, W. J.; Yeung, S.; Woodrow, C. J.; Flegg, J. A.; Das, D.; Smith, J.; Venkatesan, M.; Plowe, C. V.; Stepniewska, K.; Guerin, P. J.; Dondorp, A. M.; Day, N. P.; White, N. J. *N. Engl. J. Med.* **2014**, *371*, 411–423.

(28) Ariey, F.; Witkowski, B.; Amaratunga, C.; Beghain, J.; Ma, L.; Lim, P.; Leang, R.; Duong, S.; Sreng, S. *Nature* **2016**, *505*, 50–55.

(29) Lu, F.; Culleton, R.; Zhang, M.; Ramaprasad, A.; von Seidlein, L.; Zhou, H.; Zhu, G.; Tang, J.; Liu, Y.; Wang, W.; Cao, Y.; Xu, S.; Gu, Y.; Li, J.; Zhang, C.; Gao, Q.; Menard, D.; Pain, A.; Yang, H.; Zhang, Q.; Cao, J. *N. Engl. J. Med.* **2017**, *376*, 991–993.

(30) Basso, L. G. M.; Rodrigues, R. Z.; Naal, R. M. Z. G.; Costa-Filho, A. J. *Biochim. Biophys. Acta - Biomembr.* **2011**, *1808*, 55–64.

(31) Corral, M. G.; Leroux, J.; Stubbs, K. A.; Mylne, J. S. *Sci. Rep.* **2017**, *7*, 1–9.

(32) Yuthavong, Y. *J. Sci. Soc. Thailand* **1996**, *22*, 181–186.

(33) Lunev, S.; Batista, F. A.; Bosch, S. S.; Wrenger, C.; Groves, M. R. In *Current Topics in Malaria*; Rodriguez-Morales, A. J., Ed.; 2016; pp 235–365.

(34) Cheng, J.; Zeidan, R.; Mishra, S.; Liu, A.; Pun, S. H.; Kulkarni, R. P.; Jensen, G. S.; Bellocq, N. C.; Davis, M. E. *J. Med. Chem.* **2006**, *49*, 6522–6531.

(35) Thomé, R.; Lopes, S. C. P.; Costa, F. T. M.; Verinaud, L. *Immunol. Lett.* **2013**, *153*, 50–57.

(36) Sullivan, D. J.; Gluzman, I. Y.; Russell, D. G.; Goldberg, D. E. *Proc. Natl. Acad. Sci. U. S. A.* **1996**, *93*, 11865–11870.

(37) Saifi, A. *African J. Pharm. Pharmacol.* **2013**, *7*, 148–156.

(38) Mushtaque, M.; Shahjahan, S. *Eur. J. Med. Chem.* **2015**, *90*, 280–295.

(39) Goldberg, D. E.; Slater, A. F.; Cerami, A.; Henderson, G. B. *Proc. Natl. Acad. Sci. U. S. A.* **1990**, *87*, 2931–2935.

(40) Travassos, M. A.; Laufer, M. K. *Pediatr. Res.* **2009**, *65*, 64R–70R.

(41) Ecker, A.; Lehane, A. M.; Clain, J.; Fidock, D. A. *Trends Parasitol.* **2012**, *28*, 504–514.

(42) Wongsrichanalai, C.; Pickard, A. L.; Wernsdorfer, W. H.; Meshnick, S. R. *Lancet Infect. Dis.* **2002**, *2*, 209–218.

(43) Krogstad, D. J.; Schlesinger, P. H.; Herwaldt, B. L. *Antimicrob. Agents Chemother.* **1988**, *32*, 799–801.

(44) Kasner, E.; Hunter, C. A.; Ph, D.; Kariko, K.; Ph, D. *Expert Rev. Anti. Infect. Ther.* **2009**, *7*, 999–1013.

(45) Kannan, R.; Kumar, K.; Sahal, D.; Kukreti, S.; Chauhan, V. S. *Biochem. J.* **2005**, *385*, 409–418.

(46) Guo, Z. *Acta Pharm. Sin. B* **2016**, *6*, 115–124.

(47) Hyde, J. E. *Acta Trop.* **2005**, *94*, 191–206.

(48) Abdul-Ghani, R.; Farag, H. F.; Allam, A. F. *Acta Trop.* **2013**, *125*, 163–190.

(49) Kofoed, P.-E.; Alfrangis, M.; Poulsen, A.; Rodrigues, A.; Gjedde, S. B.; Rønn, A.; Rombo, L. *Trop. Med. Int. Heal.* **2004**, *9*, 171–177.

(50) Iyer, J. K.; Milhous, W. K.; Cortese, J. F.; Kublin, J. G.; Plowe, C. V. *Lancet* **2001**, *358*, 1066–1067.

(51) Nixon, G. L.; Moss, D. M.; Shone, A. E.; Lalloo, D. G.; Fisher, N.; O'neill, P. M.; Ward, S. A.; Biagini, G. A. *J. Antimicrob. Chemother.* **2013**, *68*, 977–985.

(52) Baggish, A. L.; Hill, D. R. *Antimicrob. Agents Chemother.* **2002**, *46*, 1163–1173.

(53) Phillips, M. A.; Lotharius, J.; Marsh, K.; White, J.; Dayan, A.; White, K. L.; Njoroge, J. W.; El Mazouni, F.; Lao, Y.; Kokkonda, S.; Tomchick, D. R.; Deng, X.; Laird, T.; Bhatia, S. N.; March, S.; Ng, C. L.; Fidock, D. A.; Wittlin, S.; Lafuente-Monasterio, M.; Benito, F. J. G.; Alonso, L. M. S.; Martinez, M. S.; Jimenez-Diaz, M. B.; Bazaga, S. F.; Angulo-Barturen, I.; Haselden, J. N.; Louttit, J.; Cui, Y.; Sridhar, A.; Zeeman, A.-M.; Kocken, C.; Sauerwein, R.; Dechering, K.; Avery, V. M.; Duffy, S.; Delves, M.; Sinden, R.; Ruecker, A.; Wickham, K. S.; Rochford, R.; Gahagen, J.; Iyer, L.; Riccio, E.; Mirsalis, J.; Bathhurst, I.; Rueckle, T.; Ding, X.; Campo, B.; Leroy, D.; Rogers, M. J.; Rathod, P. K.; Burrows, J. N.; Charman, S. A. *Sci. Transl. Med.* **2015**, *7*, 1–31.

(54) Schwöbel, B.; Alifrangis, M.; Salanti, A.; Jelinek, T. *Malar. J.* **2003**, *2*, 1–7.

(55) Fisher, N.; Majid, R. A.; Antoine, T.; Al-Helal, M.; Warman, A. J.; Johnson, D. J.; Lawrenson, A. S.; Ranson, H.; O'Neill, P. M.; Ward, S. A.; Biagini, G. A. *J. Biol. Chem.* **2012**, *287*, 9731–9741.

(56) Akhoon, B. A.; Singh, K. P.; Varshney, M.; Gupta, S. K.; Shukla, Y.; Gupta, S. K. *PLoS One* **2014**, *9*, 1–12.

(57) Kessl, J. J.; Ha, K. H.; Merritt, A. K.; Lange, B. B.; Hill, P.; Meunier, B.; Meshnick, S. R.; Trumpower, B. L. *J. Biol. Chem.* **2005**, *280*, 17142–17148.

(58) Spillman, N. J.; Kirk, K. *Int. J. Parasitol. Drugs Drug Resist.* **2015**, *5*, 149–162.

(59) Rottmann, M.; Mcnamara, C.; Yeung, B. K. S.; Lee, M. C. S.; Russell, B.; Seitz, P.; Plouffe, D. M.; Dharia, N. V; Tan, J.; Cohen, S. B.; Spencer, K. R.; González-Páez, G. E.; Lakshminaranyana, S. B.; Goh, A.; Suwanarusk, R.; Jegla, T.; Schmitt, E. K.; Beck, H.; Brun, R.; Nosten, F.; Renia, L.; Dartois, V.; TH, K.; Fidock, D.; Winzeler, E.; Diagana, T. *Science (80-.).* **2010**, *329*, 1175–1180.

(60) Goldgof, G. M.; Durrant, J. D.; Ottilie, S.; Vigil, E.; Allen, K. E.; Gunawan, F.; Kostylev, M.; Henderson, K. A.; Yang, J.; Schenken, J.; LaMonte, G. M.; Manary, M. J.; Murao, A.; Nachon, M.; Stanhope, R.; Prescott, M.; McNamara, C. W.; Slayman, C. W.; Amaro, R. E.; Suzuki, Y.; Winzeler, E. A. *Sci. Rep.* **2016**, *6*, 1–13.

(61) Huskey, S. E. W.; Zhu, C. Q.; Fredenhagen, A.; Kühnöl, J.; Luneau, A.; Jian, Z.; Yang, Z.; Miao, Z.; Yang, F.; Jain, J. P.; Sunkara, G.; Mangold, J. B.; Stein, D. S. *Drug Metab. Dispos.* **2016**, *44*, 672–682.

(62) Yeo, S.-J.; Liu, D.-X.; Kim, H. S.; Park, H. *Malar. J.* **2017**, *16*, 1–9.

(63) Kimura, T.; Shirakawa, R.; Yaoita, N.; Hayashi, T.; Nagano, K.; Horiuchi, H. *FEBS Lett.* **2014**, *588*, 3673–3676.

(64) Naim, M. J.; Alam, O.; Alam, J.; Bano, F.; Alam, P.; Shrivastava, N. *Int. J. Pharm. Sci. Res.* **2016**, *7*, 51–62.

(65) Lu, B.; Luo, Y.; Liu, L.; Ye, L.; Wang, Y.; Zhang, L. *Angew. Chemie - Int. Ed.* **2011**, *123*, 8508–8512.

(66) Bandini, M.; Eichholzer, A. *Angew. Chemie - Int. Ed.* **2009**, *48*, 9608–9644.

(67) Gribble, G. W. *Pure Appl. Chem.* **2003**, *75*, 1417–1432.

(68) Bartoli, G.; Bencivenni, G.; Dalpozzo, R. *Chem. Soc. Rev.* **2010**, *39*, 4449–4465.

(69) Chadha, N.; Silakari, O. *Eur. J. Med. Chem.* **2017**, *134*, 159–184.

(70) Dalpozzo, R. *Chem. Soc. Rev.* **2015**, *44*, 742–778.

(71) Tiwari, R. K.; Singh, D.; Singh, J.; Yadav, V.; Pathak, A. K.; Dabur, R.; Chhillar, A. K.; Singh, R.; Sharma, G. L.; Chandra, R.; Verma, A. K. *Bioorg. Med. Chem. Lett.* **2006**, *16*, 413–416.

(72) El-Sayed, M. T.; Suzen, S.; Altanlar, N.; Ohlsen, K.; Hilgeroth, A. *Bioorganic Med. Chem. Lett.*

2016, *26*, 218–221.

(73) El-Sayed, M. T.; Mahmoud, K. A.; Heinemann, F. W.; Hilgeroth, A. *J. Heterocycl. Chem.* **2017**, *54*, 714–719.

(74) Choppara, P.; Bethu, M. S.; Prasad, Y. V.; Rao, J. V.; Ranjan, T. J.; Prasad, G. V. S.; Doradla, R.; Murthy, Y. L. N. *Arab. J. Chem.* **2015**, 10.1016/j.arabjc.2015.05.015.

(75) Chen, M.; Shao, C. L.; Fu, X. M.; Xu, R. F.; Zheng, J. J.; Zhao, D. L.; She, Z. G.; Wang, C. Y. *J. Nat. Prod.* **2013**, *76*, 547–553.

(76) Wei, M. Y.; Wang, C. Y.; Liu, Q. A.; Shao, C. L.; She, Z. G.; Lin, Y. C. *Mar. Drugs* **2010**, *8*, 941–949.

(77) Mandour, A. H.; El-Sawy, E. R.; Zahran, M. A.; Ebaid, M. S.; Mustafa, M. A. *Biohealth Sci. Bull.* **2009**, *1*, 57–67.

(78) Liu, Y.; Liu, D.; Printzenhoff, D.; Coghlan, M. J.; Harris, R.; Krafte, D. S. *Eur. J. Pharmacol.* **2002**, *435*, 153–160.

(79) Rani, P.; Srivastava, V. K.; Kumar, A. *Eur. J. Med. Chem.* **2004**, *39* (5), 449–452.

(80) Rowinksy, E. In *Holland-Frei Cancer Medicine*; Kufe, D., Pollock, R., Weichselbalaum, R., Al., E., Eds.; BC Decker, 2003.

(81) Moudi, M.; Go, R.; Yien, C. Y. S.; Nazre, M. *Int. J. Prev. Med.* **2013**, *4*, 1231–1235.

(82) Kavallaris, M.; Tait, A. S.; Walsh, B. J.; He, L.; Horwitz, S. B.; Norris, M. D.; Haber, M. *Cancer Res.* **2001**, *61*, 5803–5809.

(83) Verrills, N. M.; Walsh, B. J.; Cobon, G. S.; Hains, P. G.; Kavallaris, M. *J. Biol. Chem.* **2003**, *278*, 45082–45093.

(84) Beck, W. T. *Adv. Enzyme Regul.* **1984**, *22*, 207–227.

(85) Madadi, N. R.; Penthala, N. R.; Brents, L. K.; Ford, B. M.; Prather, P. L.; Crooks, P. A. *Bioorganic Med. Chem. Lett.* **2013**, *23*, 2019–2021.

(86) Mackie, K. *J. Neuroendocrinol.* **2008**, *20*, 10–14.

(87) Steer, M. L. *Ann. Surg.* **1975**, *182*, 603–609.

(88) Guzmán, M.; Sánchez, C.; Galve-Roperh, I. *Pharmacol. Ther.* **2002**, *95*, 175–184.

(89) Tarade, D.; Ma, D.; Pignanelli, C.; Mansour, F.; Simard, D.; Van Den Berg, S.; Gauld, J.; McNulty, J.; Pandey, S. *PLoS One* **2017**, *12*, 1–13.

(90) Hu, L.; Li, Z. R.; Li, Y.; Qu, J.; Ling, Y. H.; Jiang, J. D.; Boykin, D. W. *J. Med. Chem.* **2006**, *49*, 6273–6282.

(91) Maciejewska, D.; Rasztawicka, M.; Wolska, I.; Anuszewska, E.; Gruber, B. *Eur. J. Med. Chem.* **2009**, *44*, 4136–4147.

(92) Suryadinata, R.; Sadowski, M.; Sarcevic, B. *Biosci. Rep.* **2010**, *30*, 243–255.

(93) Ashrafian, L.; Sukhikh, G.; Kiselev, V.; Paltsev, M.; Drukh, V.; Kuznetsov, I.; Muyzhnek, E.; Apolikhina, I.; Andrianova, E. *EPMA J.* **2015**, *6*, 1–12.

(94) Paltsev, M.; Kiselev, V.; Drukh, V.; Muyzhnek, E.; Kuznetsov, I.; Andrianova, E.; Baranovskiy, P. *EPMA J.* **2016**, *7*, 1–8.

(95) Thompson, A. J.; Lummis, S. C. R. *Expert Opin. Ther. Targets* **2007**, *11*, 527–540.

(96) Hibert, M. F.; Hoffmann, R.; Miller, R. C.; Carr, A. A. *J. Med. Chem.* **1990**, *33*, 1594–1600.

(97) Ren, C.; Fang, L.; Ling, L.; Wang, Q.; Liu, S.; Zhao, L.; He, Z. *Int. J. Pharm.* **2009**, *370*, 129–135.

(98) Swan, C. E.; Breyer, R. M. **2011**, *96*, 10–13.

(99) Kaye, D. M.; Johnston, L.; Vaddadi, G.; Brunner-LaRocca, H.; Jennings, G. L.; Esler, M. D. *Hypertension* **2001**, *37*, 1216–1221.

(100) Quyyumi, A. A.; Wright, C.; Mockus, L.; Fox, K. M. *Br. Med. J. (Clin. Res. Ed).* **1984**, *289*, 951–953.

(101) Kaushik, N. K.; Kaushik, N.; Attri, P.; Kumar, N.; Kim, C. H.; Verma, A. K.; Choi, E. H. *Molecules* **2013**, *18*, 6620–6662.

(102) de Paula, R. C.; Dolabela, M. F.; de Oliveira, A. B. *Planta Med.* **2014**, *80*, 378–386.

(103) Dolabela, M. F.; Póvoa, M. M.; Brandão, G. C.; Rocha, F. D.; Soares, L. F.; de Paula, R. C.; de Oliveira, A. B. *Malar. J.* **2015**, *14*, 1–12.

(104) Chong, C. R.; Sullivan Jr., D. J. *Biochem. Pharmacol.* **2003**, *66*, 2201–2212.

(105) Rocha e Silva, L. F.; Montoia, A.; Amorim, R. C. N.; Melo, M. R.; Henrique, M. C.; Nunomura, S. M.; Costa, M. R. F.; Andrade Neto, V. F.; Costa, D. S.; Dantas, G.; Lavrado, J.; Moreira, R.; Paulo, A.; Pinto, A. C.; Tadei, W. P.; Zacardi, R. S.; Eberlin, M. N.; Pohlit, A. M. *Phytomedicine* **2012**, *20*, 71–76.

(106) Ashok, P.; Ganguly, S.; Murugesan, S. *Drug Discov. Today* **2014**, *19*, 1781–1791.

(107) Sakai, R.; Higa, T.; Jefford, C. W.; Bernardinelli, G. *J. Am. Chem. Soc.* **1986**, *108*, 6404–6405.

(108) Rao, K. V.; Donia, M. S.; Peng, J.; Garcia-Palomero, E.; Alonso, D.; Martinez, A.; Medina, M.; Franzblau, S. G.; Tekwani, B. L.; Khan, S. I.; Wahyuono, S.; Willett, K. L.; Hamann, M. T. *J. Nat. Prod.* **2006**, *69*, 1034–1040.

(109) Ichiba, T.; Corgiat, J. M.; Scheuer, P. J.; Kelly-Borges, M. *J. Nat. Prod.* **1994**, *57*, 168–170.

(110) Urgaonkar, S.; Cortese, J. F.; Barker, R. H.; Cromwell, M.; Serrano, A. E.; Wirth, D. F.; Clardy, J.; Mazitschek, R. *Org. Lett.* **2010**, *12*, 3998–4001.

(111) Alves, E.; Bartlett, P. J.; Garcia, C. R. S.; Thomas, A. P. *J. Biol. Chem.* **2011**, *286*, 5905–5912.

(112) Farias, S. L.; Gazarini, M. L.; Melo, R. L.; Hirata, I. Y.; Juliano, M. A.; Juliano, L.; Garcia, C. R. S.

Mol. Biochem. Parasitol. **2005**, *141*, 71–79.

(113) Schuck, D. C.; Jordão, A. K.; Nakabashi, M.; Cunha, A. C.; Ferreira, V. F.; Garcia, C. R. S. *Eur. J. Med. Chem.* **2014**, *78*, 375–382.

(114) Svogie, A. L.; Isaacs, M.; Hoppe, H. C.; Khanye, S. D.; Veale, C. G. L. *Eur. J. Med. Chem.* **2016**, *114*, 79–88.

(115) Svogie, A. L. Investigation of α -aryl substituted 3-indolylethanones as potential antiplasmodial agents, Rhodes University, 2015.

(116) Veale, C. G. L.; Zoraghi, R.; Young, R. M.; Morrison, J. P.; Pretheeban, M.; Lobb, K. A.; Reiner, N. E.; Andersen, R. J.; Davies-Coleman, M. T. *J. Nat. Prod.* **2015**, *78*, 355–362.

(117) Clayden, J.; Greeves, N.; Warren, S. *Organic Chemistry*, 1st ed.; Oxford University Press, 2001.

(118) Xuedong, P.; Mei, Z.; Jinzhao, Z.; Xiaolong, C. Simple synthesis method of important pharmaceutical and chemical intermediate 5-cyano indole, 2014.

(119) Sawant, D. N.; Wagh, Y. S.; Tambade, P. J.; Bhatte, K. D.; Bhanage, B. M. *Adv. Synth. Catal.* **2011**, *353* (5), 781–787.

(120) da Silva, F. P.; Fiorio, J. L.; Rossi, L. M. *ACS Omega* **2017**, *2*, 6014–6022.

(121) Ponec, R.; Setínek, K. *J. Mol. Catal.* **1985**, *32*, 201–210.

(122) Tang, W.; Kwak, Y.; Braunecker, W.; Tsarevsky, N. V.; Coote, M. .; Matyjaszewski, K. *J. Am. Chem. Soc.* **2008**, *130*, 10702–10713.

(123) Khemnar, A. B.; Bhanage, B. M. *RSC Adv.* **2014**, *4*, 13405–13408.

(124) Sundermeier, M.; Zapf, A.; Mutyala, S.; Baumann, W.; Sans, J.; Weiss, S.; Beller, M. *Chem. - A Eur. J.* **2003**, *9*, 1828–1836.

(125) Miayura, N.; Yanagi, T.; Suzuki, A. *Synth. Commun.* **1981**, *11*, 513–519.

(126) Ottoni, O.; Neder, A. de V. F.; Dias, A. K. B.; Cruz, R. P. A.; Aquino, L. B. *Org. Lett.* **2001**, *3*, 1005–1007.

(127) Xu, H.; Fan, L. *Eur. J. Med. Chem.* **2011**, *46*, 364–369.

(128) Veale, C. G. L.; Lobb, K. A.; Zoraghi, R.; Morrison, J. P.; Reiner, N. E.; Andersen, R. J.; Davies-Coleman, M. T. *Tetrahedron* **2014**, *70* (43), 7845–7853.

(129) He, M.; Yang, N.; Sun, C.; Yao, X.; Yang, M. *Med. Chem. Res.* **2011**, *20*, 200–209.

(130) Black, D. S. C.; Kumar, N.; McConnell, D. B. *Tetrahedron* **2001**, *57*, 2203–2211.

(131) Svogie, A. L. Investigation of α -aryl substituted 3-indolylethanones as potential antiplasmodial agents by, Rhodes University, 2015.

(132) Raub, S.; Jansen, G. *Theor. Chem. Acc.* **2001**, *106*, 223–232.

(133) Reed, L. H.; Allen, L. C. *J. Phys. Chem.* **1992**, *96*, 157–164.

(134) Wagner, E. L. *J. Am. Chem. Soc.* **1963**, *85*, 161–164.

(135) Markwalter, C. F.; Davis, K. M.; Wright, D. W. *Anal. Biochem.* **2016**, *493*, 30–34.

(136) Makler, M. T.; Hinrichs, D. J. *Am. J. Trop. Med. Hyg.* **1993**, *48*, 205–210.

(137) Daina, A.; Michielin, O.; Zoete, V. *Sci. Rep.* **2017**, *7*, 42717.

(138) Daina, A.; Michielin, O.; Zoete, V. *J. Chem. Inf. Model.* **2014**, *54*, 3284–3301.

(139) Benson, F. R. *Chem. Rev.* **1947**, *41*, 1–61.

(140) Dai, L.-L.; Zhang, H.-Z.; Nagarajan, S.; Rasheed, S.; Zhou, C.-H. *Med. Chem. Commun.* **2015**, *6*, 147–154.

(141) Malik, M. A.; Wani, M. Y.; Al-Thabaiti, S. A.; Shiekh, R. A. *J. Incl. Phenom. Macrocycl. Chem.* **2014**, *78*, 15–37.

(142) Tsuchimori, N.; Hayashi, R.; Kitamoto, N.; Asai, K.; Kitazaki, T.; Iizawa, Y.; Itoh, K.; Okonogi, K. *Antimicrob. Agents Chemother.* **2002**, *46*, 1388–1393.

(143) Hayashi, R.; Kitamoto, N.; Iizawa, Y.; Ichikawa, T.; Itoh, K.; Kitazaki, T.; Okonogi, K. *Antimicrob. Agents Chemother.* **2002**, *46*, 283–287.

(144) Gaurav, K.; Karmakar, S.; Kundu, K.; Kundu, S. In *Antibiotic Resistant Bacteria - A Continuous Challenge in the New Millennium*; Pana, M., Ed.; 2012; pp 487–502.

(145) Reller, L. B.; Karney, W. W.; Beaty, H. N.; Holmes, K. K.; Turck, M. *Antimicrob. Agents Chemother.* **1973**, *3*, 488–497.

(146) Noto, T.; Nehashi, T.; Endo, H.; Saito, M.; Matsubara, S.; Harada, Y.; Suzuki, S.; Ogawa, H.; Koyama, K. *J. Anitibiotics* **1976**, *29*, 1058–1070.

(147) Kariyone, K.; Harada, H.; Kurita, M.; Takano, T. *J. Antibiot. (Tokyo).* **1970**, *23*, 131–136.

(148) Bergeron, M. G.; Brusch, J. L.; Barza, M.; Weinstein, L. *Antimicrob. Agents Chemother.* **1973**, *4*, 396–401.

(149) Meyers, B. R.; Leng, B.; Hirschman, S. Z. *Antimicrob. Agents Chemother.* **1975**, *8*, 737–741.

(150) Meyers, B. R.; Hirschman, S. Z. *J. Infect. Dis.* **1978**, *137*, S25–S31.

(151) Thirumoorthi, M. C.; Dajani, A. S.; Vincent, C. V.; Maurer, M. J. *Antimicrob. Agents Chemother.* **1981**, *20*, 21–24.

(152) Shindo, H.; Kawai, K.; Ikeda, T.; Igarashi, I.; Sugawara, S. *J. Anitibiotics* **1982**, *35*, 742–754.

(153) Cornick, N. A.; Jacobus, N. V.; Gorbach, S. L. *Antimicrob. Agents Chemother.* **1987**, *31*, 2010–2012.

(154) Jones, R. N.; Barry, A. L.; Fuchs, P. C.; Thornsberry, C. *J. Clin. Microbiol.* **1986**, *24*, 1055–1059.

(155) Downs, J. T.; Andriole, V. T. *Yale J. Biol. Med.* **1980**, *53*, 149–159.

(156) Weaver, S. S.; Leblanc, B. M.; Bodey, G. P. *Antibiot. Resist. Bact. - A Contin. Chall. New Millenn.* **1980**, *17*, 92–95.

(157) Neu, H. C.; Aswapokee, N.; Fu, K. P.; Aswapokee, P. *Antimicrob. Agents Chemother.* **1979**, *16*, 141–149.

(158) Yong, D.; Yum, J. H.; Lee, K.; Chong, Y.; Choi, S. H.; Rhee, J. K. *Antimicrob. Agents Chemother.* **2004**, *48*, 352–357.

(159) Yoon, E. J.; Jo, Y. W.; Choi, S. H.; Lee, T. H.; Rhee, J. K.; Yoo, M.; Shim, M. J.; Choi, E. C. *Antimicrob. Agents Chemother.* **2005**, *49*, 2498–2500.

(160) Bae, S. K.; Chung, W.-S.; Kim, E. J.; Rhee, J. K.; Kwon, J. W.; Kim, W. B.; Lee, M. G. *Antimicrob. Agents Chemother.* **2004**, *48*, 659–662.

(161) Vera-Cabrera, L.; Castro-Garza, J.; Rendon, A.; Ocampo-Candiani, J.; Welsh, O.; Choi, S. H.; Blackwood, K.; Molina-Torres, C. *Antimicrob. Agents Chemother.* **2005**, *49*, 4351–4353.

(162) Agyeman, A. A.; Ofori-Asenso, R. *Ann. Clin. Microbiol. Antimicrob.* **2016**, *15*, 1–17.

(163) Myungsun, L.; Taeksun, S.; Youngran, K.; Ina, J.; Sang, C. N.; Clifton, B. E. *N. Engl. J. Med.* **2015**, *373*, 290–291.

(164) Im, W. Bin; Choi, S. H.; Park, J.-Y.; Choi, S. H.; Finn, J.; Yoon, S.-H. *Eur. J. Med. Chem.* **2011**, *46*, 1027–1039.

(165) Vera-Cabrera, L.; Gonzalez, E.; Rendon, A.; Ocampo-Candiani, J.; Welsh, O.; Velazquez-Moreno, V. M.; Choi, S. H.; Molina-Torres, C. *Antimicrob. Agents Chemother.* **2006**, *50*, 3170–3172.

(166) Yum, J. H.; Choi, S. H.; Yong, D.; Chong, Y.; Im, W. Bin; Rhee, D. K.; Lee, K. *Antimicrob. Agents Chemother.* **2010**, *54*, 5381–5386.

(167) Yeung, K.-S.; Qiu, Z.; Yang, Z.; Zadjura, L.; D'Arienzo, C. J.; Browning, M. R.; Hansel, S.; Huang,

X. S.; Eggers, B. J.; Riccardi, K.; Lin, P.-F.; Meanwell, N. A.; Kadow, J. F. *Bioorganic Med. Chem. Lett.* **2013**, *23*, 209–212.

(168) Wilen, C. B.; Tilton, J. C.; Doms, R. W.; Walker, B.; Mcmichael, A.; Wilen, C. B.; Tilton, J. C.; Doms, R. W.; Craigie, R.; Bushman, F. D.; Shaw, G. M.; Hunter, E. *Cold Spring Harb. Perspect. Med.* **2012**, *2*, 1–13.

(169) Kuritzkes, D. R. *Curr. Opin. HIV AIDS* **2009**, *4*, 82–87.

(170) Zhou, N.; Nowicka-Sans, B.; Zhang, S.; Fan, L.; Fang, J.; Fang, H.; Gong, Y.-F.; Eggers, B.; Langley, D. R.; Wang, T.; Kadow, J.; Grasela, D.; Hanna, G. J.; Alexander, L.; Colonno, R.; Krystal, M.; Lin, P.-F. *Antimicrob. Agents Chemother.* **2011**, *55*, 729–737.

(171) Chang, C.-S.; Lin, Y.-T.; Shih, S.-R.; Lee, C.-C.; Lee, Y.-C.; Tai, C.-L.; Tseng, S.-N.; Chern, J.-H. *J. Med. Chem.* **2005**, *48*, 3522–3535.

(172) Lee, K. Y. *Korean J. Pediatr.* **2016**, *59*, 395–401.

(173) Yi, E.-J.; Shin, Y.-J.; Kim, J.-H.; Kim, T.-G.; Chang, S.-Y. *Clin. Exp. Vaccine Res.* **2017**, *6*, 4–14.

(174) WHO. *Wkly. Epidemiol. Rec.* **2012**, *87*, 461–476.

(175) WHO. *Influenza*; 2003.

(176) Król, E.; Rychłowska, M.; Szewczyk, B. *Acta Biochim. Pol.* **2014**, *61*, 495–504.

(177) Zarubaev, V. V.; Golod, E. L.; Anfimov, P. M.; Shtro, A. A.; Saraev, V. V.; Gavrilov, A. S.; Logvinov, A. V.; Kiselev, O. I. *Bioorg. Med. Chem.* **2010**, *18*, 839–848.

(178) Bhaskar, V. H.; Mohite, P. B. *J. Optoelectron. Biomed. Mater.* **2010**, *2*, 249–259.

(179) Bicker, K. L.; Thompson, P. R. *Biopolymers* **2013**, *99*, 155–163.

(180) Witalison, E. E.; Thompson, P. R.; Hofseth, L. J. *Curr. Drug Targets* **2015**, *16*, 700–710.

(181) Jones, J. E.; Causey, C. P.; Knuckley, B.; Slack-Noyes, J. L.; Thompson, P. R. *Curr. Opin. Drug*

Discov. Devel. **2009**, *12*, 616–627.

(182) Subramanian, V.; Knight, J. S.; Parelkar, S.; Anguish, L.; Coonrod, S. A.; Kaplan, M. J.; Thompson, P. R. *J. Med. Chem.* **2015**, *58*, 1337–1344.

(183) Romagnoli, R.; Baraldi, P. G.; Salvador, M. K.; Preti, D.; Tabrizi, A. M.; Brancale, A.; Fu, X.-H.; Li, J.; Zhang, S.-Z.; Hamel, E.; Bortolozzi, R.; Basso, G.; Viola, G. *J. Med. Chem.* **2012**, *55*, 475–488.

(184) Mahindroo, N.; Liou, J. P.; Chang, J. Y.; Hsieh, H. P. *Expert Opin. Ther. Pat.* **2006**, *16*, 647–691.

(185) Tron, G. C.; Pirali, T.; Sorba, G.; Pagliai, F.; Busacca, S.; Genazzani, A. A. *J. Med. Chem.* **2006**, *49*, 3033–3044.

(186) Romagnoli, R.; Baraldi, P. G.; Cruz-Lopez, O.; Cara, C. L.; Carrion, M. D.; Brancale, A.; Hamel, E.; Chen, L.; Bortolozzi, R.; Basso, G.; Viola, G. *J. Med. Chem.* **2010**, *53*, 4248–4258.

(187) Jedhe, G. S.; Paul, D.; Gonnade, R. G.; Santra, M. K.; Hamel, E.; Nguyen, T. L.; Sanjayan, G. J. *Bioorg. Med. Chem. Lett.* **2013**, *23*, 4680–4684.

(188) Arshad, M.; Bhat, R. A.; Pokharel, S.; Kim, J.; Lee, E. J.; Athar, F.; Choi, I. *Eur. J. Med. Chem.* **2014**, *71*, 229–236.

(189) Wexler, R. R.; Greenlee, W. J.; Irvin, J. D.; Goldberg, M. R.; Prendergast, K.; Smith, R. D.; Timmermans, P. B. M. W. M. *J. Med. Chem.* **1996**, *39*, 625–656.

(190) Sparks, M. A.; Crowley, S. D.; Gurley, S. B.; Mirotsou, M.; Coffman, T. M. *Compr. Physiol.* **2015**, *4*, 1201–1228.

(191) Atlas, S. A. *J. Manag. Care Pharm.* **2007**, *13*, 9–20.

(192) Kurtz, T. W.; Klein, U. *Hypertens. Res.* **2009**, *32*, 826–834.

(193) Barreras, A.; Gurk-Turner, C. *Baylor Univ. Med. Cent. Proc.* **2003**, *16*, 123–126.

(194) Le Bourdonnec, B.; Meulon, E.; Yous, S.; Goossens, J.-F.; Houssin, R.; Hénichart, J.-P. *J. Med.*

Chem. **2000**, *43*, 2685–2697.

(195) Liu, M.; Yokomizo, T. *Allergol. Int.* **2015**, *64*, 17–26.

(196) Berger, A. *Br. Med. J.* **1999**, *319*, 90.

(197) Kanaoka, Y.; Boyce, J. A. *J. Immunol.* **2004**, *173*, 1503–1510.

(198) Hamilton, A.; Faiferman, I.; Stober, P.; Watson, R. M.; O'Byrne, P. M. *J. Allergy Clin. Immunol.* **1998**, *102*, 177–183.

(199) Bernstein, P. R. *Am. J. Respir. Crit. Care Med.* **1998**, *157*, S220–S226.

(200) Hoover, D. M.; Bendele, A. M.; Hoffman, W. P.; Foxworthy, P. S.; Eacho, P. I. *Fundam. Appl. Toxicol.* **1990**, *14*, 123–130.

(201) Wang, P.; Heitman, J. *Genome Biol.* **2005**, *6*, 10.1186/gb-2005-6-7-226.

(202) Gol'tsberg, M.; Koldobskii, G. *Chem. Heterocycl. Compd.* **1996**, *32*, 1300–1304.

(203) Otsuki, S.; Nishimura, S.; Takabatake, H.; Nakajima, K.; Takasu, Y.; Yagura, T.; Sakai, Y.; Hattori, A.; Kakeya, H. *Bioorganic Med. Chem. Lett.* **2013**, *23*, 1608–1611.

(204) Brewster M, A.; Chavez-Macgregor, M.; Brown, P. *Lancet Oncol.* **2015**, *15*, 625–634.

(205) Lund, M. J.; Trivers, K. F.; Porter, P. L.; Coates, R. J.; Leyland-Jones, B.; Brawley, O. W.; Flagg, E. W.; O'Regan, R. M.; Gabram, S. G. A.; Eley, J. W. *Breast Cancer Res. Treat.* **2009**, *113*, 357–370.

(206) Trepel, J.; Mollapour, M.; Giaccone, G.; Neckers, L. *Nat. Rev. Cancer* **2010**, *10*, 537–549.

(207) Onuoha, S. C.; Coulstock, E. T.; Grossmann, J. G.; Jackson, S. E. *J. Mol. Biol.* **2008**, *379*, 732–744.

(208) Carrigan, P. E.; Sikkink, L. A.; Smith, D. F.; Ramirez-Alvarado, M. *Protein Sci.* **2006**, *15*, 522–532.

(209) Veale, C. G. L. *Tetrahedron Lett.* **2015**, *56* (38), 5287–5290.

(210) Krieble, V. K.; Noll, C. I. *J. Am. Chem. Soc.* **1939**, *61*, 560–563.

(211) Firestone, R. A. *J. Org. Chem.* **1968**, *33*, 2285–2290.

(212) Lakshmipriya, A.; Chaudharib, S. R.; Suryaprakasha, N. *New J. Chem.* **2016**, *40*, 8118–8122.

(213) Mohite, P. . B.; Pandhare, R. B.; Khanage, S. . G.; Bhaskar, V. H. *Dig. J. Nanomater. Biostructures* **2009**, *4*, 803–807.

(214) Onyestyak, G. *Stud. Surf. Sci. Catal.* **2004**, *154*, 3044–3051.

(215) Aureggi, V.; Sedelmeier, G. *Angew. Chemie - Int. Ed.* **2007**, *46*, 8440–8444.

(216) Zamani, L.; Mirjalili, B. B. F.; Zomorodian, K.; Zomorodian, S. *South African J. Chem.* **2015**, *68*, 133–137.

(217) Lei, Y.; Li, H.; Pan, H.; Han, S. *J. Phys. Chem. A* **2003**, *107*, 1574–1583.

(218) Ren, X.-H.; Wang, H.-J. *J. Solution Chem.* **2009**, *38*, 303–313.

(219) Suzuki, T.; Moriya, M.; Sakamoto, T.; Suga, T.; Kishino, H.; Takahashi, H.; Ishikawa, M.; Nagai, K.; Imai, Y.; Sekino, E.; Ito, M.; Iwaasa, H.; Ishihara, A.; Tokita, S.; Kanatani, A.; Sato, N.; Fukami, T. *Bioorg. Med. Chem. Lett.* **2009**, *19*, 3072–3077.

(220) Aureggi, V.; Sedelmeier, G. *Angew. Chemie - Int. Ed.* **2007**, *46*, 8440–8444.

(221) Gottlieb, H. E.; Kotlyar, V.; Nudelman, A. *J. Org. Chem.* **1997**, *62*, 7512–7515.